Dissertation

submitted to the

Combined Faculties for the Natural Sciences and for Mathematics

of the Ruperto-Carola University of Heidelberg, Germany

for the degree of

Doctor of Natural Sciences

Presented by

Marion Libouban, MSc

Born in: Enghien-les-bains, France

Oral examination: 12th May 2015

The effects of Mad2 over-expression on murine lung tumorigenesis.

Referees: Dr. Cornelius Gross
Prof. Dr. Stefan Wiemann

ACKNOWLEDGEMENTS

First and foremost, I would like to thank EMBL for giving me this great opportunity to do my PhD in a vibrant and international institute. Furthermore, thanks are due to Dr. Rocio Sotillo for accepting me in her group.

I am very grateful to my thesis advisor committee, Dr. Cornelius Gross, Dr. Jan Korbel, Dr. Marcos Malumbres, Dr. Martin Jechlinger, and Dr. Stefan Wiemann for their support and valuable scientific inputs during my PhD.

Many thanks to the Dean of the graduate office Helke Hillebrand and the director of EMBL Monterotondo Dr. Philip Avner. Both helped me tremendously for finding solutions to the frequent challenges during my PhD and defending the training purpose of the PhD program.

I would like to thank my family for their support before and during my PhD, my mum Lucile Guyard, my dad Thierry Libouban, my brother Ronan Libouban, my grand-ma Ginette Guyard, my step-mother Veronique Pascal, my step-brother Julien, and his wife Estelle Siringo. Many thanks to my boyfriend Sander Timmer for constant confidence in my work and support. Thanks to my cat assistant chouchou for controlling my writing progress.

I am very grateful to Kristina Havas for the guidance, support and fun during my PhD.

Thanks to Konstantina Rowald for being my German interpret.

I would like to thank my lab members, Kristina Havas, Cristina Aguirre, Joana Passos, Martina Mantovan, Konstantina Rowald, Shravan Vishaan, and Rita Cabrita, for the fun during these last years. I also thank Özge Vargel, Stefano Comazzetto, Marcos Morgan, Stefano Gnan, Janko Gospocic, Laetitia Weinhard, Shane Morley, and Irina Pinheiro, for the great times.

I am grateful to Pino (Giuseppe Chiapparelli) and Maria Kamber for their support with my mouse work. In addition, I am very grateful to Emerald Perlas for his support and suggestions regarding histology.

Thanks to Staff association for giving me the opportunity to be involved with the things orbiting around science.

ABSTRACT

Sixty-eight percent of human solid tumors are aneuploid, which is classically associated with poor patient prognosis. Several mouse models disturbing the spindle assembly checkpoint (SAC) have been developed to study the consequences of chromosome instability (CIN) and aneuploidy *in vivo*. Current knowledge suggests that aneuploidy can promote tumorigenesis or act as a tumor suppressor.

Mad2 is found over-expressed in human tumors, and Mad2 over-expression in mice induces the development of aneuploid tumors and facilitates $Kras^{G12D}$ lung tumor relapse. A proposed mechanism of tumor acceleration by CIN is the facilitation of tumor suppressor loss of heterozygosity. In how far Mad2 over-expression influences Kras driven lung tumorigenesis in a p53 heterozygous background, remains hitherto unclear.

In this thesis, I show that Mad2 over-expression increases p53(+/–);$Kras^{G12D}$ mice survival by delaying tumor initiation and progression. Different tumor populations (expressing low, intermediate and high levels of Mad2) have co-evolved from an original population of Mad2-expressing type 2 pneumocytes. My data suggest that high Mad2-expressing lung nodules are selected against during early tumorigenesis and are mainly composed of instable aneuploid cells.

Using time-lapse microscopy on mouse embryonic fibroblasts, I analyzed the effect of Mad2 over-expression in the context of p53 heterozygosity. Upon Mad2 over-expression, the inactivation of one copy of p53 rescued mitotic cell death by inducing mitotic slippage and polyploid cells.

In vivo, high Mad2 levels impaired S phase entry in tumor cells. Moreover, p53(+/–)KM high nodules strongly induced p21 in a p53-dependent manner. This data suggests that one copy of p53 can induce G1 cell cycle arrest in tumors. Although Mad2 over-expression generates aneuploidy, it does not accelerate p53 loss of heterozygosity (LOH), since Mad2 down-regulation occurs prior to LOH. Importantly, Mad2 over-expression together with p53 heterozygosity also delayed $EFGR^{L858R}$-induced lung cancer.

ZUSAMMENFASSUNG

Achtundsechzig Prozent aller soliden Tumoren enthalten einen abnormalen Chromosomensatz. Der Aneuploidie-Status eines Tumors korreliert in den meisten Fällen zudem mit schlechter Krankheitsprognose. Um die Folgen von chromosomaler Instabilität (CIN) und Aneuploidie *in vivo* zu untersuchen, wurden zahlreiche Mausmodelle auf der Basis eines veränderten Spindel-Kontrollpunktes entwickelt. Nach derzeitigem Wissensstand kann hier CIN sowohl tumorfördernd als auch tumorinhibierend wirken. Als Mechanismus für die Tumorstimulation wurde der Verlust von Heteroyzgotie eines Tumorsupressorgens wie beispielsweise TP53 durch unausgegliche Verteilung von Chromosomen vorgeschlagen.

Die künstliche Überexpression von Mad2, einer zentralen Komponente des mitotischen Kontrollkomplexes, im Mausmodel führte zur Entstehung aneuploider Tumoren und verstärkte das Rezidiv $Kras^{G12D}$ verursachter Lungentumoren nach Onkogenentzug. Bislang ist jedoch nicht bekannt, inwiefern sich die Überexpression von Mad2 auf Tumorsuppressoren und die Tumorentwicklung im p53 heteroyzgoten Kontext auswirkt.

In meinem Projekt habe ich einen positiven Effekt von Mad2 Überexpression auf das Überleben von p53(+/–);TetO-$Kras^{G12D}$;CCSP-rtTA Mäusen aufgrund einer Verzögerung der Tumorentwicklung nachweisen können. Aus der ursprünglichen Population Mad2 überexprimierender Typ 2 Pneumozyten entwickelten sich verschiedene Subpopulationen mit unterschiedlichen Mad2 Leveln (hoch, mittel, niedrig). Tumorknoten mit hoher Mad2 Expression werden während der frühen Stadien der Tumorentwicklung gegenselektiert und bestehen aus instabilen aneuploiden Zellen. Mit Hilfe von Zeitraffer-Mikrokopie analysierte ich den Einfluss von Mad2 Überexpression of embryonale Mausfibroblasten im p53 heterozygotem Hintergrund. Zusätzlich zur teilweisen Normalisierung der Mitosedauer, förderte die p53 Heterozygotie hier das Entkommen aus dem mitotischen Zelltod durch sogenannte “mitotic slippage” und damit die Entstehung polypoider Zellen.

In vivo Analysen zeigten, dass hohe Mad2 Level in Tumorzellen den Eintritt in die S-Phase erschweren. Zudem induzierten p53(+/–)KM Knoten mit hohen Mad2 Level die Expression von p21, welche höchstwahrscheinlich auf die verbleibende Kopie von p53 zurückzuführen ist. Eine Kopie von p53 kann somit zum G1-Arrest von Tumorzellen

führen. Zusammenfassend führt Mad2 Überexpression somit zur Entstehung aneuploider Tumoren, fördert jedoch nicht den Verlust von p53 Heterozygotie, da die Herunterregulierung der Mad2 Expression dem zuvorkommt. Eine Verzögerung der Tumorentwicklung konnte zudem im Model von $EGFR^{L858R}$-induzierten Lungenkrebs beobachtet werden.

THESIS INDEX

1 INTRODUCTION

1.1 BRIEF HISTORY OF CANCER

Cancer is a phenomenon that results in a large group of diseases, which begins in the smallest unit of living systems: the cell. It relies on uncontrolled cellular growth and ultimately kills the organism. Cancer occurred before modern humans appeared on the earth; in fact, metastatic cancer has been found in the fossilized bone of a Jurassic dinosaur (Rothschild et al., 1999). Although it was not named at the time, evidence of cancer has been found in mummies and the first description of cancer appeared in an Egyptian papyrus (Breasted and New York, 1930). The Greek physician Hippocrates (460-375 BC) gave the disease the term "karkinos", which later was translated to "cancer" in Latin, by the Roman physician Celsus (25 BC-50 AD). The Greek physician Galen (130-200 AD) proposed the term "oncos", which is still used by specialists today. At that time, surgeries already existed for the treatment of cancer and methods continually improved over time (Hajdu, 2011).

Christopher Columbus (1451–1506) introduced tobacco leaves in Europe and, thus, introduced the smoking habit to the Western world. By the end of the 16th century, the consumption of tobacco was common among celebrities and several cases of tobacco-induced cancer were reported (Hajdu and Vadmal, 2010). Johannes Muller drew for the first time cancer cells (Muller, 1838) and Herman Lebert postulated that enlarged nuclei and poly-nucleation are hallmarks of malignant cells (Lebert, 1845). In 1895, Wilhelm C. Rontgen discovered the X-ray, which was immediately used for cancer diagnostics. At a later stage, the tumor-suppressing effects of X-rays were employed in radiation therapies. Further development included the use of radium based on the discovery of radioactivity by Antoine H. Becquerel and by Pierre and Marie Curie (Hajdu, 2012). Another finding of the 19th century was the link between hormones and cancer, which is now utilized in hormonal therapies (Hajdu, 2012). In 1914, Theodor Boveri demonstrated that mutations can lead to cancer and postulated that cancer cells may arise from single cells with abnormal chromosome content (Boveri, 1914).

In the 1930s and 1940s, the establishment of *in vitro* cancer cell culture and animal experimentations stimulated the search for carcinogens (Hajdu and Darvishian, 2013). Otto H. Warburg discovered that cancer cells have a different metabolism, with high glucose consumption (Warburg, 1956), a property that is now used for cancer

diagnostics (PET scan) (Hajdu and Darvishian, 2013). In terms of the background of the discovery of the structure of DNA (Watson and Crick, 1953), Renato Dulbecco, Howard M. Temin and David Baltimore discovered the interaction between tumorigenic viruses and the genetic content of a cell (Baltimore, 1970; Dulbecco, 1967; Temin and Mizutani, 1970). In 1951, researchers grew for the first time neoplastic cells of a unique human cancer, adenocarcinoma of the uterine cervix (Gey GO, 1952); 64 years later, the HeLa cells are still used in laboratories (Landry et al., 2013). In 1966, the first case of familial cancer (Lynch syndrome) was reported, and this highlighted the importance of heredity in cancer development (Lynch et al., 1966). In the 60s, Sidney Farber launched the modern use of chemotherapy by developing the first national cancer chemotherapy protocols.

In the 70s, Bishop and Varmus discovered that the retroviral proto-oncogene had a cellular origin, and when re-introduced in a cell would act as an oncogene, giving rise to tumors (Stehelin et al., 1976). In the 80s, Weinberg isolated the first human oncogene *ras* and tumor suppressor *Rb* (Der et al., 1982; Dryja et al., 1986). A study suggested that genes required the modification of both alleles to extinguish the tumor-suppressive function (Knudson, 1971). However, mutation in one tumor's suppressor allele, such as p53, can be sufficient to drive tumorigenesis (Li and Fraumeni, 1969). Similar to proto-oncogenes, the genetic mutation occurring in one of the alleles produces dominant proteins (Dittmer et al., 1993). Nowell introduced "the tumor stage" concept; specifically, in the first stage cells would proliferate without control allowing, in a second stage, additional mutations and subsequently the selection of tumor cells. In addition, he speculated that genomic instability could fuel the generation of variants with a growth advantage (Nowell, 1976). A study proposed that at least five mutational hits are required for the stepwise clone selection responsible for malignant tumor progression (Fearon and Vogelstein, 1990).

The improved understanding of tumor biology and the identification of oncogenes led to targeted therapies. To gain access to oxygen and nutrients, tumors create new blood vessels; the 70s concept of blocking angiogenesis is now being used in clinics (Kerbel and Folkman, 2002). In some cases, the over-activated growth signaling is the target of novel drugs (Lynch et al., 2004). Studies on transmissible cancers suggest that cancer can break free and metastasize in other organisms; for example, a facial cancer appeared on a female Tasmanian devil about 20 years ago. The now-evolved clone

populations keep hopping from one individual to another through bite-mediated cell inoculation (Murchison et al., 2012). Other transmissible cancers in the animal kingdom are the canine transmissible venereal tumor *via* copulation (Murgia et al., 2006) and the contagious reticulum cell sarcoma in the Syrian Hamster *via* mosquito bite (Banfield et al., 1965). In the future, a novel transmissible cancer might even appear in humans. In fact, this has already been observed following accidental inoculation by medical professionals (Gartner et al., 1996).

Nowadays, cancer is a leading cause of death worldwide, with 8.2 million deaths in 2012, and the global burden of cancer is expected to further increase during the next twenty years. In the last report by the World Health Organization (WHO), lung cancer was listed as the most diagnosed cancer type, accounting for 13% of new cases. This fact is not surprising considering that tobacco use is responsible for 22% of cancer deaths (Stewart et al., 2014). Furthermore, the increasing incidence with age and the impact of cancers due to environmental and social influences made it the most prevalent disease in developed countries (Stewart et al., 2014). The world population is growing along with the adoption of cancer-causing behaviors (Jemal et al., 2011). In 2010, the costs of cancer care in the United States were estimated at $124.57 billion, and the total cost in 2020 is projected to be $173 billion, a dramatic 39% increase in 10 years (Mariotto et al., 2011).

1.2 HALLMARKS OF CANCER

Scientists Hanahan and Weinberg have simplified knowledge on cancer biology. Their description of tumorigenesis as a stepwise progression of genetic changes leading to the consequent events of immortalization, malignant progression and metastasis became one of the most cited and known theories in the field of cancer (Hanahan and Weinberg, 2000). Like in Darwinian evolution, cells through multiple rounds of mutation will be selected for growth and will ultimately generate tumors. In this context, six hallmarks of cancer cells were identified:

- Self-sufficiency in growth signal. In adult physiological tissues, most cells are quiescent. Under certain circumstances, they receive external signals such as growth factors that instruct them to re-enter the cell cycle and divide. A cell receives signals via their trans-membrane receptors that transduce the message into the cell and activate down-stream signaling pathways, most of the time by the action of kinases and

phosphorylation. To reduce this dependency, the cancer cells can modulate these signals. Cancer cells can produce their own ligands, stimulating autocrine feedback loops. In addition, cells can increase the amount of receptors, hence its chance of activation. An alternative is to produce a constitutive active form of the receptor or its down-stream effectors.

- Insensitivity to anti-growth signal. Similar to the growth, the anti-growth signals are transduced from the outside to the inside of the cells via trans-membrane receptors and down-stream effectors. As a result, the cell can exit the cell cycle and enter the quiescent state or acquire a differentiated state. Cancer cells have many ways to impair anti-growth signals such as, for example, the inactivation of the retinoblastoma (Rb) protein (Dryja et al., 1986). The tumor suppressor Rb can sequester the E2F transcription factors, which become incapable of launching the production of proteins required for the transition from G1 to S.

- Evading apoptosis. The homeostasis of tissues is normally regulated by proliferation and apoptosis. Apoptosis is a form of programmed cell death through the equilibrium of anti-apoptotic and pro-apoptotic proteins within the mitochondria. Molecular sensors can detect triggers such as DNA damage or hypoxia and, in response, activate molecular effectors that lead to apoptosis. The action of the pro-apoptotic proteins (Bax, Bak, Bim, Bid) within the mitochondria leads to the release of Cytochrome C, which activates caspases that destroy the genome and cellular organelles. The phenomenon is characterized by morphologic changes such as cellular blebbing, nuclear fragmentation, chromatin condensation and DNA fragmentation. Professional phagocytic cells complete the elimination of the cell from the tissues. A common way of perturbing this process is the mutation of the *TP53* gene; p53 acts as a DNA damage sensor and regulator of pro-apoptotic proteins.

- Limitless replicative potential. In addition to the external signals, cells have an internal clock that limits their proliferation. The telomeres are located at the end of the chromosomes and during every S phase of the cell cycle they are shortened. When chromosomes become unprotected, cells die or enter a state of senescence. The main mechanism by which a tumor cell avoids the replicative limit is by over-expressing the enzyme telomerase, which is capable of increasing the length of telomeres.

- Sustained angiogenesis. A possible limit for tumor growth would be the lack of oxygen and nutrient supply. The ability to generate and sustain new blood vessels is usually acquired at a later stage of tumorigenesis. To add to the complexity, many

different mechanisms promote angiogenesis. *TP53* mutations are also implicated in this process by reducing the inhibitory signals for angiogenesis.

- Tissue invasion and metastasis. Explorer cells that escape the primary tumor and travel to a new fertile tissue can initiate metastasis. Almost all fatal disease outcomes are attributed to metastatic cancer. When a cell finds itself in a new territory, it will resume all the previously described characteristics. The molecular processes leading to metastasis involve the deregulation of extracellular molecules required for cell-to-cell and extracellular matrix interactions.

Ten years after the first publication of the hallmarks of cancer, the authors revisited the publication; they integrated the latest concepts and highlighted the importance of the tumor environment such as, for example, innate immunity. Two emerging and two enabling hallmarks were added to the previous list (Hanahan and Weinberg, 2011).

- Deregulation cellular energetics. Tumors require many resources for their growth; to cope with their needs, tumor cells adjust their energy production. Healthy cells use aerobic metabolism: the glucose is transformed into pyruvate in the cytosol and further reactions requiring oxygen occur within the mitochondria. Cancer cells are able to increase their glucose intake and extensively use glycolysis, especially in the case of hypoxia. This phenomenon is known as the Warburg effect (see section 1.1). A possible reason for the metabolic switch is that in addition to providing energy, it also provides substrates for the synthesis of new cellular components.

- Avoiding immune response. In an organism, the immune system is constantly monitoring and eliminating aberrant cells, blocking the generation of tumors. Thus, tumors must find a way to avoid this surveillance. It is possible that in the process of selection, only clones that do not trigger the immune system survive or that highly immunogenic cancer disables the hostile response.

- Tumor promoting inflammation. Apart from the protective function of invading immune cells, the process of inflammation has also been linked to tumor enhancement. Cells involved in the inflammatory response involve macrophages, mast cells, neutrophils, and T and B cells. An example of the tumor promotion mechanism is the recruitment of inflammatory cells (co-expressing the macrophage marker Cd11b and the neutrophil marker Gr1), which are able to suppress the anti-tumoral activity of other immune cells (e.g. natural killer cells).

- Genome instability and mutation. In order to acquire the previously described hallmarks, tumor cells undergo a succession of mutations or genome modification. Like a cycle, every mutational step will confer a growth advantage to a cell that will ultimately give rise to tumors. Additionally, epigenetic changes can modify gene expression and be part of clone selection. The increased mutational potential of tumor cells is due to the dysfunction of proteins. As an example, the frequent p53 mutations increase the probability for more mutations. Functionalities such as detection and repair of DNA damage and mutagen neutralization are reduced. Alternatively, the loss of the protective telomeres at the chromosomal extremities can lead to chromosomal breakages and unstable karyotypes. Chromosomal instability is a form of genomic instability and will be introduced at a later stage (section 1.7).

1.3 LUNG CANCER

Lung cancer is the leading cause of cancer-induced death worldwide (Jemal et al., 2011) and has a very low survival rate of five years (6.5-16% (Jemal et al., 2011)). It is known to be induced by smoking and predictions suggest that its incidence will increase (see section 1.1). Histologically, lung cancers have been classified into small-cell lung carcinoma (15%, SCLC) and the non-small-cell lung carcinoma (85%, NSCLC). The NSCLC are further separated into squamous cell carcinomas (SCC), large cell carcinomas and 55% are adenocarcinomas (Shames and Wistuba, 2014). The most common driving mutations include the proto-oncogene Kras mutated in about 20% of lung adenocarcinomas, and the oncogenic EGFR is present in 10%. Kras and EGFR mutations are mutually exclusive. Furthermore, the tumor suppressor p53 is mutated in 50% of the adenocarcinomas (Chen et al., 2014; Imielinski et al., 2012).

- EGFR: epidermal growth factor receptor. EGFR is a trans-membrane receptor (Figure 1.1). When activated by its ligand or constitutively activated in cancer, it induces proliferation via the RAS/MAPK, PI3K/AKT and STAT3/STAT5 signaling pathways. EGFR and its ligands can either be over-expressed in NSCLC or the kinase domain is over-activated. Kinase over-activation can be the result of the deletion of exon 19 or by a point mutation in the exon 21, L858R (Lynch et al., 2004). Because of its importance in lung cancer and its extracellular localization, targeted therapies affecting EGFR were developed and have been proven effective in patients (Pao et al., 2004). Unfortunately, secondary mutation of EGFR confers treatment resistance.

- Kras. Ras proteins are small GTPases downstream of EGFR (Figure 1.1), and are part of the Ras/MAPK signaling pathway that transduces proliferative signals from the extracellular environment to the nucleus. *Ras* is one of the first discovered oncogenes (Pulciani et al., 1982) and the most common in lung adenocarcinomas (Mills et al., 1995). The *Ras* genes codes for different splicing variants: Nras, Hras, and Kras, which interact with similar down-stream effectors but differ in their post-transcriptional modifications. The mutated Ras variants appear be tumors specific and Kras mutations are predominant in NSCLC. Genetic mutations can be found in codon 12: G12D, G12C and G12V, or, in codon 13 and 21. These genetic mutations lead to the constitutive activation of GTPase and they are no therapy targeting *Ras* mutations.

- P53. I would like to start this part with the following citation: "I worry a lot about p53. I'm paid to do it, but perhaps we all should, as the correct functioning of this 393 amino acid nuclear protein is apparently all that lies between us and an early death from cancer" (Lane, 1992). P53 is known as the guardian of the genome (Lane, 1992) and functions as a transcription factor after homo-tetramerization. p53 regulates the cell cycle and induces G1 arrest upon DNA damage (Kastan et al., 1992). Furthermore, p53 regulates apoptosis, and acts as a backup for Rb inactivation (Morgenbesser et al., 1994). At the beginning of the 80s, p53 was mistaken for an oncogene because of its promotion of cellular transformation (Parada et al., 1984). When the first mutations in the p53 gene were discovered, research on the topic became popular (Koshland, 1993). To date, over 20.000 mutations of p53 have been reported, of which very few lead to p53 disappearance. Most genetic alterations of the p53 gene are missense mutations, leading to the production of a stable protein with an inactive DNA-binding site and to its accumulation in the nucleus. From the mutated gene, the dominant-negative p53 protein can form hetero-dimers with the wild-type p53 produced by the remaining allele and impairs transactivation and cell cycle and apoptosis control (Soussi and Beroud, 2001). Moreover, some mutations can lead to a gain of function (Dittmer et al., 1993).

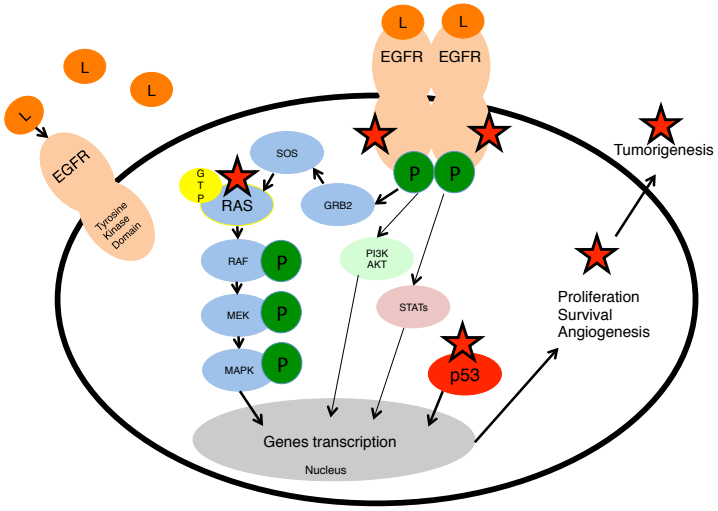

Figure 1.1: Frequent mutations in NSCLC. The binding of the ligands (L) to the EGFR receptor leads to a conformational change of the receptor and its dimerization, preceding the trans-activation of the tyrosine kinase domain by trans-phosphorylation. The activated receptor initiates a signaling cascade including the PI3K/AKT (green), the STAT (pink) pathways and the Ras/Raf/MAPK pathway (blue) orchestrated by the ras GTPase (blue and yellow) and a series of phosphorylations. The cascades lead to genes transcription regulating proliferation, cell survival and angiogenesis. In lung cancer, the EGFR receptor and its ligand can be amplified increasing the chance for receptor dimerization. The EGFR receptor can be mutated and constitutively activated. This is also the case for the Ras GTPase. The transcription factor p53 (red) can regulate proliferation, cell survival and angiogenesis via regulation of its gene targets and it is mutated in cancer. Ligand is shown in orange, ATP in yellow, phosphorylation in green. A red star indicates tumorigenic action points.

1.4 Mouse models of NSCLC

There is amplitude of mouse models and possible transgenic mouse crosses recapitulating human lung cancer. In this section, I will focus on a subset of relevant findings for this thesis.

1.4.1 First-generation mouse models

Lung cancer modeling started with spontaneous tumors in specific inbred-mouse stains or *via* induction by carcinogens. The first generation of transgenic mouse models constitutively over-expressed transgenes: oncogenes or inactive tumor suppressors. In the lung, this was done using cell-type-specific promoters. Initially, the promoter of SPC (lung surfactant protein C) was used to initiate transgene expression in type II pneumocytes and CCSP (Clara cells secretory protein) in Clara cells. The two systems

induced similar lung tumors, though the CCSP promoter is being used extensively since it was actually found active in both cell types (Meuwissen and Berns, 2005).

1.4.2 Second-generation mouse models

The next generation of mouse models includes knock-in strategies; Kras being an important oncogene in NSCLC was induced at endogenous levels and successfully induced tumors. In fact, the expression at endogenous levels appeared more tumorigenic than Kras over-expression, though the tumors were not restricted to the lung in this model (Johnson et al., 2001). The knock-in Lox-Stop-Lox-KRAS^{G12D} model overcomes this issue. The tracheal delivery of a recombinant adenovirus expressing Cre recombinase removes the Stop codon; it induces the expression of Kras and lung adenocarcinomas (Jackson et al., 2001). In addition, many Cre recombinase-carrying lines have been created for the removal of Stop codons in a cell-type-specific manner. Moreover, Cre recombinase expression can be controlled in a timely manner using inducible systems such as the Cre-RT2, where DNA excision is only possible in the presence of Tamoxifen (Brocard et al., 1997).

1.4.3 Tet-On system

The Tet-On (Figure 1.2) and Tet-off bi-transgenic models allow transgene de-induction (Gossen and Bujard, 1992). These systems consist of a first transgene where a tissue-specific promoter controls the expression of the tetracycline-controlled trans-activator (tTA) or reverse tTA (rtTA). In the absence of the regulator doxycycline (Dox), tTA activates the transcription of the second transgene by binding the tetO repeats, which are cloned upstream of the gene of interest. In these cases, the delivery of doxycycline leads to repression of the trans-activator and the transgenic system. On the contrary, the rtTA, being a mutated form of tTA, requires doxycycline for the induction of one or several target genes. The Tet-On-oncogene, CCSP-rtTA, allows transgene induction and de-induction in a temporal manner in the type II pneumocyte specifically and recapitulates human lung adenocarcinomas. An additional asset of the Tet-On system is that Dox bound to rtTA can induce more than one transgene at a time in the cell type of interest. Thus, the Tet-On system reduces the number of transgenes required for multi-parameter study. The CCSP-rtTA, TetO-Kras^{G12D,} and CCSP-rtTA, TetO-EGFR^{L858R} mouse lines successfully developed lung adenocarcinomas (Fisher et al., 2001; Politi et al., 2006) when doxycycline was administered and will be used in this

thesis in combination with other mouse models (see section 1.8.3).

1.4.4 p53

Due to the extensive interest in the role of p53 (e.g. dominant negative, gain of function or loss) in tumorigenesis, many mouse models have been generated targeting p53 or its regulators. One of the first mouse models with deficient p53 was a knockout (KO). Homozygotic p53 mice showed a very fast onset of tumorigenesis. Heterozygosity on the other hand aided tumor development (Jacks et al., 1994). This mouse model has been extensively crossed with other over-expressing oncogenes (Fisher et al., 2001). In this thesis, in a similar way, I am using the p53KO model by combining the TetO-Kras^{G12D} (Fisher et al., 2001) or TetO-EGFR^{L858R} (Politi et al., 2006) mouse models.

At a later stage, more sophisticated models have been created such as the "super p53" mice. In this model, one additional allele of p53 is added. This extra p53 allele leads to a better response to stress (e.g. cell cycle arrest and apoptosis) and mice are protected against cancer (Garcia-Cao et al., 2002). A knock-in model replacing the wild-type p53 by the R175H mutant found in human cancer has shown to be prone to fast tumor onset and metastasis (Liu et al., 2000). Further knock-in models with specific mutations in post-transcriptional modification sites, such as phosphorylation, do not generate spontaneous tumors (Chao et al., 2003; MacPherson et al., 2004). Liu et al. showed that the over-expression of p53 induces cell cycle arrest, but impairs apoptosis, and mice show a late tumor onset (Liu et al., 2004).

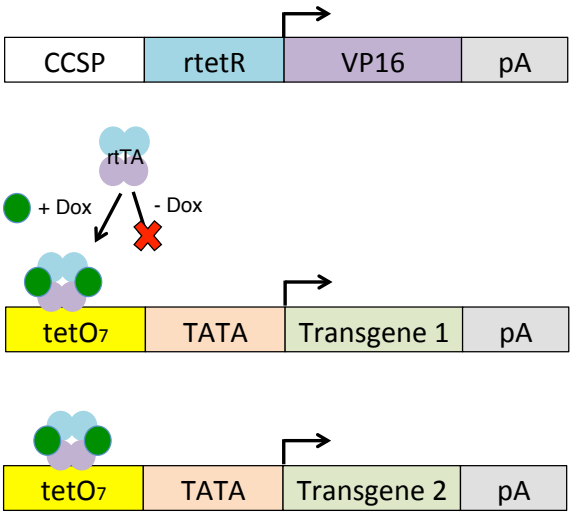

Figure 1.2: The tet-on system. The tetracycline-controlled reverse-transactivator (rtTA) consists of a mutated chimeric construct of the Escherichia coli Tn10 tetR gene (blue) and the VP16 transactivation domain from the herpes simplex VP16 protein (purple). In the presence of the inducer, doxycycline (Dox, Green), rtTA dimers bind to seven tandem repeated tetO sequences ($tetO_7$), thereby activating transcription from a minimal promoter (TATA) and simultaneously driving expression of transgenes of interest. The CCSP promoter produces rtTA in lung epithelial cells. pA: polyadenylation

1.5 Eukaryote Cell cycle

1.5.1 Definitions

The cell cycle consists of the execution of consequent events in one cell resulting in the production of two daughter cells. Importantly, cell division has three purposes for an organism: reproduction, growth and maintenance. Deregulation of the cell cycle underpins the onset of cancer.

The cell cycle is divided into four phases (Figure 1.3). DNA replication occurs in the S phase. Segregation of the replicated genetic material occurs in mitosis (M phase), which is considered the end of the cell cycle. The Gap phases, G1 and G2, are before the S phase and the M phase, respectively. In contrast to mitosis, during the G1, S and G2 phases, the cell does not change its morphology. These three phases are also defined as interphase. The majority of cells in an adult organism is neither in mitosis nor in interphase, but is quiescent. Specialized cells are an exception to this rule and continue dividing throughout life to replace cells that have a high rate of turnover (e.g. gut epithelium, hematopoietic cells).

In the late 80s, it was hypothesized that the events taking place in the cell cycle are connected; the cycle progression depends on the success of the previous phases (Hartwell and Weinert, 1989). Hartwell and Weinert introduced the concept of cell cycle checkpoints and demonstrated the existence of the DNA damage checkpoint in yeast (Hartwell and Weinert, 1989). The three eukaryotic cell cycle checkpoints maintain the integrity of the genome and viable nucleo-cytoplasmic ratio. The first checkpoint occurs in G1, the second in G2 and the last one during mitosis. During the G1 phase, a cell can commit to cell division or arrest and eventually leave the cell cycle. The restriction point, also called the G1 checkpoint, defines the time where the fate of the cell has been decided. To re-enter the cell cycle, a cell needs to receive sufficient growth signals between the previous cycle of mitosis and the restriction point. These

signals ensure the synthesis of the tools necessary for future DNA synthesis and S phase (Foster et al., 2010). Alternatively, the cell can enter a quiescent state when received signals are insufficient. The quiescent state is when a cell is not preparing to divide or dividing; it is also called Gap 0 (G0). The first purpose of quiescence is to support cell survival in extreme conditions such as nutrient deprivation, and its physiological role is to stop the growth of complex mammalian organisms (O'Farrell, 2011; Pardee, 1974). When triggered, most cells can re-enter the cell cycle in G1 and resume proliferation with the exception of terminally differentiated cells (cardiac muscle cells, neurons (Pardee, 1974)). This is in contrast with the term senescence, which defines the end of replicative life and a physiologically irreversible state. It is the final state of our molecular clock determined through the erosion of telomeres with each cellular division (Sedivy, 1998). The fact that MEFs harboring deletion of p53 and p21 can become immortal indicates that senescence can be reversible upon appropriate mutations (Deng et al., 1995; Jacks, 1996). During G2, the cell undergoes rapid growth, synthetizes proteins and prepares for the next phase of mitosis. The checkpoint at the G2/M transition, also known as the DNA damage checkpoint, ensures the repair of DNA damage experienced during the S phase prior to mitosis.

1.5.2 Regulations

The key components of the cell cycle are the cyclin-dependent kinases (CDKs) and their regulatory sub-units, the cyclins. In humans, twenty-nine cyclins have been identified from which nine appear to control the cell cycle. The CDKs are serine/threonine kinases and eleven out of the twenty members of the family have cell cycle-related activities (Malumbres, 2014). The CDKs can be regulated in three major ways. First, the fluctuation of cyclin gene expression and the degradation by the ubiquitin-mediated proteasome pathway induces oscillation in CDK activity. This oscillation regulates the transition of one phase to the next (Evans et al., 1983; Glotzer et al., 1991; Nurse, December 9,2001). Second, the activity of the CDKs can be enhanced by the CDK-activating kinase by phosphorylating the pre-formed CDK-cyclin complex (Pavletich, 1999). On the other hand, phosphorylation of the complexes can also have inhibitory effects. Third, proteins from the INK4a and Cip/Kip families (e.g p21) inhibit the CDKs. They bind the CDKs alone or those already in complexes with the cyclins (Harper et al., 1995; Malumbres, 2014; Pavletich, 1999). P21 is transcriptionally activated by p53 and can inhibit Cdk2, Cdk3, Cdk4, and Cdk6, and

increased levels of p21 induce G1 arrest (Harper et al., 1995). Moreover, these regulated transductions are tightly controlled by feedback loops responsible for the stable phases of the cell cycle.

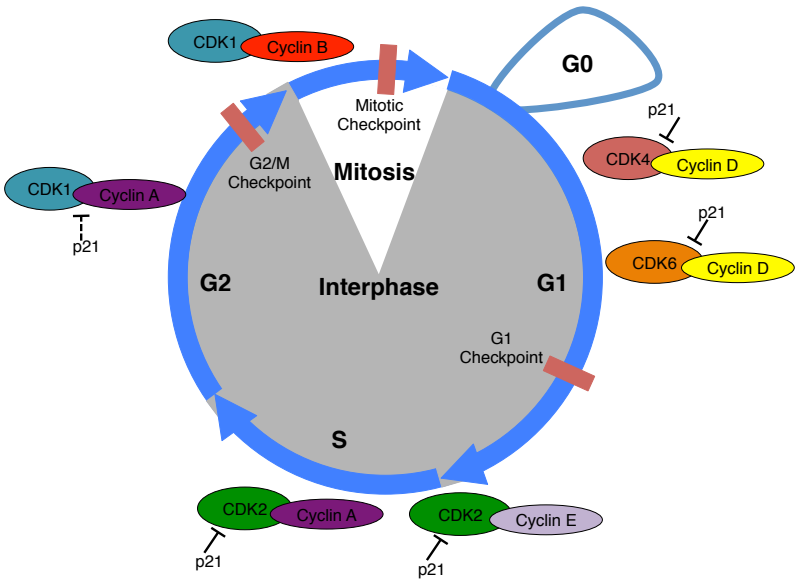

Figure 1.3: Simple view of the cell cycle. The cell cycle is composed of four phases: Gap 1 (G1), S phase (DNA synthesis), Gap 2 (G2) and mitosis (in white). Together G1, S and G2 constitute the interphase (in gray). When the conditions are not favorable for cell division the cell can reversibly escape in Gap 0 (G0) and become quiescent. Three checkpoints control for the genome integrity and cellular growth (red boxes): G1, G2 and mitotic checkpoints. The cell cycle progression is due to the CDKs enzymatic activity; CDKs operate when bound to the cyclins. The cyclins availability fluctuates during the cell cycle, hence the dominant complex forms. CDKs 4 and 6 are active when bound to cyclin D in G1. The CDK2-cyclin E complex controls the progression to the S phase. In S phase, cyclin A slowly replaces cyclin E and peaks in G2 to form the CDK1-cyclin A complex. The mitotic cyclin B binds to CDK1, the complex is called the mitosis-promoting factor (MPF). Its activity rises during the cell cycle and provokes entry into mitosis; the degradation of cyclin B is required for mitotic exit. The protein from the Cip family, p21 can directly (black line) inhibit CDK 2, 4 and 6 and produce a G1 arrest. The CDK1-Cyclin A complex is indirectly (dashed line) inhibited by p21 and contributes to a G2 arrest.

1.6 Mitosis and the spindle assembly checkpoint

1.6.1 Mitosis

Mitosis is the phase of the cell cycle in which the previously replicated chromosomes are equally separated in two nuclei, a process followed by cytokinesis, leading to the production of two generally identical daughter cells. Walther Flemming was the first to publish extensive work on the process that he called mitosis (Flemming, 1878). Altogether, mitosis is divided into five phases in animals, while plants have an additional sixth phase: in pre-prophase, the nuclei have to migrate to the cell center. The first phase is prophase: the previously replicated pairs of centrioles (centrosome) migrate at the opposite poles of the mother cell and form the spindle via elongation of microtubules from each pole of the cell. The previously replicated DNA condensates, sister chromatids are associated by cohesin at their centromeres (kinetochores) and the nuclear envelop dissolves. In metaphase, the duplicated chromosomes (sister chromatids) align at the equatorial or metaphase plate of the mother cell. The microtubules connect the kinetochores of the sister chromatids to opposite poles of the cell. In anaphase, the chromosomes have lost cohesion and are pulled by the microtubules to their respective poles. In telophase, the chromatin decondenses, the spindle disappears, the two nuclear envelops form and the physical cell division begins. Finally, in cytokinesis, the cytoplasm divides through a contracting ring at the midbody, forming the cleavage furrow, which divides two daughter cells, thus ending mitosis. The purpose of the mitotic checkpoint, or the spindle assembly checkpoint (SAC), is to ensure proper chromosome segregation during anaphase by preventing the premature separation of sister chromatids.

1.6.2 The spindle assembly checkpoint (SAC) discovery

The SAC is activated in pro-metaphase, it controls the alignment of chromosomes at the metaphase plate and proper attachment of the sister chromatids to the microtubules coming from opposite poles. The centromeric chromatin and the cohesins comprise the inner part of the kinetochores. The chromosome passenger complex is localized at the inner kinetochore in metaphase. It is composed of inner centromere protein (INCENP), Survivin, Borealin, and Aurora B. Aurora B oversees chromosome bi-orientation by ensuring the enzymatic function of the complex, which is responsible for the removal of improper microtubule-kinetochore attachments. At the outer part, there are,

respectively, binding and docking sites for the microtubules and SAC members (Sullivan et al., 2001).

Members of the SAC gene family were discovered in two screens in budding yeast for genes, which, when mutated, confer sensitivity to depolymerizing microtubule drugs (Hoyt et al., 1991; Li and Murray, 1991). Among the mitotic arrest-deficient genes are *Mad1*, *Mad2*, and *Mad3* (*BubR1* in humans). Mad2 was the first to be identified in humans (Li and Benezra, 1996). Budding inhibited by benzimidazole genes belong to Bub1 and Bub3. Bub2 was later excluded from SAC composition since it monitors the spindle position, not the interaction between microtubules and kinetochores (Bloecher et al., 2000). In addition, the SAC components were responsible for the delay of metaphase entry when the chromosomes have mutant centromeres (Spencer and Hieter, 1992). The Mps1 kinase was identified in an experiment where *mps1* mutants did not arrest mitosis upon spindle disruption (Weiss and Winey, 1996). Many more proteins were identified as part of the SAC gene family, for example Spc105, MIS12, HEC1, and MCM21, which bind to the outer kinetochores. The impairment of kinetochore assembly by acting on the microtubule motor protein CENP-E and dynein can activate the SAC.

1.6.3 The SAC mechanism

Two proteins must be eliminated in order for mitosis to be completed. First, the degradation of Securin allows the separation of sister chromatids. Second, the destruction of Cyclin B inactivates the mitotic kinase CDK1 and promotes mitotic exit. At the molecular level (Figure 1.4), the kinase Mps1 phosphorylates proteins found at the microtubule-free kinetochores, allowing the recruitment of the Bub1-Bub3 complex. Mps1 phosphorylates Bub1, which interacts with Mad1. Mad1 at the un-attached kinetochores attracts Mad2 and changes its conformation from an open to closed form. The closed Mad2 sequesters Cdc20 in the cytoplasm and, as a result, Cdc20 becomes unavailable for the anaphase-promoting complex/cyclosome (APC/C). In addition to the sub-complex Mad2-Cdc20, the mitotic checkpoint complex (MCC) includes BubR1 and Bub3. With increased complexity, the effector of the SAC has more affinity for Cdc20. When available, Cdc20, together with the APC/C, have ubiquitin ligase activity and target Securin and Cyclin B for proteolysis. Securin inhibits the enzyme Separase, which when free contributes to the separation of the sister chromatids by cleavage of the

cohesins. In summary, the recruitment of the SAC at the un-attached kinetochores leads to the change of Mad2 conformation, the sequestration of Cdc20, the inhibition of the APC/C complex, the inhibition of sister chromatid separation, the maintenance of CDK1 activity, and a pro-metaphase block.

It is intuitive to think that the SAC is inactivated when all the kinetochores are attached. However, it remains unclear how it can distinguish between correct and incorrect attachments. Since the microtubules are pooling chromosomes, the SAC might be able to sense inadequate tension due to incorrect binding and remain active, or, alternatively, become inactive upon bi-polar attachment or both.

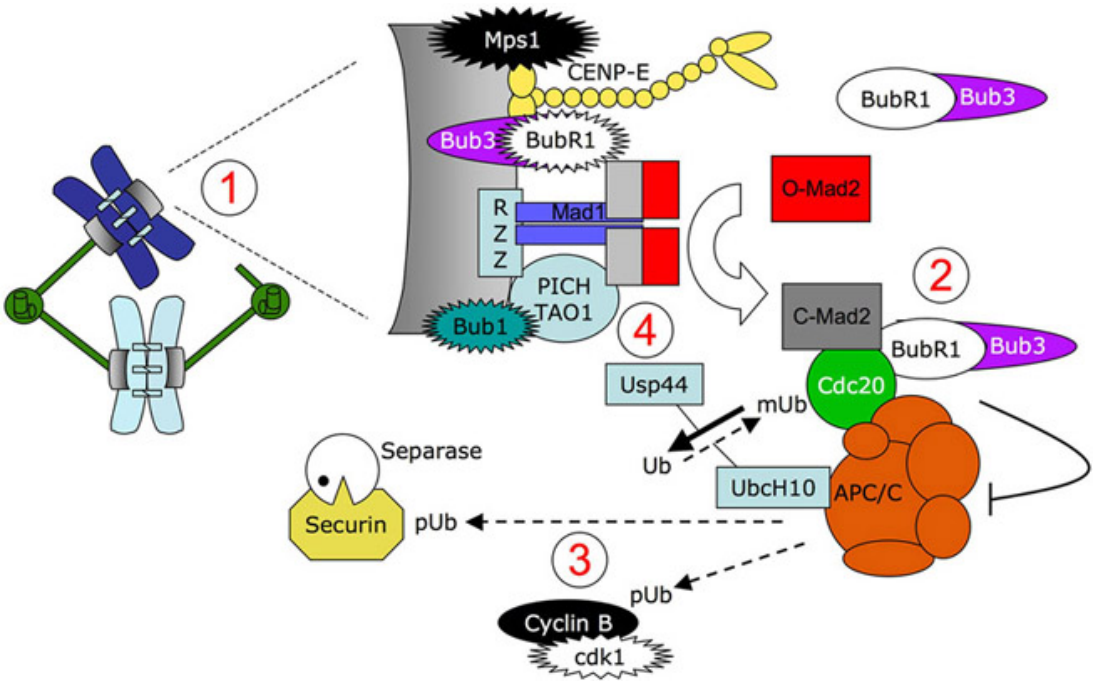

Figure 1.4: The mitotic checkpoint or SAC. Figure taken from Geert JPL Kops, Frontiers in Bioscience 13, 2606-3620, May 1, 2008. "Schematic model of molecular aspects of mitotic checkpoint signalling. Unattached kinetochores (1) specifically recruit proteins that participate in production of the Mitotic Checkpoint Complex (MCC) (2), an inhibitory complex that prevents poly-ubiquitination (pUb) and subsequent degradation of cyclin B and Securin (3) by the APC/C. Integrity of the MCC is further maintained by Usp44, a de-ubiquitinating enzyme that counteracts Cdc20 multi-ubiquitination (mUb) by the APC/C and its E2 co-enzyme UbcH10 (4)."

1.7 Genomic instability, Chromosome instability, and aneuploidy

1.7.1 Genomic instability

Genome instability (GI) has been recently associated with the acquisition of initial cancer hallmarks (Hanahan and Weinberg, 2011). Genomic instability can be divided into two categories: microsatellite instability and chromosome instability. Microsatellites are composed of large sequences of tandem repeats and ((CA)n is the most frequent) at the chromosome centromere (Ellegren, 2004). During DNA replication, the DNA polymerase is prone to slippage at the microsatellites, producing insertion-deletion loops and inactivating frame-shift mutations. DNA mismatch repair proteins normally correct these errors. Thus, microsatellite instability is a result of mutation or silencing of DNA mismatch repair. An example of microsatellite instability is found in a colon carcinoma cell line, where the DNA mismatch repair gene *MSH2* is mutated as well as the pro-apoptotic protein BAX, the latter due to a frame-shift mutation (Zhivotovsky and Kroemer, 2004).

1.7.2 Chromosome instability: structural

Among the different forms of GI, chromosome instability (CIN) is the most prevalent (Lengauer et al., 1997). Structural and numerical are the two types of chromosome instability. Structural instability can be promoted by dysfunction of the DNA damage sensor and repair mechanisms such as DNA damage checkpoint, DNA double strand breakage, non-homologous end-joining and homologous recombination. Moreover, structural instability can be a consequence of telomere attrition and end-to-end chromosome fusion. As a result, chromosomes can break and enter chromosomal break-fusion-bridge cycles (Zhivotovsky and Kroemer, 2004). Chromosome translocations are the most common form of structural changes (Mitelman et al., 1997). The first example of a translocation was discovered in myeloid leukemia. The reciprocal translocation between chromosome 9 and 22 led to the fusion of two genes (BCR and Abl). This fusion led to the production of an oncogenic protein, a structural anomaly known as the Philadelphia chromosome (Look, 1997; Nowell P, 1960). Tumors are not always the result of one structural modification; in fact, they appear to have a high rate of chromosomal rearrangements (Abdel-Rahman et al., 2001). This frequent chromosome re-configuration confers instability and heterogeneity to tumors and supports the selective advantage of the cancerous population.

1.7.3 Chromosome instability: numerical, aneuploidy

Where whole chromosomal instability relates to the dynamic rate of chromosomal changes, aneuploidy relates to a state: non-diploid DNA content. Physiological aneuploidy exists in the liver, skin, and brain (Duncan et al., 2010; Gandarillas and Freije, 2014; Rehen et al., 2005), and the stable karyotype can be transmitted to the cells. The majority of human solid tumors are aneuploid (Storchova and Kuffer, 2008) and generally continue to evolve throughout tumor cell generation. Such evolution is classically associated with poor patient prognosis (Choi et al., 2009; Lengauer et al., 1997). As mentioned for structural changes, whole chromosomal instability or the constant change of karyotype might fuel the selection of transformed clones. Examples of mechanisms leading to numerical chromosome instability are merotelic attachments and mitotic checkpoint defects. Interestingly, these mechanisms can induce each other.

- Merotelic attachments consist of the simultaneous attachment of a kinetochore by the microtubules from the two opposite poles. If the merotelic attachments are not resolved, it results in lagging chromosomes. Although Aurora B-dependent mechanisms can correct the placement of the wrongly attached microtubules, their removal seems to be a limiting factor (Bakhoum et al., 2009; Thompson and Compton, 2011). For this reason, the hyper-stabilization of the microtubule at the kinetochore can be a cause of aneuploidy. In fact, over-expression of Mad2 increases kinetochore-microtubule stability and leads to aneuploidy and tumorigenesis in mice (Kabeche and Compton, 2012; Sotillo et al., 2007). Additionally, the mitotic checkpoint is not efficient in sensing the merotelic attachments enabling the dividing cell to proceed through the end of mitosis, resulting in aneuploid daughter cells (Thompson and Compton, 2008). Cohesion dysfunction in between two sister chromatids can also be a source of merotelic attachments since it can increase kinetochore accessibility for the microtubules. Another known cause of merotelic attachments is an abnormal centrosome number, which is common in cancer cells (Nigg, 2002) and can lead to the formation of a multi-polar spindle. In an environment with microtubules emerging from many poles, it is very likely that a kinetochore will find several attachments. In the context of structural modification, a chromosome can have multiple attachment sites and will trigger numerical instability.

- Mitotic checkpoint defects. On the one hand, a weak SAC does not arrest the cells when the microtubules are not properly attached to the kinetochores. This can lead to premature anaphase and aneuploid progeny. Alternatively, an over-activated SAC alters the mitotic timing by blocking cells in mitosis and might be overcome by mitotic slippage or mitotic catastrophe. The two outcomes are accidental mitotic exit where the first one leads to viable progeny and the second one to cell death. How this choice is made remains largely unclear. The outcome seems to depend on the balance between apoptotic signals and SAC-independent gradual degradation of Cyclin B (Gascoigne and Taylor, 2008). Deficient (too weak or too strong) SAC function, in the majority of cases, results in improper chromosomal segregation and aneuploidy. Depending on the severity of the damage to and the status of p53, the cell might arrest in G1 or undergo apoptosis in interphase. In the absence of functional p53, the aneuploid cell could continue cycling and increase the levels of aneuploidy. Several mouse models disturbing the SAC have been developed to study the consequences of CIN and aneuploidy *in vivo* (Schvartzman et al., 2010).

1.8 Aneuploidy Model organisms and Aneuploidy paradox

Although representing a common feature in cancer, aneuploidy has been shown to have detrimental effects on cell growth and fitness. The contradictory findings together with the lack of consensus in studies has led to the concept of "aneuploidy paradox", describing its beneficial or detrimental effects on tumorigenesis, depending on context. In this section, I am summarizing the results relevant for this thesis. It is important to remember that aneuploidy corresponds to a stable state of non-diploid karyotype. On the contrary, chromosome instability (CIN) corresponds to the dynamic rate of karyotype changes, meaning that CIN cells can also be aneuploid.

1.8.1 Aneuploidy with out transgenic mouse models

At the cellular level, *in vitro* studies indicate that aneuploidy impairs cellular fitness. Yeast strains and mouse cell lines carrying extra chromosomes have impaired growth and immortalization. As a consequence of the increase in gene products, cells need an enhanced metabolism; this phenomenon is called proteotoxic stress (Pavelka et al., 2010; Torres et al., 2007; Williams et al., 2008). In people, aneuploidy is the leading cause of miscarriage. Only autosomal trisomies of chromosomes 13, 18 and 21 are compatible with human life, though these result in phenotypes with severe

developmental problems such as mental retardation and reduced survival (Hassold et al., 2007). Despite the development of a phenotype at puberty, aneuploidy of sex chromosomes is better tolerated in childhood. In healthy tissues, mitosis leading to aneuploid progeny can occur (Hartwell and Smith, 1985), though with the control mechanisms being intact, the cells are eliminated or kept in rare physiological cases (e.g. skin). On the contrary, 68% of the pathologic human solid tumors are aneuploid (Duijf et al., 2012). The constant evolution of tumor karyotypes has been linked to tumor heterogeneity, resistance to therapy and poor prognosis including lung adenocarcinomas (Choi et al., 2009; Gao et al., 2007; Kuukasjarvi et al., 1997).

1.8.2 First-generation mouse models: weakened SAC

Initial *in vivo* studies on the effect of aneuploidy addressed whether aneuploidy by itself is sufficient to induce tumorigenesis. Alternatively, aneuploidy could be a "passenger" accompanying selected mutations. Since the complete abrogation of the mitotic checkpoint and the deletion of its components are lethal (Hassold et al., 2007; Kalitsis et al., 2000; Michel et al., 2004), the first mouse models were aimed solely at weakening the checkpoint. In this weakened condition, the aneuploidy is induced by premature separation of the sister chromatids, and many models display an increase in susceptibility to spontaneous tumors with late latencies, especially in the lung. The mouse embryonic fibroblasts derived from the mouse models were aneuploid and disabled. In most cases, however, no correlation could be found between the *in vitro* levels of aneuploidy with the *in vivo* disease outcome. As examples, Mad2, CENP-E, Mad1 heterozygous and Bub1 hypomorphic mice showed an increase in the incidence of spontaneous lung tumors (Iwanaga et al., 2007; Jeganathan et al., 2007; Michel et al., 2001; Weaver et al., 2007). On the contrary, Bub1 and Bub3 haplo-insufficiency and consequent CIN did not affect spontaneous tumorigenesis (Jeganathan et al., 2007; Kalitsis et al., 2005). These results indicate that a weakened SAC can induce aneuploidy and tumorigenesis, and for undetermined reasons the lung tissue is particularly prone to tumors.

1.8.3 Second-generation mouse models: SAC over-activation

Gene down-regulation leading to a weakened checkpoint is extremely rare (e.g. mosaic variegated syndrome), especially in human tumors (Haruki et al., 2001). In fact, the over-activation of the SAC is more likely to cause of aneuploidy in tumors.

Accordingly, a study extrapolated a 70 gene-expression signature corresponding to aneuploid human tumors, in which most SAC genes were up-regulated (Carter et al., 2006). Furthermore, the commonly lost tumor suppressors Rb and p53 are critical negative regulators of the SAC, also leading to SAC component up-regulation (Schvartzman et al., 2011). These studies can be misleading since it is possible that equal up-regulation of the SAC components due to high proliferation or mutations does not affect SAC functionality. It would be interesting to analyze the SAC stoichiometry and confirm that it is unbalanced and hyper-activated in human tumors. Nevertheless, it appears that aneuploidy as a result of SAC over-activation is relevant for the human disease. Studies with Mad2, Hec1 or Bub1 over-expression have shown that hyper-activation of the SAC induces CIN, which is sufficient for tumor initiation (Diaz-Rodriguez et al., 2008; Ricke et al., 2011; Sotillo et al., 2007). Moreover, upon the de-induction of the Mad2 transgene, the tumor persisted, indicating that Mad2 was not required for tumor maintenance. Mad2 over-expression leads to SAC hyper-activation and CIN (Sotillo et al., 2007). It is important to consider that phenotypes can be obtained by SAC-independent functions of the subject proteins. For instance, in addition to its effect on the SAC, Mad2 leads to Aurora B mis-localization and impairs the correction of merotelic attachments, leading to lagging chromosomes (Kabeche and Compton, 2012). These data shows that the over-activation of SAC induces aneuploidy and tumorigenesis.

1.8.4 Mouse model combinations

The effect of CIN and aneuploidy on tumorigenesis was further investigated through the combination of CIN and tumor-prone mouse models. The cumulative outcome was that CIN could both promote and impair tumorigenesis. Mad2 over-expression enhanced Myc-induced lymphomagenesis (Sotillo et al., 2007). Furthermore, Kras-induced lung tumorigenesis increased relapse incidence after oncogene withdrawal when Mad2 was over-expressed during primary tumorigenesis (Sotillo et al., 2010). CENP-E heterozygosity impaired tumorigenesis in two different systems: carcinogen-induced tumors together with tumor-suppressor knockout (Weaver et al., 2007). Moreover, BubR1 deficiency favored colon tumorigenesis, but inhibited intestinal tumors (Rao et al., 2005). Furthermore, Bub1 haplo-insufficiency, in the context of tumor-suppressor partial inactivation, had surprising outcomes. It accelerated tumorigenesis on two occasions (p53, APCmin) and inhibited tumor development once

(Pten) (Baker et al., 2009). A simple explanation for the tumor-promoting effect in the context of tumor-suppressor heterozygosity is that CIN promotes the loss of the remaining wild-type allele. Actually, Bub1 insufficiency promotes p53 loss of heterozygosity and the gain of the mutant allele (Baker et al., 2009). Nevertheless, it remains unclear how CIN inhibits tumorigenesis in tumor-prone models with impaired tumor-suppressor function. A recent study has revealed that the effect of CIN on tumorigenesis depends on the rate of chromosome mis-segregation (Silk et al., 2013). Tumor suppressors (*e.g* p53) are responsible for the elimination of aneuploid cells (Li et al., 2010). It is, therefore, possible that tumor-suppressor inactivation may increase the mis-segregation rate, shifting the balance towards tumor cell death. This hypothesis is tested in the present thesis.

1.9 AIM

Lung cancer is the leading cause of cancer-related death. The lung tissue is particularly sensitive to aneuploidy, and lung tumors develop in many spontaneous mouse models of tumorigenesis with impaired SAC. It is known that aneuploidy can promote and inhibit tumorigenesis, though the decisive factors shifting the balance remain unclear. CIN can promote tumorigenesis by inducing tumor suppressor loss of heterozygosity; however, how CIN inhibits tumorigenesis remains unclear. Two points will be addressed in this thesis:

- Weather Mad2 over-expression leads to p53 loss of heterozygosity in a model of lung cancer?

- How aneuploidy inhibits lung tumorigenesis in lung cancer mouse models?

2. MATERIALS AND METHODS

2.1 MOUSE MODELS

All transgenic mice were maintained in a mixed background (129-C57Bl/6-FvB) and were generated previously: TetO-HAMad2 (Sotillo et al., 2007), TetO-Kras^{G12D} (Fisher et al., 2001), TetO-EGFR^{L858R} (Politi et al., 2006) and p53KO (Jacks et al., 1994). Mice were kept in pathogen-free housing at EMBL Mouse Biology Unit, Monterotondo, in accordance with the Italian legislative decree on animal experiments Nr. 116/92 and approved by the Italian Ministry of Health (Decree nr. 233/2011-B). Mice were monitored on a regular basis and sick animals were sacrificed humanely in accordance with the guidelines for Humane End Point for animal used in biomedical research. Animals were kept on 12h light, 12h night cycle with constant temperature (21 degrees Celsius) and humidity (55%). Animals were weaned at 3 weeks and house grouped with a maximum of five per cage with pellet food and water *ad libitium*. The Doxycycline was impregnated in the food pellet (625 mg/kg; Harlan-Teklan) and the experimental mice were switched to a doxycycline-enriched diet at 4 weeks. BrdU was dissolved in the drinking water (1g/L, Sigma), protected from light and was given to the mice for 48h or 24h.

For genotyping, DNA was extracted by incubating the tail with 200 μl 0.05M NaOH at 98°C degrees for 40 minutes and neutralized with 20μl 1M Tris HCL, pH 7.5. PCR reactions were used for transgene detection using 1μl of the supernatant coming from the tail digestion. The primers used for genotyping are indicated in table 2.1 and the PCR condition in table 2.2. PCR products were run on 1.5% agarose gel with ethidium bromide (Sigma), except for p53 with 2% agarose.

Step	Temperature (°C)	Time (min)	Cycles
Denaturation	95	05:00	1X
Denaturation	94	00:30	28X
Annealing	60	01:00	
Elongation	72	01:30	
Elongation	72	05:00	1X
Hold	10	for ever	NA

Table 1:PCR program p53 genotyping

Step	Temperature (°C)	Time (min)	Cycles
Denaturation	95	05:00	1X
Denaturation	94	00:30	29X
Annealing	60	00:30	
Elongation	72	00:30	
Elongation	72	01:00	1X
Hold	10	for ever	NA

Table2: PCR program for other genotypes

Genotypes	Forward	Reverse
CCSP-rtTA	AAGGTTTAACAACCCGTAAACTCG	GTGCATATAACGCGTTCTCTAGTG
TetO-Kras	GGGAATAAGTGTGATTTGCCT	GCCTGCGACGGCGGCATCTGC
TetO-Mad2	CCATCCACGCTGTTTTGACCTC	GGCTTTCTGGGACTTTTCTCTACG
p53	commun/ ATAGGTCGGCGGTTCAT	WT/ CCCGAGTATCTGGAAGACAG
		Mutant/ CCTCGTGCTTTACGGTATCGC
CMV-rtTA	GTGAAGTGGGTCCGCGTACAG	GTACTCGTCAATTCCAAGGGCATCG
TetO-EGFR	ACTGTCCAGCCCACCTGTGT	GCCTGCGACGGCGGCATCTGC

Table 3: Genotyping primers

2.2 HISTOLOGY

2.2.1 NECROPSY

Mice were euthanized by CO_2 suffocation and were perfused with PBS in the left ventricle of the heart and the liquid evacuated from the sectioned inferior vena cava. In order to further clean the lungs, tracheal PBS perfusion was performed. For DNA and RNA, tumor and lung samples were snap frozen in liquid nitrogen and conserved at -80°C. For immunofluorescence, healthy lung samples were embedded in O.C.T. compound (Tissue-Tek), and conserved at -80°C. For immunohistochemistry, lungs were fixed in 10% neutral buffered formalin solution over-night at room temperature. After PBS washing the sample were dehydrated in Leica ASP300S and embedded in paraffin. For both Cryo (Cryostat CM3050S, Lieca) and paraffin tissues (RM 1235 microtome, Leica), the 8μm sections were put on Super-frost Glass slides (Thermo scientific).

2.2.2 HEMATOXYLIN AND EOSIN (H&E)

The paraffin tissue sections were de-paraffinized as follow: two times incubation with Xylene for 15 minutes, three time with 100% ethanol for 3 minutes, 3 minutes in 96% ethanol, 3 minutes in 70% ethanol, two time washes in water for 5 minutes. For H&E staining, the sections were incubated for 1 minute with hematoxylin QS (Vector) and washed in water. The tissue was counter stained with eosin 1% (Bio optic) and washed. The section were dehydrated as follow: 3 minutes in 70% ethanol, 3 minutes in 96% ethanol, two times 3 minutes is 100% ethanol, two times 15 minutes in xylene. DPX mounting media was used (VWR #360294H). Leica LMD 7000 mounted with the Leica CD310 digital camera and the Leica LASV3.7 software were used to acquire images.

2.2.3 Immunohistochemistry on parafin sections.

Sample hydration was done as for H&E. Sections were subjected to antigen retrieval by steamed treatment for 30 min in 0.09% (v/v) antigen unmasking solution (Vector Lab). After cooling, endogenous peroxidases were inactivated by incubation is 3% H_2O_2 for 15 minutes. After two PBS washes of 5 minutes each, sections were blocked with 10% serum in PBS for 30 minutes (serum specie depend on the primary antibody, Vectastain ABC rat or rabbit kit, Vector laboratory). Primary antibodies were diluted in the previous blocking solution and incubated for 2 hours at room temperature. Primary antibodies included: anti-HA (1:200 dilution, #11867423001 Roche), anti-Prosurfactant Protein C (proSP-C, 1:400 dilution, #AB3786 Millipore), anti-Ki67 (1:500 dilution, # VP-K451, Vector laboratories), anti-BrdU (1:200, #ab6326, Abcam). After two PBS washes of 5 minutes each, sections were incubated for one hour with the appropriate Biotinylated secondary antibody diluted in blocking solution (Vectastain ABC rat or rabbit kit). Sections were washed twice 5 minutes with PBS and incubated with HRP conjugated antibody for 30 minutes and washed. Staining was reveled by peroxidase reaction using the DAB peroxidase substrate kit (Vector) and stopped when the stain comes visible, less than 2 minutes. After wash in water the section were counterstained with Hematoxylin for 10 seconds, de-hydrated, mounted and imaged as for H&E.

Whole mount Senescence staining was done using Senescence β galactosidase staining Kit (#9860 Cell signaling). TUNEL assay was performed by Joana Passos using ApopTag® (#S7100, Millipore) and p21 staining was performed at the histology facility of the CNIO (Madrid, Spain). Aneuploidy was quantified by measuring nuclear volumes in tissues as described previously (Perez de Castro et al., 2013). Briefly, area of nuclei were measured using ImageJ, the radius was determined and the volume was calculated using the following sphere formula: $4/3*\pi*r3$.

2.2.3 Immunofluorescence on cryo-section

Cryo-section was chosen for immunofluorescence (IF) of healthy lung because the paraffin section together with the lung auto-fluorescence gave to much background for the detection of specific fluorescence. Cryo-samples are stored at -80°C and were left for 20 minutes to equilibrate to -20°C before cutting. After cutting sections were left for one hour at room temperature to dry and attach to the slides. Sections were briefly fixed with paraformaldehyde to avoid background (4%, 4 minutes) and incubated 30 min with

2M HCL at 37°C for 30 minutes for antigen retrieval. The section were washed three times 10 minutes in PBS and blocked for 1 hour with 5% goat serum in PBS (Jackson ImmunoResearch). Sections were incubated with primary antibodies in the previous blocking solution at 4°C over-night. Primary antibodies included: anti-Prosurfactant Protein C (proSP-C, 1:400 dilution, #AB3786 Millipore), anti-BrdU (1:100, #ab6326, Abcam). The next day the sections were washed three times 10 minutes and incubated with the conjugated secondary antibodies in blocking solution for one hour. Secondary antibodies were: Alexa 647 goat anti rat IgG, Alexa 488 goat anti rabbit IgG (1:1000 dilution, # A21247, #A11034, Invitrogen). Sections were washed 3 times with PBS for 10 minutes and the last wash included DAPI for nuclei counter staining. Leica TCS SP5 confocal microscope was use to acquire and ImageJ to analyze the images.

2.3 Lung FACS

After animals were sacrificed, tracheal PBS was used to clean the lungs. Auxiliary lymph nodes were dissected and single cell solution was obtained by mechanic dissociation and the use of 40μm filters. To make single lung cells suspension, 2ml of dispase (Roche) followed by 2ml of liquid low melting agarose (Promega) was delivered to the lungs *via* the trachea. After the agarose solidified the lungs were taken and further incubated in 2ml of dispase and incubated for 45 minutes under agitation. Auxiliary lymph nodes were dissected. To terminate the digestion DMEM (Life Technology) media was added and contained DNase I (5mg/ml Sigma, #D4527), to prevent the clamping of dead cells. The lung was mechanically dislocated and passed trough 70μm and 40μm nylon filters (Falcon). Red blood cells were eliminated by incubated with red blood cell lysis buffer (Sigma, #R7757) for 1 minute. The antibodies solutions were prepared according to the cell count.

For cell death staining, the lung single cell suspension was washed with the apoptosis-staining buffer, incubated for 30 min in the dark with annexin V at RT and before analysis the live cell die Cytoxblue was added (Annexin apoptosis Detection kit FITC, eBioscience). For inflammation staining in the lung and in the lymph nodes, single cell suspensions were blocked with CD16/32 block (clone 93 eBioscience). T cells were excluded using their positivity for CD8 and CD4 (CD8-alexafluor 488 clone 53-6.7 bd Farmigene, CD4-PE clone L3T4 eBioscience). B cells were eliminated using the marker B220 (B220-PE clone RA3-6B2 eBiosceince). Macrophage were further

identified based on CD11b high expression (Cd11b-APC clone M1/870, eBioscience) and activation was monitor with the CD54 marker (CD54 FITC clone yN1/.7.4 Biolegend). For this procedure all the antibodies were added (1/50 dilution) in the same time and incubated for 10 minutes at RT, washed and cells were analyzed. PBS supplemented with 2% FBS was used for washes.

2.3 Cell culture

2.3.1 Mouse embryonic fibroblasts: MEFs

Mouse embryonic fibroblast (MEFs) was obtained from embryos of 12.5 after conception. The day of conception was known by the appearance of a white plug at the entry of the mouse genitals and the male was removed from the cage. Later, 12.5 days, the mouse was examined for pregnancy and in the positive case it was euthanized and the embryos dissected out. The visible liver or the embryo was mechanically removed and the head taken for genotyping. The body was incubated over night in 0.5 ml of 0.05% trypsin (Life technology) at 4°C for digestion. During incubation the heads were digested and genotyped as it is done for the tails (section 2.1). The next day, the selected embryos were further mechanically dissociated and the cell suspension was plated in 150 cm dish, with DMEM medium. The DMEM media was complemented with 10% Tet-free serum (FBS, Clontech Cat#631106), L-Glutamine for a final concentration of 2mM (Life technology) and Penicillin/Streptomycin for a final concentration of 100U/mL (Life technology). When the plate was confluent (about 3 days), the MEFs were divided in 4 vials and frozen. Freezing media consisted of 90% serum and 10% DMSO (Sigma). For cell growth and immortalization experiments, MEFs vials were thawed and platted in two 10cm dish. After 3 days the MEFs have expanded and can be distributed in different plates for experiments. After being collected 20μl of MEFs suspension was inserted in cell counting chamber and counted automatically (Cellometer). For immortalization, one million MEFs was platted per dish with or with out doxycycline (1mg/ml), twice a week they were counted and one million was re-plated until the end of the experiment. After platting the cells pellet was frozen for further analysis. For cell growth, 70.000 MEFs were plated in each well of a 6 well plate and one well was counted everyday, after counting the cells were frozen for protein samples.

2.3.1 TIME LAPSE IMAGING

In order to visualize the DNA with the time-lapse recording, and because primary MEFs do not get transfected, they were transduced with H2B-GFP (Yamamoto et al., 2004). The construct containing H2B-GFP was a kind gift from Rocio Sotillo and amplified by bacterial transformation.

Frozen competent cells were thawed on ice for 20 minutes and were incubated with 1μl of the given preparation for 20 minutes on ice. The mixture was put at 42ºC for 1 minute for heat shock and cells were allowed to recover for 2 minutes on ice. 500μl of LB media was added and the mixture placed at 37ºC for one hour allowing the bacteria to grow. 50μl was platted on a 10cm LB agar ampicillin plate and incubated at 37ºC over night. The day after, the transformed clone were further gown until enough bacteria were collected for maxi-prep, which was done using Qiagen Plasmid Maxi Kit. Transformed bacteria were also frozen for LB-ampicillin inoculation when more plasmid was needed.

For the production of retrovirus containing H2B-GFP (Yamamoto et al., 2004), I used the Phoenix retrovirus packaging cell line. The phoenix cells were transfected with the H2B-GFP constructs using the calcium phosphate method (ProFection Kit, Promega). In brief 15ng of construct was first mixed with calcium 62μl 2M $CaCl_2$ and sterile, deionized water for a total of 500μl. The mixture was slowly added to tube containing 500μl 2X HBS upon agitation. The combined solution was left at room temperature for 30 minutes and done in duplicate. The two mixtures were delivered drop wise onto two plates of 70% confluent Phoenix cells in normal DMEM media. After over-night incubation the media was replaced and Phoenix cells were transduced as seen by their Green fluorescence. Phoenix cells were producing retrovirus-containing H2B-GFP found in the media.

As soon as MEFs vials were platted in two 10cm dish, they were incubated with the Phoenix filtered media (0.45 μM, Millex HA), which contains the H2B-GFP virus. In order to enhance the virus infection efficiency, Polybrene (Final concentration 4μg/ml, Sigma) was added to the media. MEFs were repetitively infected, twice a day for 4 days. The transduction efficiency remaining low the MEFs were sorted for green fluorescence and directly platted in a 35mm high μ-plate (Ibidi). MEFs were left to

recover and attach to the plate for 5 hours. In order to synchronize their entry in mitosis they were serum starved (0.1% serum) for 72h. When the cells were released by adding media with 10% serum, the Doxycycline (1mg/ml) was also included to induce transgene expression. Release and Dox induction occurred 20h prior to imaging. To observe cell death TO-PRO-3 iodide (1:1000 dilution, #T3605, Molecular Probes) was added to the media just before the imaging started. Imaging was recorded on an inverted spinning disk confocal (Perkin Elmer Ultraview-Vox): 3μm stack across 27μm, 10 minutes frames during 48 hours. Volocity version 6.2 (Improvision-Perkin Elmer) was used for image acquisition and analysis.

2.4 Molecular methods

2.4.1 PCR and real time PCR

DNA and mRNA were isolated from flash frozen nodules and from MEFs using the DNA/RNA Micro kit (Qiagen) and the pestle ruptor method was chosen to disrupt the tissues. For p53 PCR, 150ng of genomic DNA was used and the primers were the same as the one used for genotyping (see section 2.1). Band intensities were measured using the Chemidoc XRS+ with image lab software (Biorad).

RNA from the extractions was measured using a Nanodrop (Thermo Scientific), 0.2 to 0.5 μg of RNA was reversed transcribed into cDNA using Superscript III RT kit (Invitrogen). Quantitative PCR was done using LightCycler 480 SYBR Green I Master and Light Cycler 480 (Roche). The reaction program is indicated in table 2.4 and primers in table 2.5. The fold changes in gene expression were calculated using the ΔΔCt method. Reactions were run in triplicate, the fold changes were calculated using two references genes and normalized to reference sample.

Step	Temperature (°C)	Time (s)	Cycles
Denaturation	95	300	1X
Denaturation	95	10	45X
Annealing	60	15	
Elongation	72	10	
Denaturation	95	5	1X
Annealing	65	60	1X
Denaturation	95	N/A	Continuous
Cooling	40	10	1X

Table 2.4: Real time PCR program.

Genes	Forward	Reverse
LC37	TCTGTGGCAAGACCAAGATG	GACAGCAGGGCTTCTACTGG
PPIa	CGCGTCTCCTTCGAGCTGTTTG	CGCGTCTCCTTCGAGCTGTTTG
HA-Mad2	GGCTTACCCATACGATGTTCC	CGACGGATAAATGCCACG
Bax	TGGAGCTGCAGAGGATGATTG	TGGGATGCCTTTGTGGAACT
p21	CAGATCCACAGCGATATCCA	GGCACACTTTGCTCCTGTG
PUMA	GCGGCGGAGACAAGAAGA	AGTCCCATGAAGAGATTGTACATGAC
GADD45	ATTACGGTCGGCGTGTACGA	CAGCAGGCACAGTACCACGTTA
Mdm2	AGCAGCGAGTCCACAGAGA	ATCCTGATCCAGGCAATCAC

Table 2.5: Real time PCR primers sequences.

2.4.2 Western blot

Protein were obtained using RIPA buffer complemented with PMSF and complete mini protease inhibitor cocktails (Roche), half tablet for 12.5ml. Cell pellet were incubated for 10 minutes on ice and spin at the maximum speed for 10 minutes. Supernatant was collected and protein was measured using the Bradford method (Biorad protein Assay). Before leading the protein were denatured at 98°C for 2 minutes. Preparation of 12% SDS-PAGE and the stacking gel was done using a Biorad system. Isopropanol was used to ensure a strait 12% gel and removed before pouring of the stacking gel. The composition of the 12% gel was as followed: 12% acrylamide, 0.1 M Tris (pH 8,8), 0.01% ammonium persulfate, and TEMED was added for fast polymerization. The composition of the stacking gel was as followed: 5% acrylamide, 0.1 M Tris (pH 6,8), 0.01% ammonium persulfate, and TEMED was added for fast polymerization. After leading the samples and the molecular weight marker (Kaleidoscope, Biorad) the gels were submerged with running buffer and run at 100V for 1h30. The composition of Tris-Glycine running buffer was as followed: 25mM Tris, 250 mM Glycine, and 0.1% SDS. For transfer, the nitrocellulose membranes were submerged in methanol for 2 min, washed with water and transfer buffer. Filters, the papers, and the pads were submerged in transfer buffer. All the components were mounted for wet transfer and submerged with transfer buffer, and run at 40V over-night at 4°C. The composition of transfer buffer was as followed: 48 mM Tris, 39 mM Glycine, 0.037% SDS, and 20% methanol. After transfer, blots were blocked for 1hour with 1% Bovine Serum Albumin (Sigma). Blots were probed with antibodies directed against, p44/42 MAP Kinase (Cell Signaling technology), HA (#H9658, Sigma), Kras (F234, SC-30, Santa-Cruz), Mad2 (BD Transduction Laboratories), and Actin (#A2066,

Sigma). HRP conjugated anti-mouse or rabbit were used as secondary antibodies and proteins were visualized and quantified using Chemidoc XRS+ with image lab software (Biorad).

2.5 Statistics

Student *t* test, F analysis or log-rank tests were performed using Graph Pad Prism 5 and error bars represent mean ± SEM. Statistical significance was concluded at $p < 0.05$. Samples images were quantified using ImageJ (National Institutes of Health, Bethesda, Maryland).

3. Results

3.1 In vivo characterisation of the p53(+/–)K and p53(+/–)KM cohorts

3.1.1 Over-expression of Mad2 delays Kras induced lung tumors with impaired p53

It has previously been reported that Mad2 over-expression accelerates Kras induced lung tumorigenesis by inducing chromosome instability (Sotillo et al., 2010). Current knowledge supports a model where tumor suppressor inactivation may lead to Mad2 over-expression that results in CIN and aneuploidy, which in turn may contribute to tumor progression. However, it remains unclear to what extent CIN can contribute to tumorigenesis since some tissues are more prone to tumor formation than others, pointing out the importance of the cellular context and genetic landscape in mice (Sotillo et al., 2007). p53 impairment is found in a majority of lung tumors and importantly it is a critical regulator of aneuploidy (Schvartzman et al., 2011; Thompson and Compton, 2010). My supervisor, Dr. Rocio Sotillo and I, hypothesized that Mad2 over-expression would affect $Kras^{G12D}$ induced tumorigenesis -either further acceleration or via inhibition- when a copy of p53 is inactivated.

To test this hypothesis, I monitored mice overexpressing tetracycline inducible Mad2 (M) and $Kras^{G12D}$ (K) in a p53(+/–) background. The control cohort of p53(+/–)K mice died of lung tumors with a median latency of 33 weeks and the over-expression of Mad2 led to an significant increased lifespan of around 13 weeks (46 weeks; Figure 3.1).

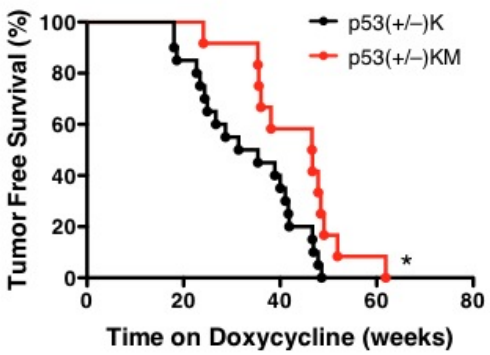

Figure 3.1: Mad2 over-expression delays p53(+/–)Kras driven lung tumorigenesis. Mice were feed doxycycline-impregnated food from 4 weeks of age and monitored for lung tumors. Tumor free survival of p53(+/–)Kras (black, median survival: 33.4 weeks, n=20) and p53(+/–)Kras Mad2 mice (red, median survival: 46.65 weeks, n=12; Mantel-cox test $^{*}p<0.05$).

3.1.2 KINETICS OF TUMORIGENESIS

Upon observation of the Mad2 inflicted delay on Kras driven lung tumorgenesis in the p53(+/–) background, I set out to determine the window in which Mad2 was exerting it's influence. As in the absence of MRI qualifying mice as humane end point can be challenging with mouse models of lung cancer, I used an alternative approach that was originally utilized for the initial characterization of this Kras mouse models (Fisher et al., 2001). I analyzed the kinetics of tumorigenenes by histology, selecting different time points of doxycycline induction, and I calculated the percentage of tissue occupied by tumors.

There was noticeably little tumor development during the first 10 weeks of doxycycline induced transgenes expression (Figure 3.2 A and B). At a later time point between 10 and 20 weeks - I observed that the tumors in the p53(+/–)KM lungs were occupying a significantly smaller surface than in the p53(+/–)K lungs (5.67% *Vs*. 45.61%, Figure 3.2 A and B). However, this difference diminished at longer induction times, from more that 20 weeks induction to humane end point (31.42% *Vs*. 51.68%, Figure 3.2 A and B). This is probably due the fact that in the control cohort (p53(+/–)K), the lungs were soon saturated with tumors, with at 10-20 weeks time point the tumors occupied close to half of the lungs. The >20 weeks time point did not show significant increases beyond the 10-20 week time point for this cohort (Figure 3.2 A and B). Fifty percent of tumor in the lung is probably the maximum tolerated by the mice before they classify as humane end point. The cohort over-expressing Mad2 had only 5.67% of tumors at the 10 to 20 weeks time point, and as the lungs were not yet saturated with tumors, it was possible to observe the their growth. At the >20 weeks time point, the tumors were occupying 31.42% of the lungs in the p53(+/–)KM cohort. I observed that the lungs over-expressing Mad2 initially have an impaired tumorigenesis however, the tumors eventually developed to occupy a significant portion of the lungs, albeit with slower kinetics (10-20weeks: 5.67%, >20 weeks: 31.42%, $p<0.05$, Figure 3.2 B), suggesting a compensation mechanism for Mad2 over-expression.

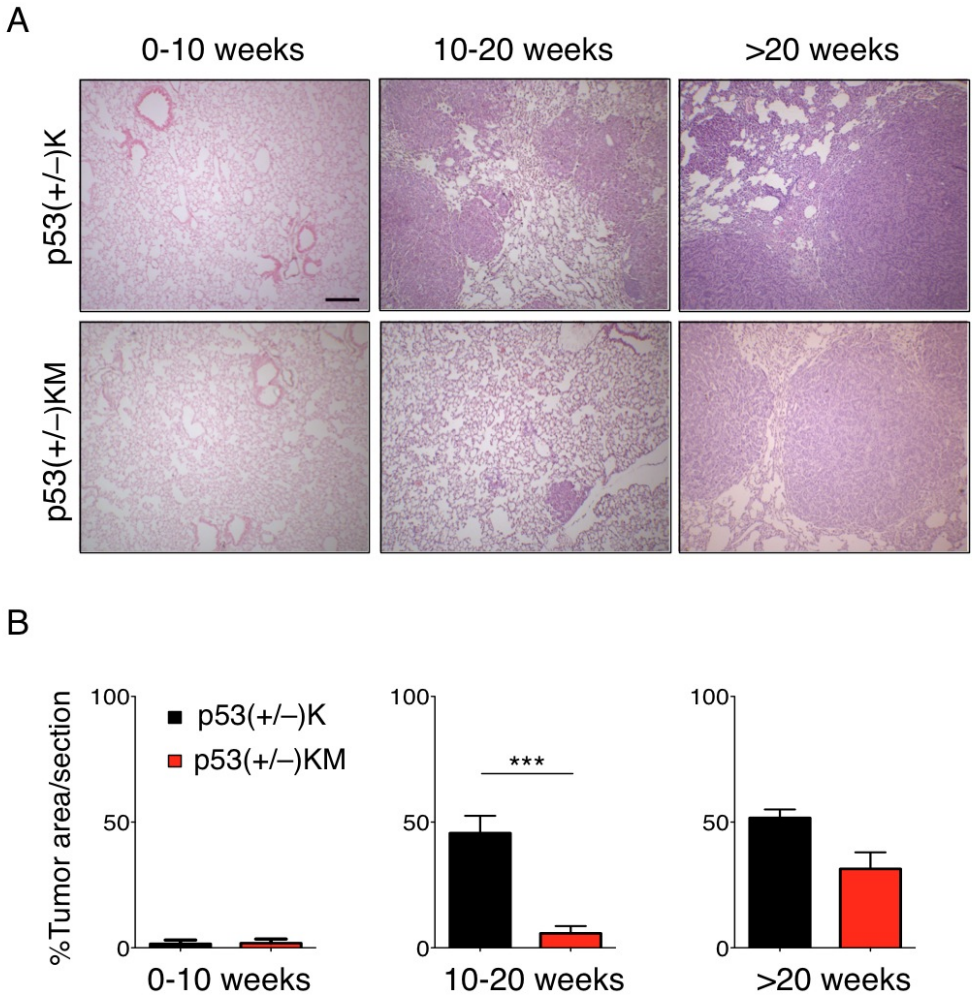

Figure 3.2: Kinetics of tumorigenesis in the p53(+/–)Kras and p53(+/–)Kras Mad2 cohorts. **A)** H&E staining at 0-10 weeks, 10-20 weeks and >20 weeks after transgenes induction. Scale bar 200µm. **B**) Percentage of tumor area per lung section indicating a maximum delay in tumorigenesis between 10 and 20 weeks. Time point 0-10 weeks; p53(+/–)K= 1.47% n= 7 mice, p53(+/–)KM= 1.83% n= 9 mice. Time point 10-20 weeks; p53(+/–)K= 45.61% n= 6 mice, p53(+/–)KM= 5.76% n= 6 mice, unpaired *t*-test ***p<0.001. Time point >20 weeks; p53(+/–)K= 51.68% n= 7 mice, p53(+/–)KM= 31.42% n= 17 mice.

3.2 Early effect of Mad2 over-expression, prior tumorigenesis

3.2.1 Mad2 over-expression inhibits the proliferation of type 2 pneumocytes prior to tumorigenesis

The observation that lung tumors arise in the p53(+/–)K and in the p53(+/–)KM mice cohorts at different times (Figure 3.1 and 3.2), suggested that over-expression of Mad2 may have an inhibitory effect on p53(+/–)Kras-induced tumor initiation. The lung is a

very slowly proliferating tissue, therefore it is challenging to monitor it is physiological turnover: proliferation and cell death. To address the negative effect of Mad2 over-expression on cell proliferation on pseudo-healthy lung, the mice were feed doxycycline for 4 days and pulsed with BrdU (a nucleotide analogue) in the drinking water for 48hours. When new DNA is synthetized the BrdU is faulty incorporated; this method allows the cumulative labeling of cells that have entered S phase. First, Mad2 expression at this early time point was confirmed by immunohistochemistry against the HA tag in the p53(+/–)KM samples (Figure 3.3 A). Importantly, samples with no trans-activator did not show positive staining for HA-Mad2 confirming the tight control of transgenes induction. In a first step, I calculated the ratio of BrdU positive area per nuclei area (Magenta/DAPI). Since both marker are nuclear, the number reflects the percentage of BrdU positive cells per total lung cells and I observed a non-significant increase in the p53(+/–)K lungs (data not shown). The transgenic system induces the expression of the transgenes specifically in the type 2 pneumocytes (TIIPN). The TIIPN secrete pulmonary surfactant and can be visualized using the Surfactant protein C (SpC) as a marker. In a second step, I counted the percentage double positive cells (SpC and BrdU) from the total BrdU positive cells. Finally, I calculated the percentage of double positive cells per total lung cells using the BrdU values for conversion. As an example, if 5% of the total lung cells are BrdU positive and only 10% of the BrdU nuclei are also SpC, then 0.5% of the total cells are double positive cells (SpC and BrdU).

In the lung physiological lung (mice lacking the transactivator rtTA), I found very few proliferating TIIPN: 0.5% double positive cells (SpC and BrdU). The TIIPN proliferation was significantly increased in the p53(+/–)K lungs and upon Mad2 over-expression the percentage of proliferative TIIPN was significantly reduced: 1.9% *Vs*. 0.6% double positive cells (Figure 3.3 D and E). These results suggest a very early negative effect of Mad2 over-expression on the TIIPN, at this stage it is more likely due to an over-activation of the mitotic checkpoint rather than a decrease of cell fitness due to aneuploidy.

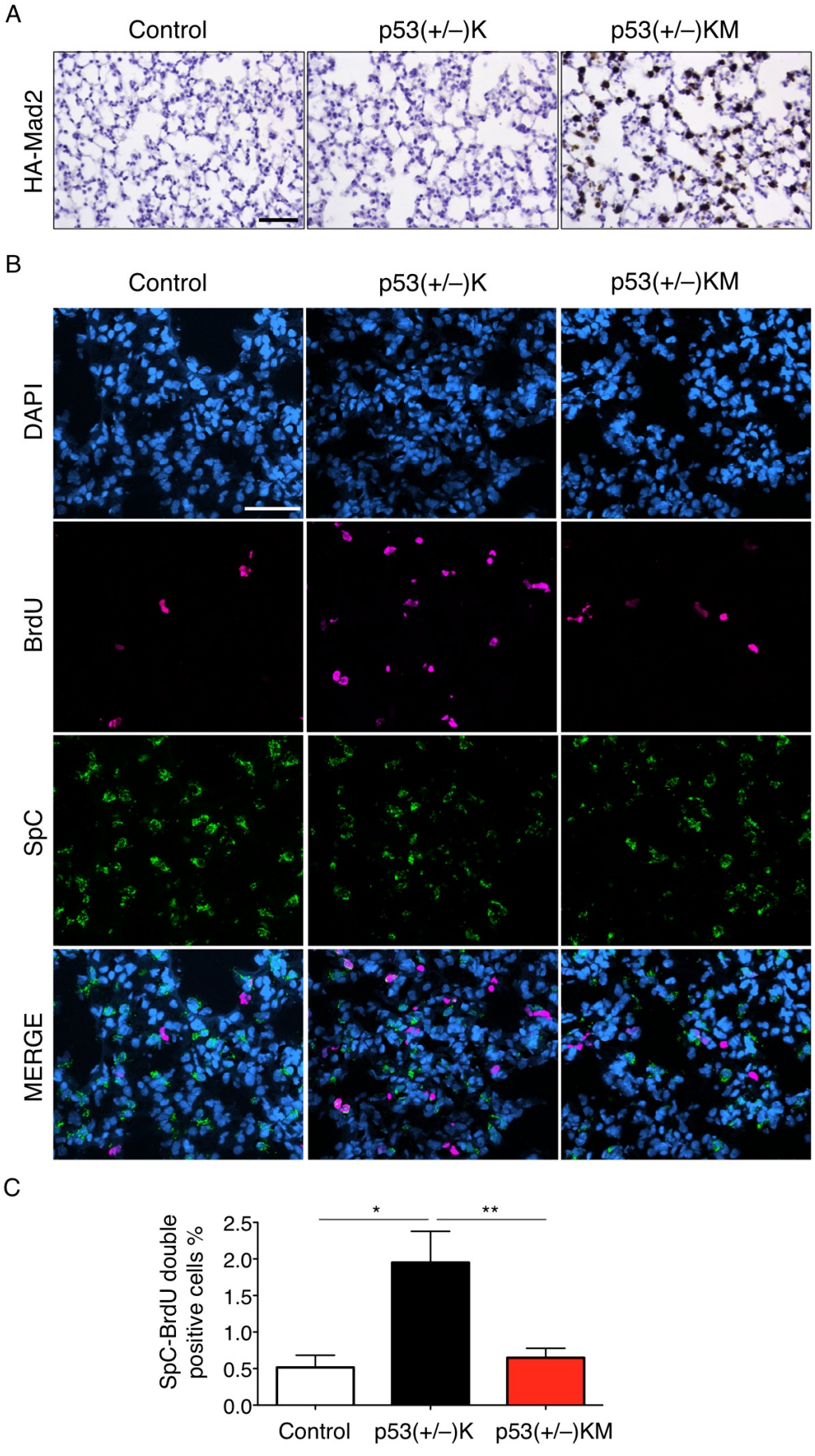
A
Control
p53(+/–)K
p53(+/–)KM
HA-Mad2
B
Control
p53(+/–)K
p53(+/–)KM
DAPI
BrdU
SpC
MERGE
C
SpC-BrdU double positive cells %
2.5
2.0
1.5
1.0
0.5
0.0
*
**
Control
p53(+/–)K
p53(+/–)KM

Figure 3.3: Mad2 over-expression inhibits type 2 pneumocytes proliferation. Mice were feed doxycycline-impregnated food at 4 weeks of age and scarified after 4 days including 2 days with BrdU provided in the drinking water. **A**) HA IHC of lung samples confirming the induction of HA-Mad2 exclusively in p53(+/–)KM samples. Control is a p53(+/–)KM lung without the rtTA. Scale bar 50 μm. **B**) IF staining on lung sections induced for 4 days and pulsed with BrdU for 48hours before sacrifice. Scale bar: 50μm. **C**) Quantification of double positive cells (BrdU, SpC). Mice that are lacking the trans-activator were used to measure the physiological lung proliferation (0.5% of proliferating TIIPN (0.5158 ± 0.1667 n=7 mice). This number was significantly increased in the p53(+/–)K lungs (1.951 ± 0.4266 n=9 mice, unpaired *t*-test, $^{*}p<0.05$). Upon Mad2 over-expression the percentage of proliferative TIIPN was significantly reduced to 0,6% (0.6476 ± 0.1302 n=13 mice, unpaired *t*-test, $^{**}p<0.01$).

3.2.2 CELL DEATH *IN VIVO*: LACK OF EVIDENCE

To test whether the inhibition of proliferation induced by Mad2 over-expression (Figure 3.3) is due to cell death, I analyzed TUNEL immunohistochemistry performed by Joana Passos (Lab Technician) at different time point of transgenes induction. After 4 days of induction, I could detect only sporadic positive cells. As the time point can be critical for *in vivo* observations, I also analyzed TUNEL at later stages of induction, which were also not conclusive (Figure 3.4 A), probably due to the rapid turn over apoptotic cells. Another possible limitation for the detection of apoptotic cells can be due to the small amount of tissue that can be quantified by immunohistochemistry.

In order to detect more apoptotic cells, I decided to analyze the entire lung by FACS (fluorescence activated cell sorting). After preparing a single cell suspension from the lung on doxycycline for 4 weeks, I excluded the macrophages and followed cell death using Annexin V staining combined with a live cell dye (Figure 3.4 B). It allows measuring live, early and late apoptosis as well as necrotic cells; in this experiment I did not observe an increase of cell death upon Mad2 over-expression (Figure 3.4 C). However, this method might lead to a type II error: the amount of dying cells generated by the procedure could mask small variations between the genotypes. Overall, I did not observe the induction of apoptosis upon Mad2 over-expression, however this might be due to the *in vivo* condition.

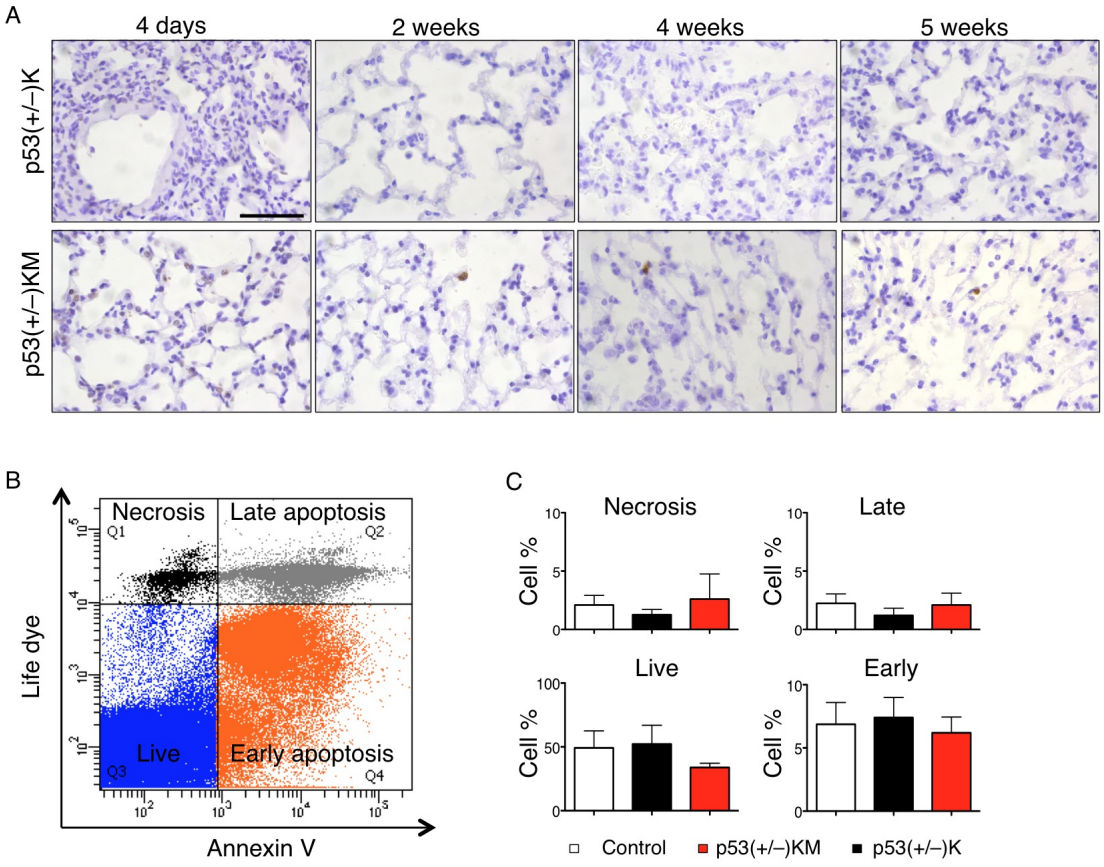

Figure 3.4: Cell death *in vivo*. A) TUNEL staining showing occasional dead cells at 4 days, 2, 4, 5 weeks time points. Scale bar 50 µm. **B)** Annexin V and cytoxblue staining showing live, early and late apoptotic cells, necrotic cells; from lung cell suspension depleted from its macrophages. **C)** Quantification of the different population (n=3 mice) showing no difference across the genotypes (n=3 mice), p53(+/–) mice were used as control.

3.2.3 Inflammation *in vivo*: lack of evidence

The detection of apoptotic cells is very challenging *in vivo*, to retain tissue homeostasis alveolar macrophages clear apoptotic and necrotic bodies. They are usually kept in a quiescent state in the lungs and can be classically or alternatively activated. The classic macrophages are the primary "killers" and induce inflammation, the alternative macrophages are involved in tissue repair and appear to promote tumor growth (Galdiero et al., 2013). Alveolar macrophages have been shown to transport pathogens to lymph nodes to trigger adaptive immunity, a feature that has been long consider exclusive to dendritic cells (Kirby et al., 2009). I hypothesized that if Mad2 would induce cell death *in vivo*, it could lead to the infiltration of macrophages in the lungs, their activation and possibly their migration to the axillary lymph nodes. After preparing a single cell

suspension from the lung, I isolated the macrophages (CD11b+, Figure 3.5 A) and followed their activation (CD54, Figure 3.5 B) by FACS.

Using wild-type mice, I observed a high number of Cd11b+ cells populating the lung compare to the axillary lymph nodes (Figure 3.5 C) and on the contrary, activated Cd11b+ cells were the most represented in the axillary lymph nodes (Figure 3.5 D). These results are in accordance with the physiological function of macrophages. I then performed the similar analysis on mice fed with doxycycline during 4 weeks (Figure 3.5 E-H) and I did not observe an effect of Mad2 over-expression on macrophage recruitment and activation in the lung or axillary lymph nodes. These results indicates that none of the induced transgenes leads to the infiltration or activation of the alveolar macrophages in p53(+/–) mice after 4 weeks of induction.

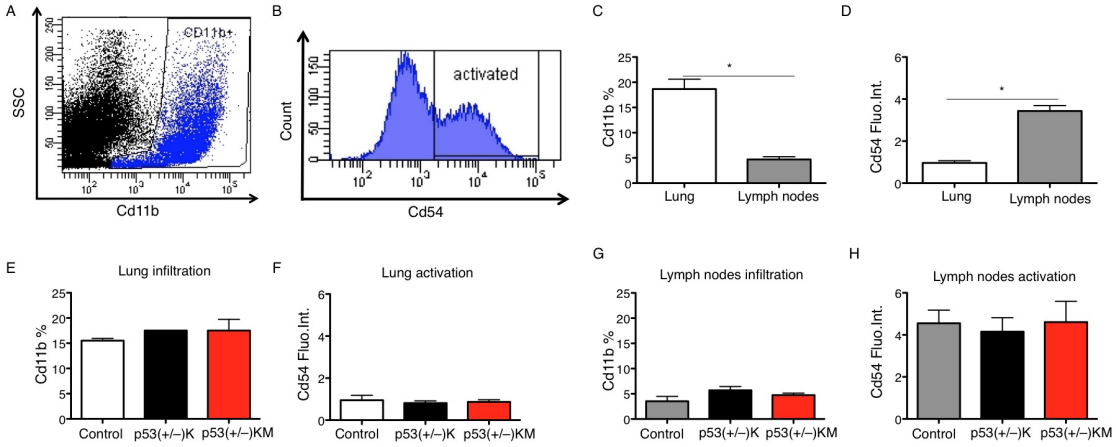

Figure 3.5: Inflammation. The B and T cells populations were excluded from the single cell suspension of lungs and lymph nodes. **A)** Macrophages population identified on the basis of the Cd11b expression and Side Scatter (SSC). **B)** Macrophages activation was followed on the basis of CD54 expression. **A.B)** Cd11b and Cd54 X-axis represent log fluorescence intensity. **C**) Percentages of Cd11b+ cells found in the lung and in the axillary lymph nodes in wild-type mice showing the abundance of macrophages in the lungs (n=3 mice paired *t*-test $^{*}p<0.05$). **D**) Macrophages activation in the lung and in the axillary lymph nodes in wild-type mice showing activated macrophages in the axillary lymph nodes (n=3 mice paired *t*-test $^{*}p<0.05$). **E-H)** Macrophages percentages and activation from control (p53(+/–)) and experimental mice showing no differences between the cohorts (n=3 mice except for **E**: n=1 mouse).

3.2.4 MAD2 OVER-EXPRESSION IMPAIRES CELLULAR GROWTH *IN VITRO*

As it is very challenging to study the consequences of Mad2 over-expression at the cellular level *in vivo*. I utilized an alternative *in vitro* approach and generated murine embryonic fibroblast (MEFs) isolated from day 12.5 mouse embryos. To induce transgenes expression in MEFs the ubiquitous CMV promoter controls the rtTA expression as described previously (Sotillo et al., 2007). I first tested the expression of the transgenes by western blot. At 24 hours post doxycycline induction there was no leakage in the transgenic system and the exogenous HA tagged Mad2 was produced in p53(+/–)KM cells (Figure 3.6 A). In order to test for activation of Kras signaling following doxycycline driven transgenes expression, I preformed a western blot for the downstream phospho-Erk, which I found elevated in both p53(+/–)KM and p53(+/–)K MEFs (Figure 3.6 A).

I assessed the MEFs growth rate by plating a fixed amount of cells and following their proliferation for 6 days. Oncogenic Ras can induce cell cycle arrest and senescence (Serrano et al., 1997), which would render the use of MEFs for the study of cancer properties futile. Importantly, the p53(+/–) clones over-expressing Kras were able to grow in culture indicating that MEFs could be used for further experiments (Figure 3.6 B). The detrimental effect of Mad2 on MEF growth has previously been reported in the p53 wild-type background (Sotillo et al., 2007), I obtained similar results (Figure 3.6 C) as well as in the context of Kras over-expression (Figure 3.6 D). Moreover, Mad2 over-expression impaired the MEFs growth with or without Kras over-expression in the p53 heterozygote background (Figure 3.6 E and F). These results indicate that Mad2 over-expression has a dominant detrimental effect on MEFs growth, independent of oncogene over-expression and partial tumor suppressor inactivation.

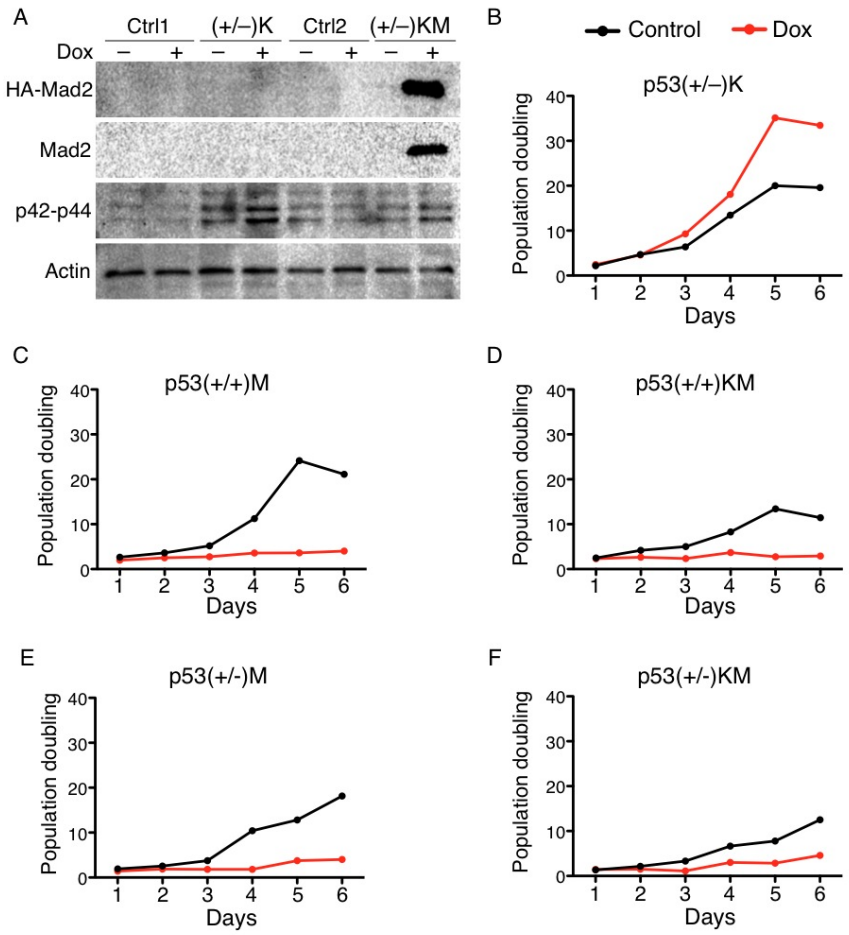

Figure 3.6: Mad2 over-expression impairs cellular growth *in vitro*. **A**) Western Blot from MEFs showing the specific expression of HA–Mad2 and the activation of the down-stream effector of Kras (p42-p44) after 24hours of doxycycline (Dox). Actin was used as loading control. Control 1; MEFs lacking the trans-activator, Control 2: MEFs lacking Kras and Mad2 transgenes. **B-F**) Representative MEFs growth curves showing the dominant detrimental effect of Mad2 over-expression. Control with out Dox in black and with Dox in red. 70000 cells were platted at day 0 and the cells were counted during the 6 following days. The Y axis shows the doubling population normalized to day 0. **B**) p53(+/–)K, **C**) p53(+/+)M, **D**) p53(+/+)MK, **E**) p53(+/–)M, **F**)p53(+/–)M.

3.2.5 Inactivating one copy of p53 rescues the mitotic death induced by Mad2 over-expression and generates polyploid MEFs

Mad2 over-expression confers a growth dis-advantage to MEFs over-expressing Kras in the p53 wild-type and p53 heterozygote background (Figure 3.6). However the effect of Mad2 over-expression on Kras induced lung tumorigenesis differs depending on the p53 background, with an acceleration in the wild-type background (Sotillo et al., 2010) and a delay when p53 is partially inactivated (Figure 3.1). It is then possible that

the preliminary detrimental effect of Mad2 is mediated by two distinct mechanisms that would have different effects during the long process of tumorigenesis. High Mad2 levels have been shown to induce aneuploidy and mitotic cell death when p53 is functional (Sotillo et al., 2007). In an attempt to understand the effect of Mad2 over-expression in the context of p53 heterozygosity, I used p53(+/+)KM, p53(+/–)K and p53(+/–)KM MEFs and time-lapse microscopy. To monitor the early effect of Mad2 over-expression on the first mitosis and to visualize the DNA, I infected the cells with a retrovirus expressing Histone 2B fused to the green fluorescent protein (H2B-GFP). Because of the low efficiency of primary cell transduction, I cell sorted the positive cells using the GFP reporter. After allowing them to recover for 5 hours, I serum-starved the cells for 3 days and released them 20 hours prior imaging allowing them to enter mitosis coincidentally with the beginning of imaging. Upon release doxycycline was added and the transgenes induced. I first verified by western blot the maintenance of the transgenes expression at 72 hours post doxycycline (the endpoint of the imaging). I observed that Kras was induced upon doxycycline treatment in all the chosen genotypes and as expected the exogenous Mad2 was overexpressed in p53(+/+) and p53(+/–)KM MEFs (Figure 3.7 A).

I followed the duration and the outcome of mitosis by imaging the cells for a total duration of 52 hours. Control p53(+/–)K MEFs underwent a rapid mitosis (51 min) with 87% of the cells giving rise to two daughter cells and 13% becoming tetraploid (Figure 3.7 B upper panel, C and D). Over-expression of Mad2 in combination with Kras -p53(+/+)KM- led to a dramatic increase in the time spent in mitosis (5h48min) while having just one copy of wild-type p53 reduced this time to 3h10min (Figure 3.7 B and C). As expected, over-expression of Mad2 in p53(+/–)K cells increased the number of tetraploid cells by 2.5 fold (13.1% *Vs*. 32.6%; Figure 3.7 D). In addition to the partial rescue of the mitotic timing, p53 heterozygosity almost completely rescued the mitotic cell death of p53(+/+)KM MEFs (2.8% *Vs*. 32.7% Figure 3.7 D). Moreover, I failed to detect cell death in interphase during the time of imaging. These results are consistent with the previous *in vivo* data, where the over-expression of Mad2 did not induce cell death in the p53(+/–) background at early time points of transgene induction.

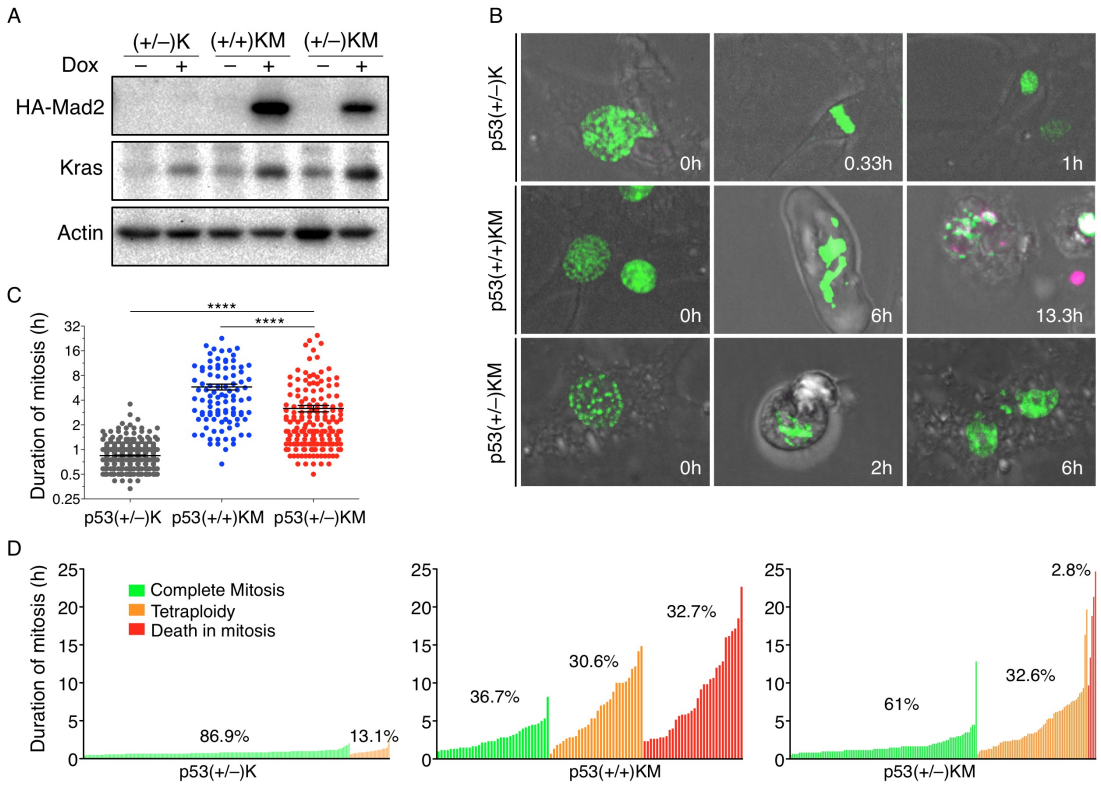

Figure 3.7: Mad2 over-expression induces aneuploidy in p53(+/–)Kras MEFs. **A**) Western Blot from MEFs showing the specific over-expression of HA–Mad2 and Kras after 72hours of doxycycline (Dox). Actin was used as loading control. **B**) Time-lapse microscopy of MEFs showing the course of mitosis between 24 hours and 72hours after induction. Upper: p53(+/–)K cell entering mitosis at T=0 min and completing cytokinesis by 1hour. Middle: representative p53(+/+)KM cell arrested in mitosis for more than 6hrs and dying in mitosis indicated by the To-PRO staining (magenta). Lower: p53(+/–)KM cell completes mitosis after 6 hrs. **C**) Duration of mitosis, Y axis log2 scale. Control p53(+/–)K MEFs completed mitosis in 50 minutes (0.8451 ± 0.01150 hours, n=624 mitosis); p53(+/+)KM MEFs ended mitosis in an average time of 5.8 hours (5.799 ± 0.4717, n=98 mitosis) and in p53(+/–)KM cells mitosis was completed in an average time of 3.2 hours (3.165 ± 0.2810 n=177 mitosis). P53(+/–)KM mitosis was longer than p53(+/–)K and shorter than p53(+/+)KM mitosis (unpaired *t*-test ****p<0.0001). **D**) Single cell analysis of the out come of mitosis showing an increased percentage of p53(+/+)KM cells dying compared to p53(+/–)KM and showing an increase of cells becoming tetraploid in the p53(+/–)KM compare to p53(+/–)K.

It was surprising to find that the removal of only one copy of p53 was sufficient for rescuing the mitotic death induced by Mad2 over-expression. I next hypothesized that, in this settings, the p53(+/–) cells were similar to the true p53 Knock out (KO) and performed the experiment using p53(–/–)KM clones. The effect of Mad2 over-expression together with Kras in the p53 complete KO was similar to what we observed in the p53(+/–)KM cells: mitotic block but only rare mitotic death and the generation of

tetraploid cells (Figure 3.8 A). To rule out that the p53(+/–) cells lost the wild-type copy of p53, I verified the presence of the p53 wild-type allele during the experimental processing of the p53(+/–) MEFs (Figure 3.8 B). These results suggest that half of the p53 dosage is enough to allow mitotic slippage and the generation of aneuploid cells in the presence of high Mad2 levels. This permissiveness could explain the apparent tumor suppressor effect of Mad2 in the p53(+/–) background *in vivo*.

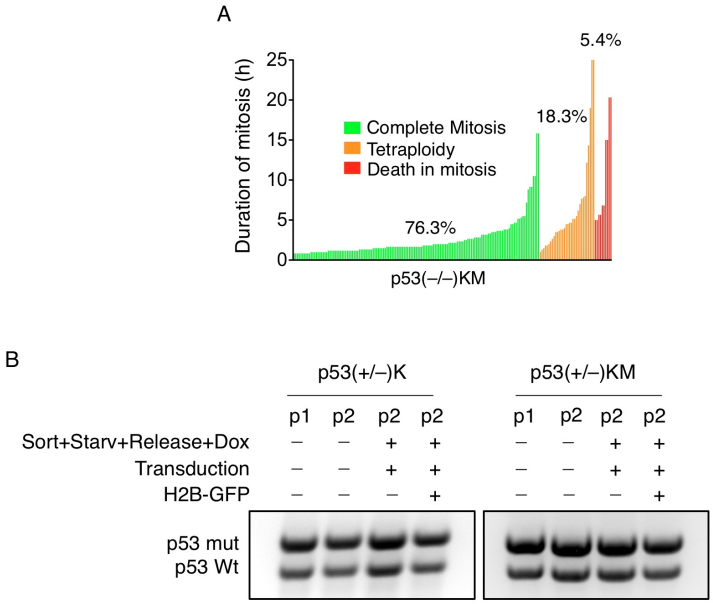

Figure 3.8: Mad2 over-expression induces aneuploidy in p53(–/–)Kras MEFs. A) Mitotic timing and outcome of mitosis of single p53(–/–)KM cells after 24 hours on doxycycline (n=185 mitosis). **B)** PCR for mutant and wild-type p53 from MEFs at different steps before time-lapse imaging. p53(+/–) K and KM MEFs retained their wild-type copy of p53 after being transduced with H2B-GFP, cell sorted, plated, starved, released and induced for 24hours.

3.5.6 Early sings of p53-p21 mediated G1 arrest *in vivo*

I could not detect any sign of cell death in the p53(+/–)KM lungs, interestingly the time-lapse experiments indicated that two copies of p53 are required to trigger mitotic death. I decided to look again for cell death but this time I compared p53(+/+) and p53(+/–)KM early induction lung samples. Once again I failed to detect evidence of cell death (data not shown). I then explored the opposite situation, cell cycle arrest, by following the activation of the p53 target p21. I hypothesized that if the two copies of p53 are able to kill cells in mitosis they should be also more potent in inducing cell cycle arrest following a defective mitosis. This approach also had the advantage that

contrary to dead cells; arrested cells should remain for a while in the lung before clearance or cell cycle re-entry.

I controlled for the HA-Mad2 and p21 induction by IHC after 4 days of doxycycline (Figure 3.9 A). I counted the number of p21 positive cells and normalized it by the quantity of tissue present on the images. In general I found a very low average of p21 positive cells per tissue area, further analysis should focus on the cell type on interest, the type II pneumocytes. I observed p21 positive cells with very large nuclei in the p53(+/+)KM lungs, this phenomenon was less frequent in in the samples with only one copy of p53 (Figure 3.8 B and C). Cell type specific analysis and the use of more samples could confirm the primary observations. In addition to the slight increase in the number of p21 cells, the fact that half of the p21 positive cells in the p53(+/+)KM have enlarged nuclei suggest a p53-p21 mediated G1 arrest due to Mad2 over-expression. These results support the hypothesis that at a very early time point (4days), the removal of one copy of p53 reduces the control of a defective mitosis *in vivo*. Additionally these data suggest that the inhibitory effect of Mad2 on type II pneumocyte described earlier (Figure 3.3) is most likely due to the mitotic block and not the activation of p53.

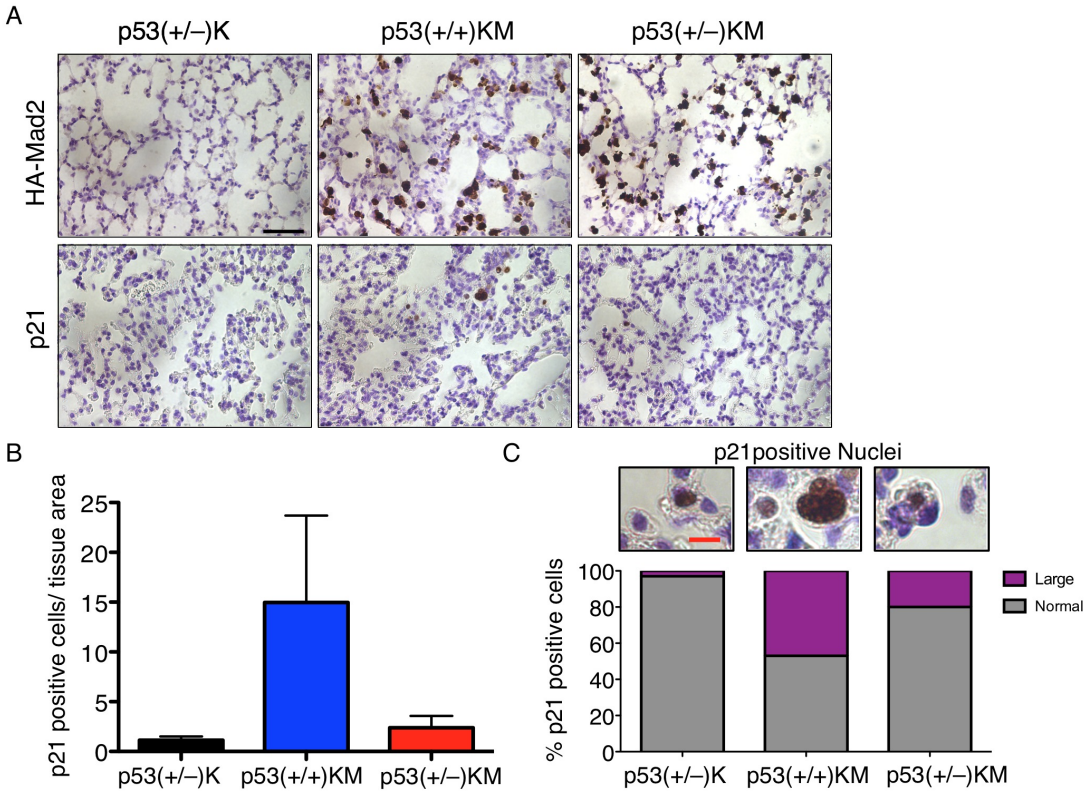

Figure 3.9: Early sings of p53-p21 mediated G1 arrest *in vivo*. Mice were feed doxycycline-impregnated food at 4 weeks of age and scarified after 4 days. **A**) HA and p21 IHC of lung samples. Black scale bar 50 μm. **B**) Quantification showing the normalized number of p21 positive cell per lung tissue surface. p53(+/–)K lungs were used as negative control (1.1±0.4 positive cells, n=4 mice). The p53(+/+)KM were variable however seem to have more p21 positive cells than p53(+/–)KM lungs (15.0 ± 8.7 n=6 *Vs*. 2.4 ± 1.2 n=9, n.s). **C**) Classification of the nuclear size of p21 positive cells and their distribution in the different genotypes, normal nuclear size in gray and large nuclei in purple. p53(+/–)K: normal 97%, large 3 %, n=31 p21 nuclei. p53(+/+)KM: normal 53%, large 47 %, n=183 p21 nuclei. p53(+/–)KM: normal 80%, large 20 %, n=54 p21 nuclei. Red scale bar 10 μm.

3.3 Effect of Mad2 over-expression on p53(+/–)K tumor

3.3.1 Mad2 over-expressing nodules are selected against

I observed that Mad2 over-expression delays lung tumorigenesis induced by Kras in the p53(+/–) background (Figure 3.1). Moreover, in the p53 wild-type background, I found a high incidence of cell death *in vitro* whereas the p53(+/–) background was more permissive to Mad2 over-expression (Figure 3.7). I then suspected that high levels of Mad2 are generally detrimental for tumorigenesis *in vivo* but to different extents depending of the p53 background. To address this question, I verified the expression of the Mad2 transgene in lung nodules, taking advantage of an HA tag upstream of the initiation codon.

I described that both low and high HA-Mad2 expressing nodules (Figure 3.10 A) were present within the same lung. A population with intermediate levels of Mad2 was consistently found across genotypes (Figure 3.10 A), probably due to the difficulty of classifying some nodules in one category using this empirical method. Control p53(+/+)KM lungs had an average of 46.6% of high Mad2 (HA-Mad2) expressing nodules whereas the removal of one copy of p53 reduced the incidence to 14.4% (Figure 3.10 B). These data demonstrate the evolutionary disadvantage of high Mad2 expressing tumors in the context of p53 partial inactivation. Yet, these results are intriguing since the removal of one copy of p53 initially enhanced cell survival *in vitro*.

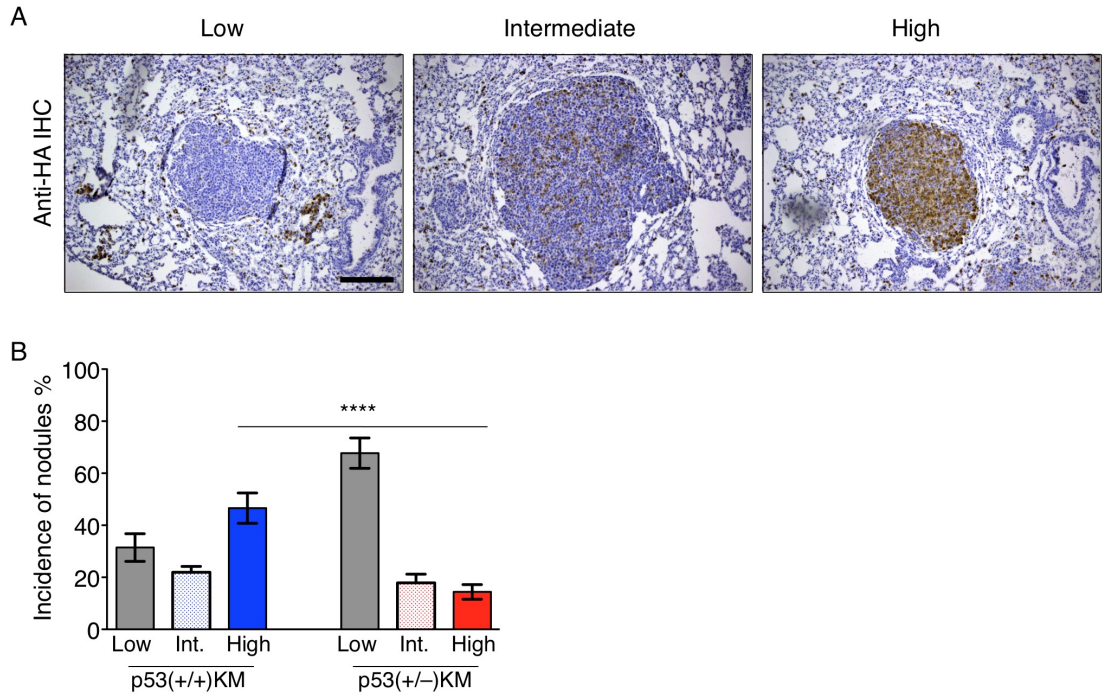

Figure 3.10: Mad2 over-expressing tumors are selected against. A) Representative staining of HA-Mad2 lung nodules indicating different levels of Mad2 expression: low, intermediate and high. Mice were selected for having at least 10 tumours and transgenes were induced at different time points. **B)** Percentage of nodules with low, intermediate (Int.) or high Mad2 levels shows a decrease in high expressing nodules in p53(+/–)KM mice compared to p53(+/+)KM (p53(+/–)KM: 14.4%, n=13 mice *Vs*. p53(+/+)KM: 46.6% n=13 mice, *t*-test ****p<0.0001) and similar percentage of nodules with Ha-Mad2 intermediate levels in the 2 genotypes.

3.3.2 MAD2 OVER-EXPRESSING NODULES ARE COMPOSED OF ANEUPLOID CELLS

The removal of one copy of p53 rescued the mitotic death induced by Mad2 over-expression and lead to the generation of polyploid cells *in vitro* (Figure 3.7), paradoxically, high Mad2 nodules were most selected against in the p53(+/–) background (Figure 3.10). Since chromosomal instability and aneuploidy have been shown to have tumor promoting and tumor suppressor effects (Weaver et al., 2007), I hypothesized that the initial permissiveness produced by the removal of one copy of p53 was generating highly instable tumors, which in turn was detrimental to tumorigenesis. It has previously been reported that increased chromosome copy number correlates with an increase in nuclear size (Knouse et al., 2014). To confirm that cells overexpressing Mad2 in p53(+/–) animals had undergone chromosome mis-segregation, I measured the nuclear size and converted to nuclear volumes in the different tumor sub-categories, the normal nuclear volumes of type II pneumocytes were used for

normalization.

Generally tumors cells showed very large nuclei compare to healthy cells (Figure 3.11 A and B), it is not surprising since 68 % of solid tumors are aneuploidy (Duijf and Benezra, 2013). It has been previously shown that Mad2 over-expression induces aneuploidy in Kras induced tumors (Sotillo et al., 2010), accordingly, Mad2 over-expression in this study led to the generation of polyploid cells as indicated by the dramatic increase in the tumor cell nuclear size, in both p53 backgrounds (Figure 3.11 A and B). However the nuclear volume variability was significantly higher in the p53(+/–) background (Figure 3.11 B), reflecting the diverse DNA contents thus the increased instability. Moreover, p53(+/–)KM low tumors had larger and variable nuclei size compared to p53(+/–)K nuclei (Figure 3.11 B), suggesting persistent low over-expression of Mad2 or an earlier transient Mad2 over-expression in this population. These data are compatible with the possibility that sustained high levels of Mad2 over-expression may lead to an evolutionary disadvantage in p53(+/–) KM mice due to increased aneuploidy and chromosomal instability.

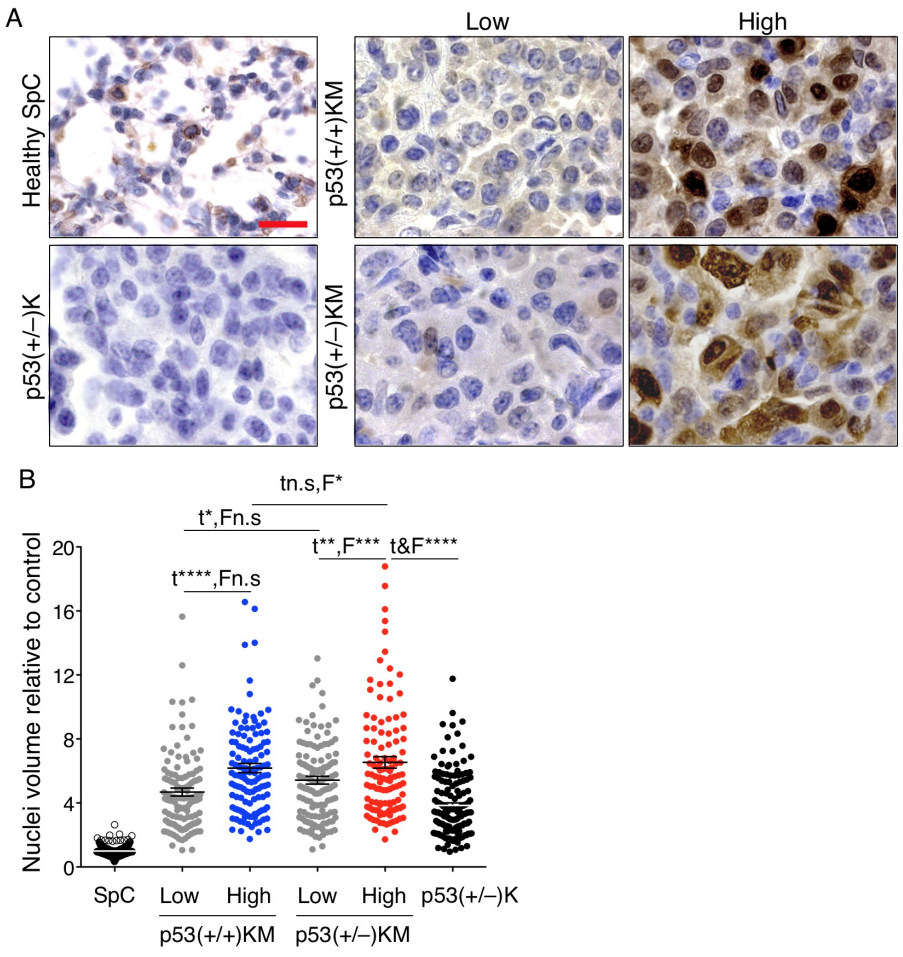

Figure 3.11: Mad2 over-expressing tumors are mainly composed of aneuploid cells. A) SpC staining of healthy wild-type type II pneumocytes or tumorigenic cells from p53(+/–)K mice and mice over-expressing Mad2 in the p53(+/+) or (+/–) backgrounds. **E**) Quantification of the nuclear size relative to wild-type control cells, Y axis log2 scale, indicating an increase of the nuclear size (unpaired *t*-test) and increase of size variability (F test) upon Mad2 over-expression. Average volumes were: healthy TIIPN: 1 (0.9988 ± 0.01975, n=256 nuclei), p53(+/+)KM low: 4.7 (4.678 ± 0.2475 n=126 nuclei), p53(+/+)KM high: 6.2 (6.181 ± 0.2864 n=125 nuclei), p53(+/–)KM low: 5.4 (5.423 ± 0.2415, n=129 nuclei), p53 (+/–)KM high: 6.5 (6.535 ± 0.3584, n=118 nuclei), p53(+/–)K: 3.8 (3.842 ± 0.1641, n=147 nuclei). Scale bar 20 μm.

3.3.3 MAD2 OVER-EXPRESSION INDUCES P21 AND INHIBITS P53(+/–)KRAS TUMOR PROLIFERATION

I reasoned that if Mad2 over-expressing cells were first selected against (Figure 3.10 and 3.11), the detrimental effect of Mad2 may be eventually lost during malignant transformation. To test this hypothesis I analyzed early tumors coming from p53(+/–)K and p53(+/–)KM mice, at 15 weeks post-transgenes induction. Using immunohistochemistry, I first classified the tumors depending on their genotype and their HA-Mad2 expression (Figure 3.12 A) and I stained the sections with markers of cell death, proliferation and cell cycle arrest.

Once again, I observed very few cell death events in all subtypes (Figure 3.12 B) and I failed to detect any differences in the amount of proliferating cells assessed by Ki67 staining (Figure 3.12 C). Ki67 stains the cells at any phase of the cell cycle, including cells arrested in G1 and G2, for this reason it might not be the best marker for measuring tumor proliferation in this thesis. I next used BrdU labeling; I started by giving a BrdU pulse to the mice via injection 2 hours before sacrifice, in this experiment only few tumors cells were labeled in comparison to the control intestinal tissue (data not shown). It is relatively intuitive to think that tumors are highly proliferative but in fact they are relatively slow compared to other normal tissues (e.g intestine data not shown). Furthermore, using the 2hours BrdU labeling I did not observe differences between the tumors subtypes (data not shown), I hypothesized that the difference of proliferation between tumor subtypes could not be seen because of the small amount of labeled tumor cells. With two hours BrdU pulse, only cells that enter S phase in the two hour window will be stained. Increasing the pulse of BrdU to 24hours will cumulatively stained cells entering S phase, and importantly, cells completing cell division will give

arise to two BrdU positive cells and amplify the proliferation signal. By increasing the labeling to 24 hours, I observed a significant decrease in the number of BrdU positive cells in High Mad2 nodules compared to the control tumors (Figure 3.12 D), thus Mad2 over-expression impairs proliferation.

Moreover, p53(+/–)KM high nodules had a very high number of p21 positive cells compared to the other nodule types (Figure 3.12 E). This result was surprising since p53(+/–)KM and p53(–/–)KM MEFs showed similar behavior (Figure 3.7 and 3.8) where the removal of only one copy of p53 rescued the mitotic death induced by Mad2. In this experiment, at an early tumor stage, the cells with only one copy of p53 are able to activate the down stream effector p21. Importantly, these result indicate that the p53(+/–)K tumors over-expressing Mad2 are arrested in G1.

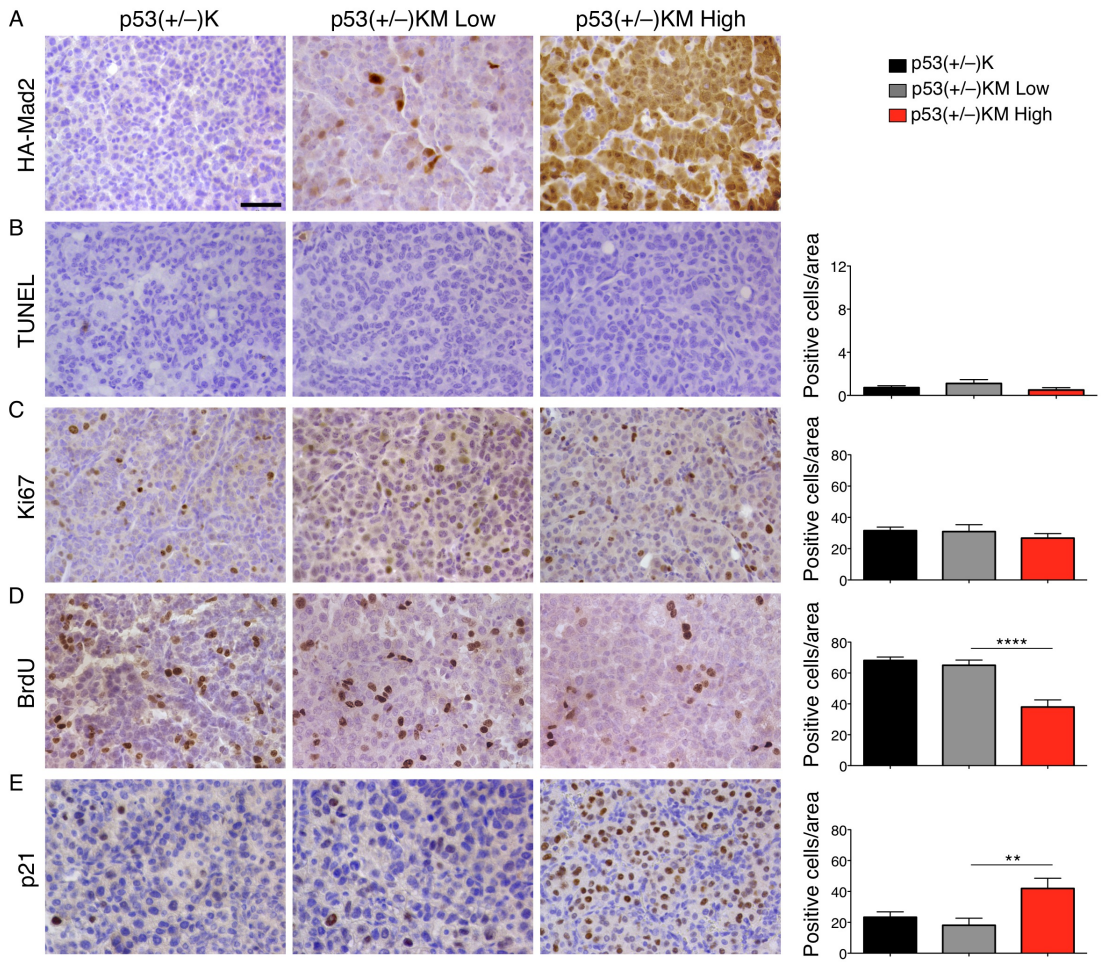

Figure 3.12: Mad2 expression in early p53(+/–)Kras lung nodules induces p21 and inhibits proliferation. A) HA immunostaining of early tumors after 15 weeks of transgenes induction. Scale bar 50 μm. **B)** TUNEL staining showing occasional dead cells (p53(+/–)K n=18 tumors from 6 mice, p53(+/–)KM Low n= 9 tumors from 3 mice, p53(+/–)KM High n=10 tumors from 4 mice). **C)** KI67 staining showing similar number of cycling cells in all the tumors sub-types (p53(+/–)K n=23 tumors from 5 mice, p53(+/–)KM Low n=15 tumors from 3 mice, p53(+/–)KM High n=15 tumors from 4 mice). **D)** BrdU staining after 1day of labelling showing the reduced number of BrdU positive cells in High Mad2 tumors indicating the decrease of proliferation upon Mad2 over-expression (p53(+/–)K: 68.16 ± 2.174 n=96 tumors from 11 mice, p53(+/–)KM Low: 65.04 ± 3.342 n=38 tumors from 7 mice, p53(+/–)KM High : 38.00 ± 4.559 n=24 tumors from 8 mice, unpaired *t*-test ****p<0.0001). **E)** P21 staining showing the high number of p21 positive cells in High Mad2 tumors indicating a G1 arrest upon Mad2 over-expression (p53(+/–)K: 23.30 ± 3.517 n=44 tumors from 6 mice, p53(+/–)KM Low: 18.12 ± 4.575 n=22 tumors from 4 mice, p53(+/–)KM High : 41.98 ± 6.624 n=24 tumors from 3 mice, unpaired *t*-test **p<0.01).

The previous results indicated that p53(+/–)K tumors cells over-expressing Mad2 are able to activate the p53 target p21 (Figure 3.12), however previous experiments suggested that p53(+/–)KM MEFs are similar to p53(–/–)KM, it is then possible that the activation of p21 in the tumors is independent of p53. To test whether the activation of p21 was due to p53 activation, I took advantage of the rare p53(–/–)KM mice that survived long enough to develop tumors. I observed equal amounts of p21 positive cells in p53(–/–)K, p53(–/–)KM low and high tumors. These data demonstrate that the p21 induction in p53(+/–)KM high nodules was due to the remaining wild-type copy of p53, since p53(–/–)KM nodules did not induce p21 despite expressing high levels of Mad2 (Figure 3.13).

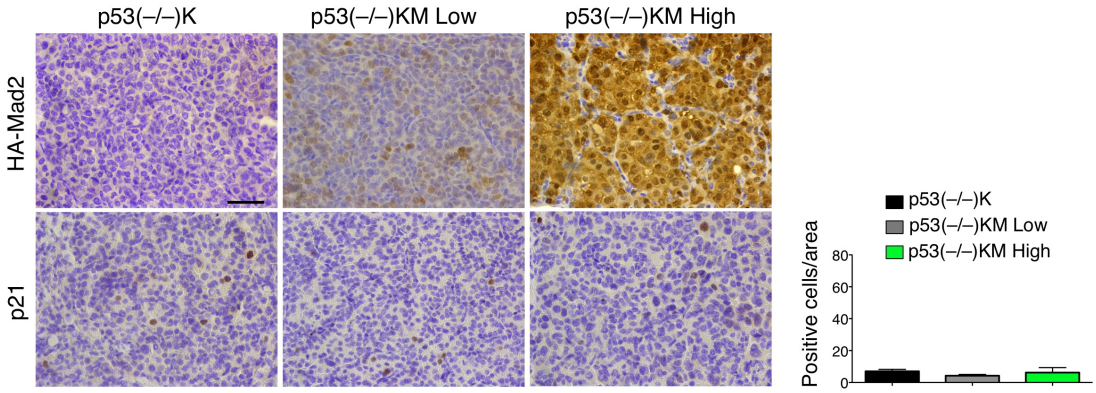

Figure 3.13: Mad2 expression in p53(–/–)Kras early lung nodules doesn't induces p21. Upper panel) HA immunostaining of early p53 null tumors, around 13 weeks of transgenes induction. Scale bar 50 μm. **Lower panel)** p21 staining of early p53 null tumours showing that the activation of p21 is p53 dependant (p53(–/–)K: 7.037 ± 1.225 n=27 tumors from 6 mice,

average induction time =13.8 weeks, p53–/–)KM Low: 4.252 ± 0.8074 n=20 tumors from 4 mice, average induction time =13.2 weeks, p53(–/–)KM High: 6.231 ± 3.099 n=13 tumors from 6 mice, average induction time =13 weeks).

At early stage, the fact that p53(+/–)KM high tumors had reduced BrdU and increased p21 suggests that Mad2 over-expression remained detrimental in these tumors by preventing cell proliferation (Figure 3.12). At later stage of tumorigenesis, I observed that the proportion of lungs occupied by the tumors in p53(+/–)KM lungs became close to the tumor proportion found in the p53(+/–)K control lungs (more than 20 weeks, Figure 3.2). Therefore, I hypothesized that the growth repression induced by p21 could be released at later stages during tumor growth. Immunohistochemistry staining against p21 on aged-tumors (humane end point) from p53(+/–)KM animals remained positive for p21 upon Mad2 over-expression (Figure 3.14) however, it was decreased in the p53(+/–)KM high aged-tumors compare to the early ones (42 *Vs*. 21 positive cells per tumor area, Figure 3.12 E and 3.14). At the contrary to early tumors, I was not able to assess proliferation-using BrdU labeling in the late stage tumors (data not shown). It is important to keep in mind that at this stage around 50% of the lungs are occupied by tumors in the p53(+/–)K cohort and it appeared that the BrdU was un-evenly distributed in the lungs probably due to their general obstruction, or that the large tumors have reached a physiological limit. All together these results suggest that one wild-type copy of p53 is sufficient to activate p21 and at later tumor stages high Mad2 expressing nodules might have lost the control of p21 expression, probably due to the loss of the wild-type copy of p53.

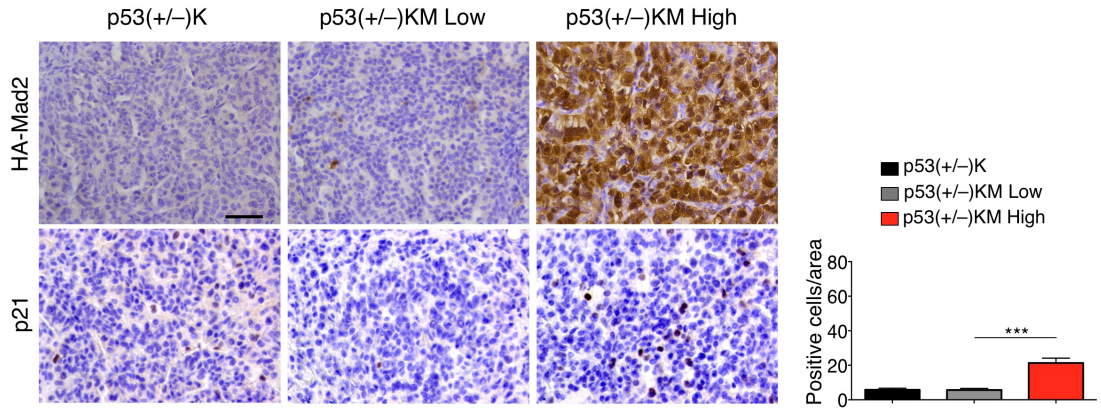

Figure 3.14: Mad2 expression in late stage p53(+/–)Kras lung nodules induces p21. Upper panel) HA immunostaining of late tumors, more than 20 weeks after transgenes induction.

Scale bar 50 μm. **Lower panel)** Representative images of p21 immunostaining in late stage tumors showing a p21 induction upon Mad2 over-expression (p53(+/–)K: 5.815 ± 0.9184 n=42 tumors from 6 mice, p53(+/–)KM Low: 5.649 ± 0.9188 n=37 tumors from 6 mice, p53(+/–)KM High : 21.30 ± 2.835 n=36 tumors from 6 mice, unpaired t-test $^{****}p<0.0001$).

3.3.4 MAD2 OVER-EXPRESSION DOES NOT INDUCE SENESCENCE

In remained unclear to me how high levels of Mad2 can induce p21 and cell cycle arrest but does not lead to cell death (Figure 3.12). A possible explanation would be that after a long arrest the cells would re-enter the cell cycle or enter senescence; at the contrary to cell cycle arrest and similar to cell death, in theory senescence is irreversible. Using a conditional mouse model with an oncogenic Kras-V12 allele that is activated by Cre recombinase, a study has shown that Kras induces senescence in pre-malignant tumors called adenomas (Collado et al., 2005). The progression of these tumors toward a more aggressive form; adenocarcinomas is characterized by the fact that the tumors overcome senescence. Thus the authors claim that lung adenomas are composed of many senescence cells seen by an intense senescence associated β-galactosidase blue staining (β-gal), whereas adenocarcinomas show only rare positive cells. I have observed activation of p21 in the tumors over-expressing Mad2 in the p53(+/–) background (Figure 3.12-14), and p21 is increased in senescent human fibroblast (Tahara et al., 1995). To test whether the activation of p21 and the G1 arrest would push the tumors cells into senescence, I performed a β-gal staining on p53(+/–)K with out Mad2, Mad2 low and high tumors.

I did not observe the previously described intense blue staining at the center of the tumors characteristic of adenomas in any of the tumors category suggesting that in this p53(+/–)Kras model of cancer the tumors were all adenocarcinomas (Figure 3.15). Accordingly, the MEFs over-expressing did not shown evidence of senescence as suggested by their growth in culture (Figure 3.6). Initially adenomas were chemically induced in mouse, however, adenocarcinomas are one of the lung cancer sub-types frequently found in humans, thus some genetically engineered models were developed which could directly give rise to adenocarcinomas (Kazushi Inoue, 2013). Moreover, I observed senescent cells only at the periphery of the tumors, where they appear to form an external layer that encapsulates the heart of the tumors. In the center, where the p21 or BrdU positive cells were found I saw occasional senescent cells (Figure 3.15). This pattern was very consistent across the different tumors type. It is been previously shown

that p21 is not required for the induction of senescence (Pantoja and Serrano, 1999), thus, p21 induction in high Mad2 expressing tumors doesn't mean that cells will enter senescence. In fact, it appears that senescence is not the route taken by the cells after being p21 positive and arrested in G1, it could be because in this model of cancer the tumors have already bypassed this difficulty to arise. The reduction of arrested cells over-time in the tumor over-expressing Mad2 can be due to 2 non-mutuality exclusive possibilities. The p21 positive cells can be progressively eliminated, or they can by-pass the arrest and re-enter the cell cycle.

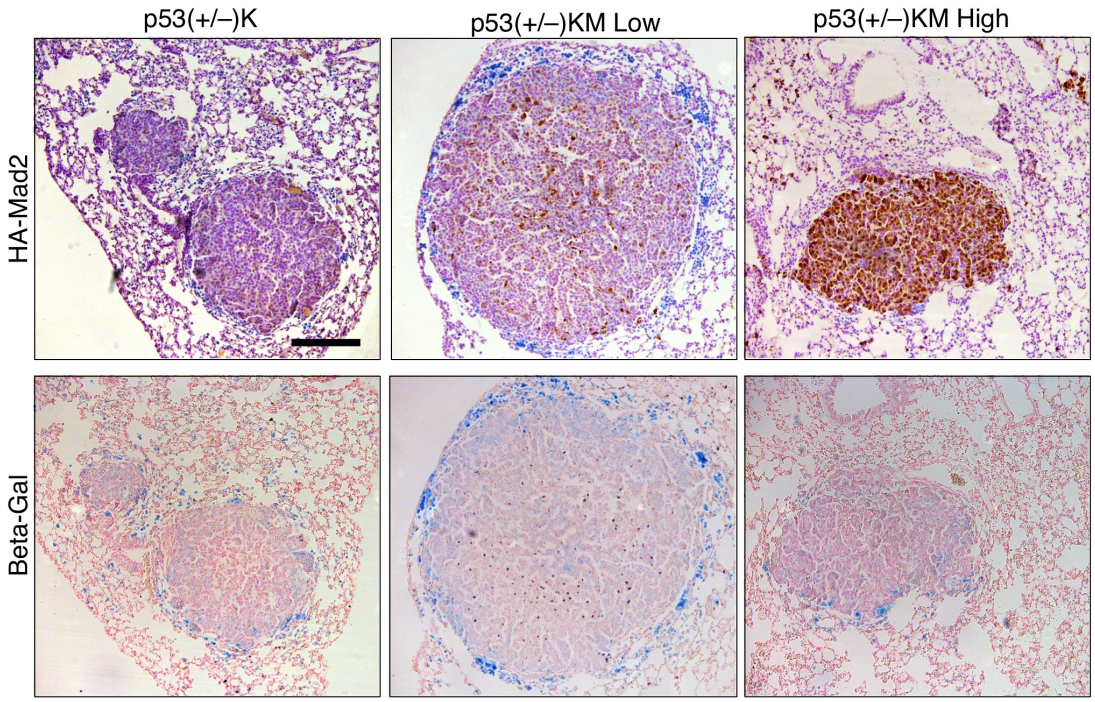

Figure 3.15: Mad2 expression doesn't induce senescence in early lung nodules. Upper panel) HA immunostaining of early tumors after 15 weeks of transgenes induction, showing he different types of tumors: p53(+/–)K with out, low or high Mad2. Scale bar 200μm. **Lower panel)** β-galactosidase staining showing senescent cells at the tumor peripheries, independently of the tumor type.

3.4 P53 LOSS OF HETEROZYGOCITY

3.4.1 MAD2 OVER-EXPRESSION DOES NOT INCREASE P53 LOH

P53 loss of heterozygosity normally occurs in human lung cancer. It has been shown that p53 heterozygosity in human cancers is achieved via mutation of one copy of p53, which correlates with the removal of corresponding intact copy. This phenomenon is called p53 loss of heterozygosity (p53 LOH) and leads to the inactivation of both copies

of the tumor suppressor (Mallakin et al., 2007; Zienolddiny et al., 2001). Because it was unclear how chromosome instability can drive tumorigenesis, a study addressed the possibility that chromosome instability promotes tumor suppressor loss of hetorozygosity. The study shows that reduced levels of the mitotic checkpoint protein Bub1 induce p53 LOH, however, it doesn't induce the LOH of other tumor suppressors (Baker et al., 2009). The previous results show that Mad2 over-expression impairs Kras induced lung tumors in the context of partial p53 inactivation (Figure 3.1 and 3.2). However, when I screened by immunohistochemistry the p53(+/–)KM lungs, I observed that 15% of tumors were able to develop with very high levels of Mad2 (Figure 3.10) and the p53 mediated induction of p21 decreased over-time (Figure 3.12-14). I therefore looked into possible compensatory mechanisms and tested whether Mad2 over-expression induces p53 LOH. I explored this possibility by performing PCR for the two alleles of p53 (Figure 3.16 A upper panel), and I calculated the ratio between the mutant and wild-type bands, I used control healthy lungs to normalize (Figure 3.16 A lower panel). A ratio with a value of 1 corresponds to the normal genotype p53(+/–), more the value is close to zero more the wild-type copy of p53 is underrepresented compare to the mutant one in the sample (Figure 3.16 A and C).

The results indicated that both Kras and Kras/Mad2 genotypes could give rise to tumors with p53 LOH and Mad2 over-expression has no influence on p53 LOH (Figure 3.16 A). To better understand the significance of p53LOH, I performed qPCR analysis for the Mad2 transgene on the same nodules. As expected, p53(+/–)K tumors did not express exogenous Mad2 and the pattern of Mad2 expression on p53(+/–)KM nodules was very heterogeneous as previously seen by imunohistochemistery (Figure 3.16 B and 3.10). Since the p53(+/+)KM cohort was not originally included in this thesis, I obtained fewer p53(+/+)KM nodules. In the case of the p53(+/+)KM, late stage nodules were over-expressing the Mad2 transgene (Figure 3.16 B). I hypothesized that the Mad2 low expressing nodules could mask a relationship between Mad2 over-expression and p53LOH. The correlation between the two parameters indicated that although LOH was not a prerequisite for high expressing Mad2 nodules, the p53 wild-type allele was under-represented in the most high expressing nodules (Figure 3.16 C). In this model p53LOH is the result of selection pressure, an opportunistic way to adapt to the detrimental effect of Mad2. Yet, it is not Mad2 induced chromosome instability that is responsible for p53LOH since it occurs with the same frequency in the control tumors.

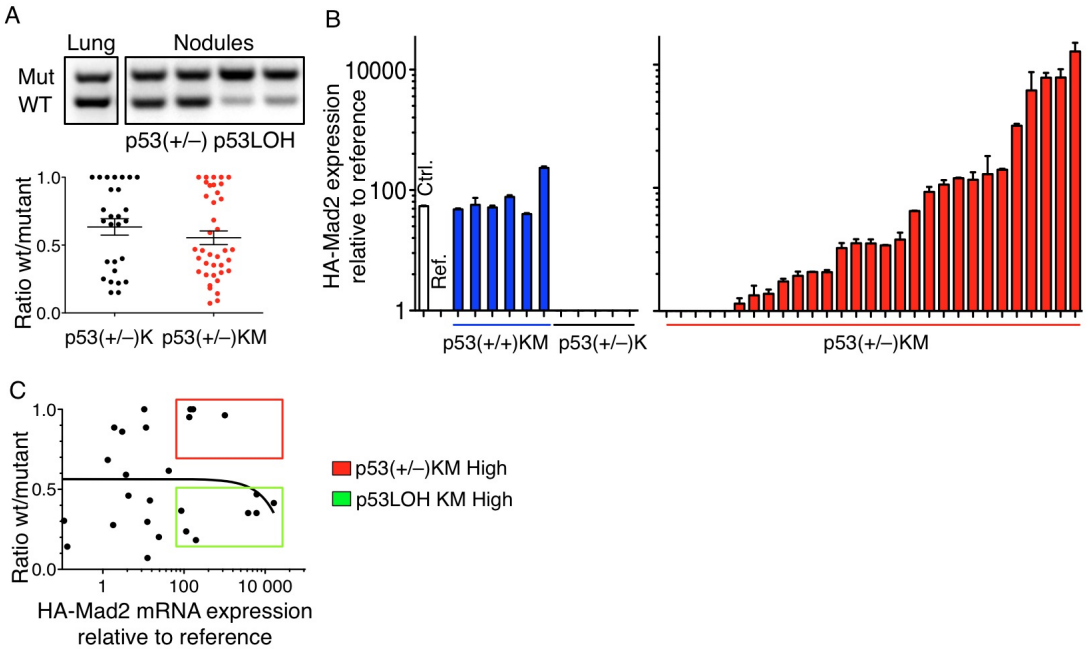

Figure 3.16: Mad2 over-expression doesn't induce p53 LOH. A) PCR example of p53(+/–) and p53 LOH (upper panel); lower panel: quantification of p53 LOH in nodules: a value of 1 corresponds to p53(+/–) and 0 to p53 LOH. **B**) qPCR analysis of Mad2 transgene in individual nodules from p53(+/+)KM n=6 tumors from 3 mice (blue) p53(+/–)K n= 5 tumors from 3 mice (black) and p53(+/–)KM n=19 tumors from 7 mice (red). Ref. used was a p53(+/–)KM lung without the rtTA and p53(+/–)M healthy lung on doxycycline was used as positive control. **C**) Regression analysis showing that Mad2 over-expression and p53LOH in p53(+/–)KM nodules do not correlate. On the Y axis: values used in A and on the X axis: Mad2 over-expression. Red square: nodules with p53(+/–) and high Mad2 levels. Green square: p53 LOH and high Mad2 levels.

3.4.2 MAD2 OVER-EXPRESSION INDUCES THE EXPRESSION OF P53 TARGET GENES

To functionally confirm the complete p53 loss in the different nodules I performed real time PCR for some p53 target genes. P53(+/–)K nodules were used as a negative control and p53(+/+) nodules expressing Mad2 were used as positive controls. I defined two groups of nodules in p53(+/–)KM mice: those that expressed high Mad2 which remained p53(+/–) and the ones that underwent p53 LOH (Figure 3.16 C). It has been shown that p53 can negatively regulate Cdc20 and positively p21 (Kidokoro et al., 2008; Macleod et al., 1995). I observed that Mad2 over-expression led to down regulation of Cdc20 and induction of p21 in the p53 heterozygous background and the

regulations were similar to the one in the p53 wild-type samples (Figure 3.17 A and B). As expected, p53LOH suppressed these p53-mediated regulations. These results confirm that high Mad2 levels induce cell cycle arrest in nodules with only one functional copy of p53. It was challenging to reliably quantify cell death on tumor sections using TUNEL due to the physiological clearance of the lung tissue. Therefore, I took an alternative approach and I analyzed the expression of the two pro-apoptotic genes PUMA and Bax and observed their up-regulation upon Mad2 over-expression that was abolished upon p53LOH (Figure 3.17 C, D). Similar results were obtained with GADD45, an effector of the DNA damage-signaling pathway that is regulated by p53 (Figure 3.17 E). Importantly, GADD45 is able to induce a G2 arrest. Since G1 and G2 arrest are not distinguishable and cell death is rare *in vivo* it is possible that the nodules over-expressing high levels Mad2 are arrested in the two phases of the cell cycle and ultimately dying. Moreover, the p53 negative regulator Mdm2 was found down regulated upon p53LOH (Figure 3.15 F) indeed, it is no longer needed in the absence of functional p53. In summary, Mad2 over-expression induces the expression of p53 targets when one or two copies of p53 are functional while the p53 mediated regulation is abolished in the p53(+/–) tumors that experienced p53LOH. The fact that Mad2 delays tumorigenesis (Figure 3.1) shows that the late stage random occurrence of p53LOH in Mad2 expressing nodules was not sufficient to restore tumorigenesis.

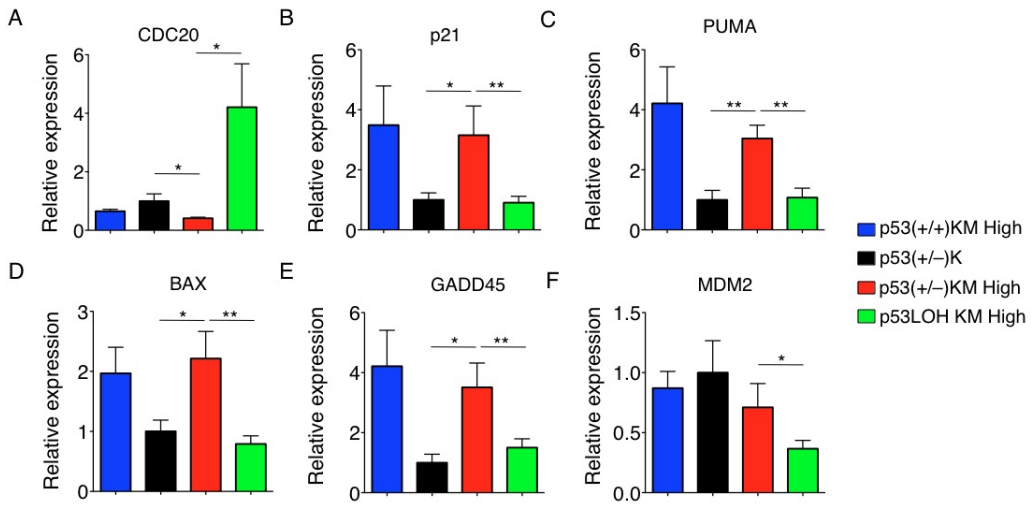

Figure 3.17: Mad2 over-expression induces the up-regulation of the p53 targets in the p53 heterozygote background and it is abolished upon p53LOH. A-F) qPCR analysis of p53 target genes in p53(+/+)KM (blue), p53(+/–)K (black), p53(+/–)KM high (red) and p53(+/–)KM

LOH high (green) (At least n=4 nodules per group were analysed, unpaired *t*-test $^{*}p<0.05$ or $^{**}p<0.01$). For all expect Cdc20, p53(+/+)KM n=4 tumors from 3 mice, p53(+/–)K n= 4 tumors from 4 mice, p53(+/–)KM high n=4 tumors from 4 mice, p53(+/–)KM LOH high n=8 from 4 mice. For Cdc20, p53(+/+)KM n=5 tumors from 3 mice, p53(+/–)K n= 5 tumors from 2 mice, p53(+/–)KM high n=4 tumors from 4 mice, p53(+/–)KM LOH high n=6 from 3 mice. **A)** Cdc20 **B)** p21 **C)** PUMA **D)** Bax **E)** Gadd45 **F)** MDM2

3.4.3 MAD2 OVER-EXPRESSING CELLS ARE SELECTED AGAINST IN THE P53(+/–) AND P53(–/–) KRAS BACKGROUND *IN VITRO*

To better understand the sequence of events during lung tumorigenesis, I followed p53(+/–)KM MEFs during immortalization after continuous passage, twice a week as described previously (Sotillo et al., 2001). Contrary to the results obtained previously (Figure 3.6 F), Mad2 over-expression had no effect on the MEFs growth (Figure 3.18 A). This is due to the two very distinct goals and settings of the two experiments. In the previous experiment (Figure 3.6), I assed the initial cell fitness by following their short-term growth (day 0 to day 6), when the cells were counted it was the end of the experiment. In the long-term immortalization experiment, the one described in this part, the continuous passage promotes the growth and selection of the fittest, mimicking the phenomenon of transformation *in vivo,* where only one transformed cell needs to make it through the initial selection for a tumor to form. Even if Mad2 has been previously shown to have a detrimental effect on cellular growth (Figure 3.6), the cells that do not find a compensatory mechanism in this experiment will be eliminated early allowing the culture to be overtaken by low or non-expressing clones.

Previous results indicated that p53LOH might help restoring tumorigenesis (Figure 3.13 and 3.17), to test this hypothesis I followed the immortalization of p53(–/–)KM and p53(+/–)KM MEFs. The growth curves showed no differences between the two genotypes or to MEFs grown in the absence of doxycycline (Figure 3.18 A). In fact, with and without doxycycline p53(+/–)KM MEFs became immortal by losing the wild-type copy of p53 around passage 8 (Figure 3.18 B). Interestingly, doxycycline induced p53(+/–)KM cultures were quickly over-taken (at passage 4) by low Mad2 expressing cells before LOH took place (Figure 3.18 C). These results correlates with the situation *in vivo* where low expressing nodules were found as early as 15 weeks of transgenes induction (Figure 3.12) and at a later time point, the high Mad2 expressing nodules

show sign of p53LOH (reduced p21 activation, Figure 3.14). Interestingly, p53(–/–) MEFs were able to sustain high levels of Mad2 for a longer time in comparison to p53(+/–) MEFs (until passage 10, Figure 3.16 C). In this setting, p53LOH was again not a consequence of Mad2 induced aneuploidy since non-induced p53(+/–)KM cells lost the wild-type allele at similar frequencies compared to induced cells (Figure 3.16 B). These results indicates that complete p53 inactivation slightly increases the tolerance for Mad2 over-expression *in vitro*.

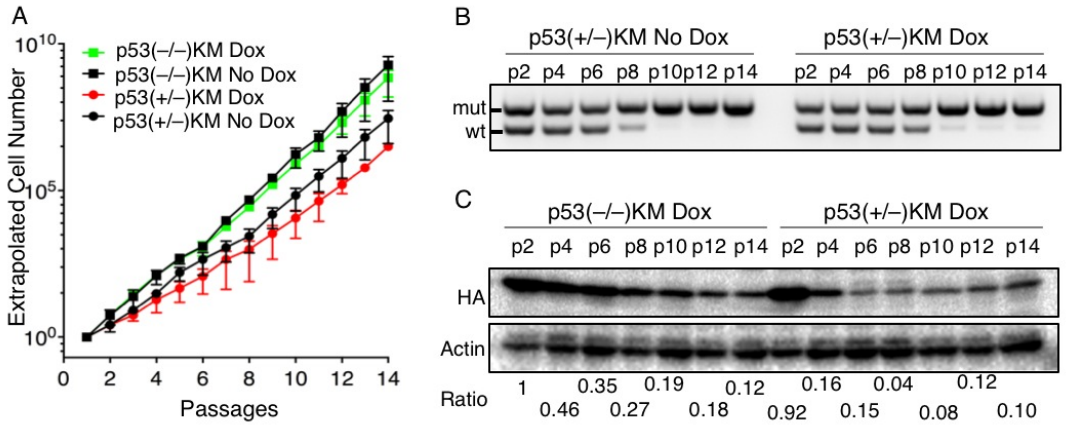

Figure 3.18: p53LOH is independent of Mad2 over-expression *in vitro*. A) Growth curve of p53(+/–)KM or p53(–/–)KM MEFs in culture with and without doxycycline from two experiments. **B)** PCR analysis of p53 LOH at different passages showing that LOH is independent of Mad2. **C)** Western blot analysis of HA-Mad2 shows reduction of Mad2 levels relative to control (Actin) prior to p53 LOH. The analysis shows that p53(–/–)KM MEFs keep higher Mad2 levels longer than p53(+/–)KM, indicating that p53 loss tolerate better Mad2 over-expression.

3.4.4 p53 complete inactivation does not restore Kras tumorigenesis upon Mad2 over-expression

The fact that the remaining wild-type copy of p53 in the p53(+/–)KM mice is sufficient to induce the regulation of the p53 targets in the tumors over-expressing Mad2 (Figure 3.12-14 and 3.17) suggests that the complete inactivation of p53 from the beginning of the transgenes induction could restore the normal course of tumorigenesis. To test this hypothesize, I analyzed the size and the incidence of the tumors appearing in the rare p53(–/–)K mice and compared it to the herein previously described p53(+/–)K tumors, with or with out Mad2. Because the p53 null mice die very early in

comparison to the other lung tumor models used here, I used early time points of transgene induction in this experiment, about 15 weeks.

In both p53 backgrounds I found again that the Mad2-high expressing nodules were smaller than the low expressing ones (Figure 3.19 A and B). Contrary to the p53(+/–) mice, the majority of nodules in p53(–/–) mice were expressing high levels of Mad2 (Figure 3.19 C) at 15 weeks. The results indicate that the maximum detrimental effect of Mad2 during p53(+/–)K tumorigenesis occurs prior tumorigenesis, where Mad2 high expressing cells are selected against due to their increased aneuploidy and remaining p53 activity. The fact that low expressing nodules are generated in the p53(–/–)K background together with the fact that high Mad2 nodules remain smaller suggest that even if complete loss of the p53 tumor suppressor helps tolerating high levels of Mad2, it would not be enough to restore the normal course of tumorigenesis. Previous results indicated that the inactivation of the two copies of p53 first led to the generation of polyploid cells (Figure 3.8) and then suppressed rescuing mechanisms (e.g. cell cycle arrest, Figure 3.13 and 3.17). In the absence of p53, it is possible that the double tolerance (in mitosis and in G1) for Mad2 over expression turn out to be harmful. It would be interesting to study what are the molecular mechanisms impairing the development of aneuploid tumors in the absence of p53.

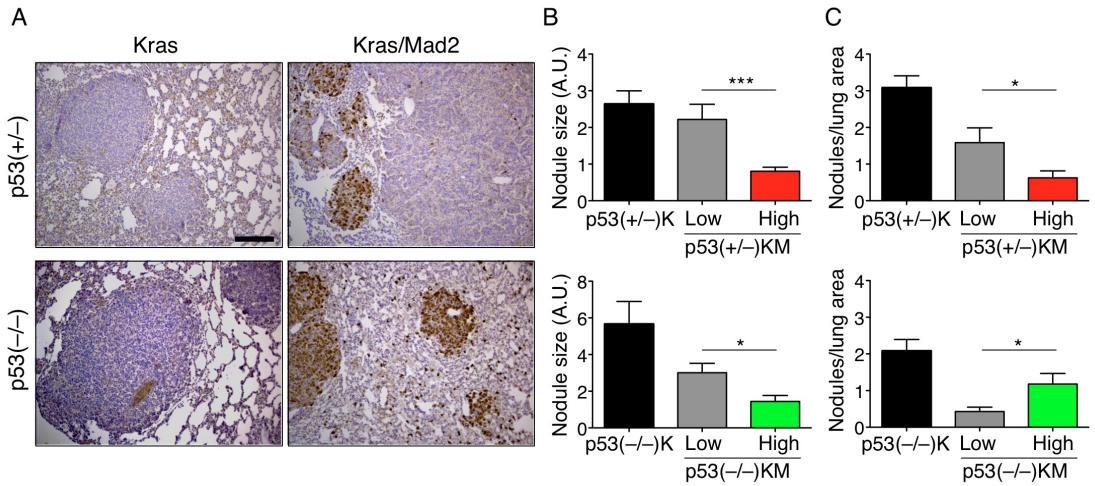

Figure 3.19: High Mad2 nodules are smaller than control nodules in the complete p53 knock out. A) HA-Mad2 staining showing the size of p53(+/–)K , p53(+/–)KM low and high, p53(–/–)K and p53(–/–)KM low and high nodules. Scale bar: 200µm **B)** Graph representing the decreased nodules size (arbitrary unit) upon Mad2 over-expression independently of the p53

background (p53(+/–)K n=103 tumors from 6 mice, p53(+/–)KM low n=45 tumors from 4 mice, and high n=52 tumors from 4 mice; p53(–/–)K n=63 tumors from 5 mice, p53(–/–)KM low n=24 tumors from 4 mice and high n=27 tumors from 4 mice, unpaired *t*-test $^{*}p<0.05$ or $^{***}p<0.001$) **C**) Graph showing reduced incidence of high Mad2 nodules compared to the low ones in p53(+/–) lungs and an increased incidence of high Mad2 nodules in the complete null p53 background (p53(+/–)KM n=24 lung fields from 6 mice, p53(–/–)KM n=26 lung fields from 7 mice, unpaired *t*-test $^{*}p<0.05$).

3.5 *IN VIVO* CARACTERIZATION OF THE EGFR COHORTS OVER-EXPRESSING MAD2

3.5.1 MAD2 OVER-EXPRESSION DELAYS EGFR DRIVEN LUNG TUMORIGENESIS UPON P53 PARTIAL INACTIVATION BUT NOT IN THE P53 WILD-TYPE BACKGROUND

Mad2 over-expression together with the Kras oncogene has been shown to accelerate tumorigenesis (Sotillo et al., 2010) while the similar combination in the context of partially impaired p53 delays tumorigenesis (Figure 3.1). In the field, whether aneuploidy is promoting or suppressing tumorigenesis is often attributed to the cellular context since all the studies aiming to better understand this opposite behavior have yet to reach a consensus. I hypothesized that regardless of the oncogene driving tumorigenesis Mad2 is detrimental in the context of a partially inactivated p53. After Kras, EGFR is the second most common oncogene found in lung cancer (Imielinski et al., 2012). I took advantage of mice expressing an inducible a human EGFR oncogene: $EGFR^{L858R}$ (Politi et al., 2006) (E) and crossed them with the inducible Mad2 mice in a wild-type or p53 heterozygous background.

I observed that the EGFR mice had a very fast onset of tumorigeneis in comparison to the Kras model (Figure 3.1 and 3.20 A). Here again, the combination of Mad2 over-expression in the p53(+/–) background delayed lung tumorigenesis (Figure 3.20 A). However, contrary to what was described in the Kras model, Mad2 over-expression seem to have no impact on EGFR driven tumorigenesis in a p53-wild-type background (Figure 3.20 B). A possible explanation for this finding is that the EGFR tumor onset is so fast that it cannot be further accelerated by Mad2 over-expression, or, that the EGFR cells are highly proliferative and thus do not tolerate an hyper-active mitotic checkpoint. In other words, the treading of aneuploidy for the cost of a mitotic block is no longer producing benefits in the EGFR model. I speculate that aneuploidy could accelerate

EGFR tumorigeneis in the p53 wild-type background, only with a permissive mitotic checkpoint.

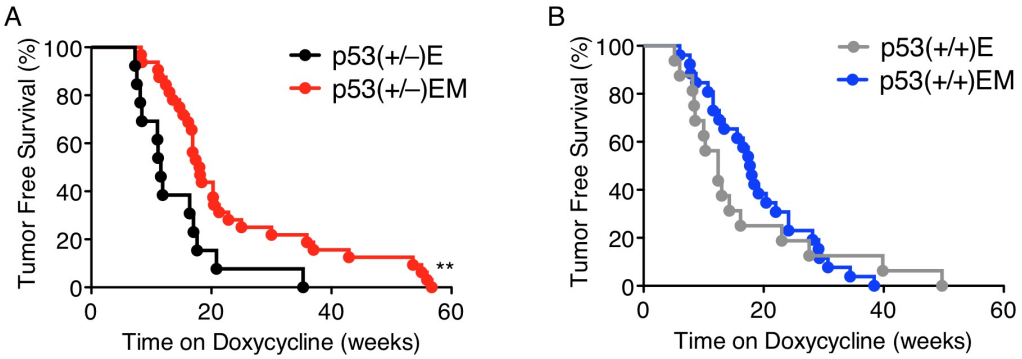

Figure 3.20: Mad2 delays lung tumorigenesis in the EGFR lung cancer models. A) Tumor free survival of mice expressing $EGFR^{L858R}$ oncogene (E) in the p53(+/–) background. Median survival time of p53(+/–)E: 11.57 weeks, n=17 (black) and p53(+/–)EM: 18.05 weeks, n= 41 (red) (Mantel-cox test $^{**}p<0.01$). **B)** Tumor free survival of mice expressing $EGFR^{L858R}$ oncogene (E) in the p53 wild-type background. Median survival time of p53(+/+)E: 12.43 weeks, n=21 (gray line), p53(+/+)EM: 17.86 weeks, n=41 (blue).

3.5.2 MAD2 OVER-EXPRESSING NODULES ARE SELECTED AGAINST IN THE EGFR MODEL

I have seen that in the Kras model different types of tumors appeared in the cohorts over-expressing Mad2 (Figure 3.10). I performed the same analysis in the EGFR cohorts; by immohistochemistry I classified the incidence of low, intermediate and high Mad2 expressing nodules (Figure 3.21 A and B). The induction of EGFR led to the generation of a different type of tumors, bronchioloalveolar carcinoma (BAC or diffuse tumors) that contrary to confined nodules colonizes the entire lung. I also noticed variable levels of Mad2 in this tumor type (Figure 3.21 C and D). Independent of the p53 background, the high Mad2 expressing tumors sub-type was extremely under-represented (Figure 3.21). I speculate that in a perfect mouse model where only high Mad2 nodules would be generated, the tumorigenesis of EGFR in the p53 wild-type background would also be delayed. The advantage of this model, at the contrary to the Kras one, is that the different types of tumors are equally represented in both p53 backgrounds with very rare high Mad2 expressing nodules (Figure 3.10 and 3.21). In this case, it is possible to affirm that it is the low expressing Mad2 nodules that are

responsible for the death of the animals in the two p53 backgrounds.

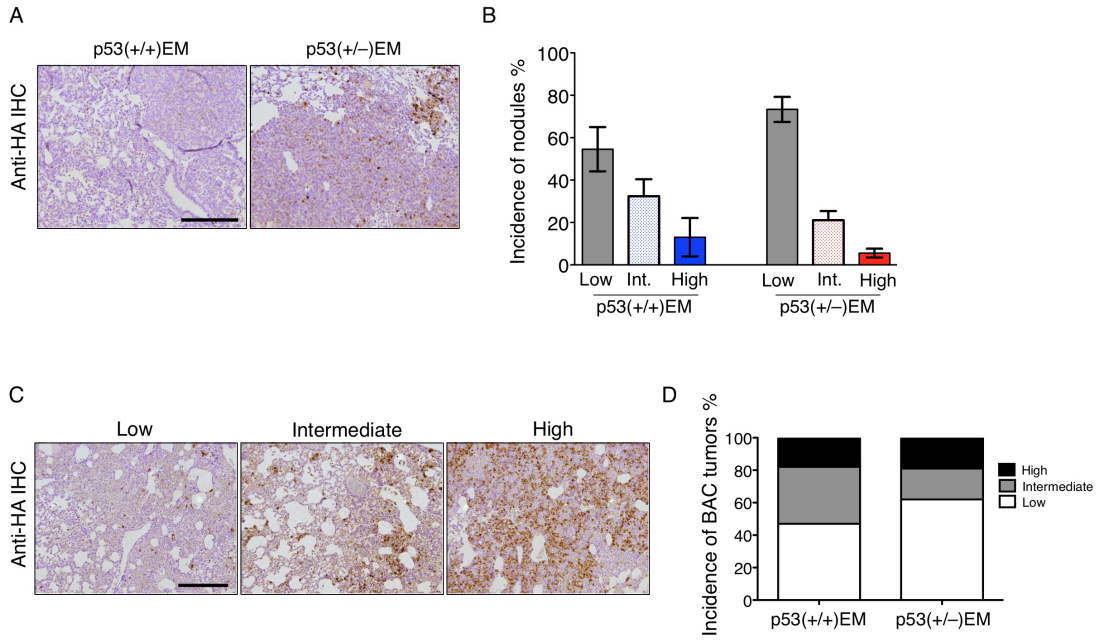

Figure 3.21: Mad2 High nodules are selected against in the EGFR models. A) Representative staining for HA-Mad2 showing low Mad2 nodules in the EGFR model. Scale bar 500 μm. **B**) Quantification of nodule incidence depending on Mad2 expression (p53(+/+) n=10 mice; p53(+/–) n=13 mice). **C**) Representative staining of a low, intermediate and high HA-Mad2 in bronchioalveolar carcinomas (BAC) of p53(+/–)EM mice. Scale bar 500μm. **D**) Percentage of BAC tumors depending of HA-Mad2 levels.

3.5.3 Mad2 over-expressing nodules are mainelly composed of aneuploid cells

Previous results indicate that the removal of one copy of p53 predisposed Kras cells to high aneuploidy and instability due to their in-efficiency to die during prolonged mitosis (Figure 3.7). In fact high expressing Mad2 tumor cells in the Kras, p53(+/–) background showed an increased nuclear size suggesting higher levels of aneuploidy, additionally the nuclear sizes were highly variable reflecting the increased chromosomal instability (Figure 3.11). Similar analysis in the EGFR tumors indicated that once again the size of the nuclei and the variability in size were increased upon Mad2 over-expression, especially in the cohort where one copy of p53 was lacking (Figure 3.22). These results support the hypothesis that Mad2 over-expression and the removal of one copy of p53 increases chromosomal instability and the level of aneuploidy, which is

selected against very early in tumorigenesis. Further analysis on this model remains challenging mainly due to two reasons: the generation of diffuses tumors and the low incidence of nodules over-expressing Mad2, it impairs tumor measurement and staining quantifications in tumors sub-categories.

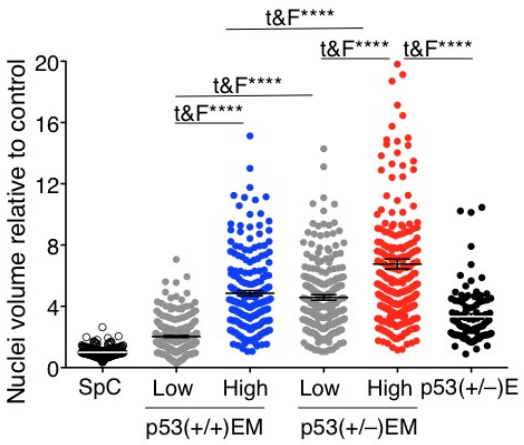

Figure 3.22: Mad2 High nodules are mainly composed aneuploidy cells. Quantification of the nuclear size relative to wild-type control cells, Y axis log2 scale, indicating an increase on the nuclear size and size variability upon Mad2 over-expression (unpaired *t*-test and F test: ****p <0.0001). The average volumes: p53(+/+)EM low: 2 (2.030 ± 0.06550 n=259 nuclei), p53(+/+)EM high: 4.9 (4.851 ± 0.1750 n=204 nuclei), p53(+/–)EM low: 4.6 (4.579 ± 0.1746 n=247 nuclei), p53 (+/–)EM high: 6.8 (6.757 ± 0.3193 n=276 nuclei), p53(+/–)E: 3.3 (3.337 ± 0.1752 n=101 nuclei).

3.6 High levels of Mad2 impairs Kras lung tumor growth in the p53 wild-type background.

3.6.1 Kinetics of Kras tumorigenesis in p53 wild-type compare to p53 heterozygote, with or with out Mad2 over-expression

It appeared to me that the combination of Mad2 over-expression together with impaired p53 is detrimental in the EGFR model (Figure 3.20) and Mad2 is detrimental for p53(+/–)Kras tumorigenesis (Figure 3.1). Detailed analysis of the p53(+/–)Kras model suggested that the detrimental effect of Mad2 is predominantly exerted prior to tumorigenesis, as a result very few nodules with high levels of Mad2 were generated in the p53 heterozygote background (Figure 3.10 and 3.19). This particular fatal combination seems to be due to permissiveness produced by the inactivation of one

copy of p53 towards the aneuploidy generated by Mad2 (Figure 3.7). However, since one copy of p53 is able to induce cell cycle arrest in the Mad2 expressing tumors, it remained unclear to me how Mad2 over-expression benefits Kras tumors progression in the p53 wild-type background, in which they are two functional p53 copies. For these reasons, I decided to compare the effect of Mad2 over-expression on Kras tumorigenesis in the p53 wild-type and p53(+/–) backgrounds simultaneously.

Because the method is faster and commonly employed than survival curves for monitoring lung tumorigenesis, I followed the kinetics of tumorigenisis by histology in the four following mice cohorts: p53(+/+)K, p53(+/+)KM, p53(+/–)KM, and p53(+/–)KM at two time points of transgene induction, 15 weeks and more than 20 weeks (Figure 3.23 A). In this experiment the more than 20 weeks time point has a sharper time window (25 to 29 weeks) than in the figure (Figure 3. 2). In the previous experiment the mice were humane end point and exceeded this time window. First I observed that at 15 weeks of transgenes induction, the tumorigenesis in the p53(+/–)K was more advanced than in the p53(+/+)Kras lungs, until the lungs reached saturation in both cohorts (at >20 weeks, 50% of the lungs were occupied by tumors, Figure 3.23 B and C). Furthermore, Mad2 over-expression delayed p53(+/–)K induced tumorigenesis at 15 weeks and this difference faded over time (Figure 3.23), these results confirms previous findings (Figure 3. 2). In the p53 wild-type background, Mad2 over-expression delayed Kras tumorigenesis (Figure 3.23 B and C) however, it remains unclear what would be the long-term effect on mice survival. In fact, Mad2 over-expression in the p53 wild-type EGFR background appeared to be detrimental since high Mad2 expressing nodules were selected against however; the mice survival was not significantly prolonged. Therefore, it is possible that Mad2 over-expression in the p53 wild-type background would have no effect or could increase the Kras tumor free survival of the mice. Importantly at 15 weeks, the detrimental effect of Mad2 was more visible in the p53(+/–)K cohort, since the default tumorigenesis was more potent (Figure 3. 23 B). In a simple model where tumor would grow exponentially, the earlier and the strongest Mad2 detrimental effect is, the later mice will succumb of lung tumors.

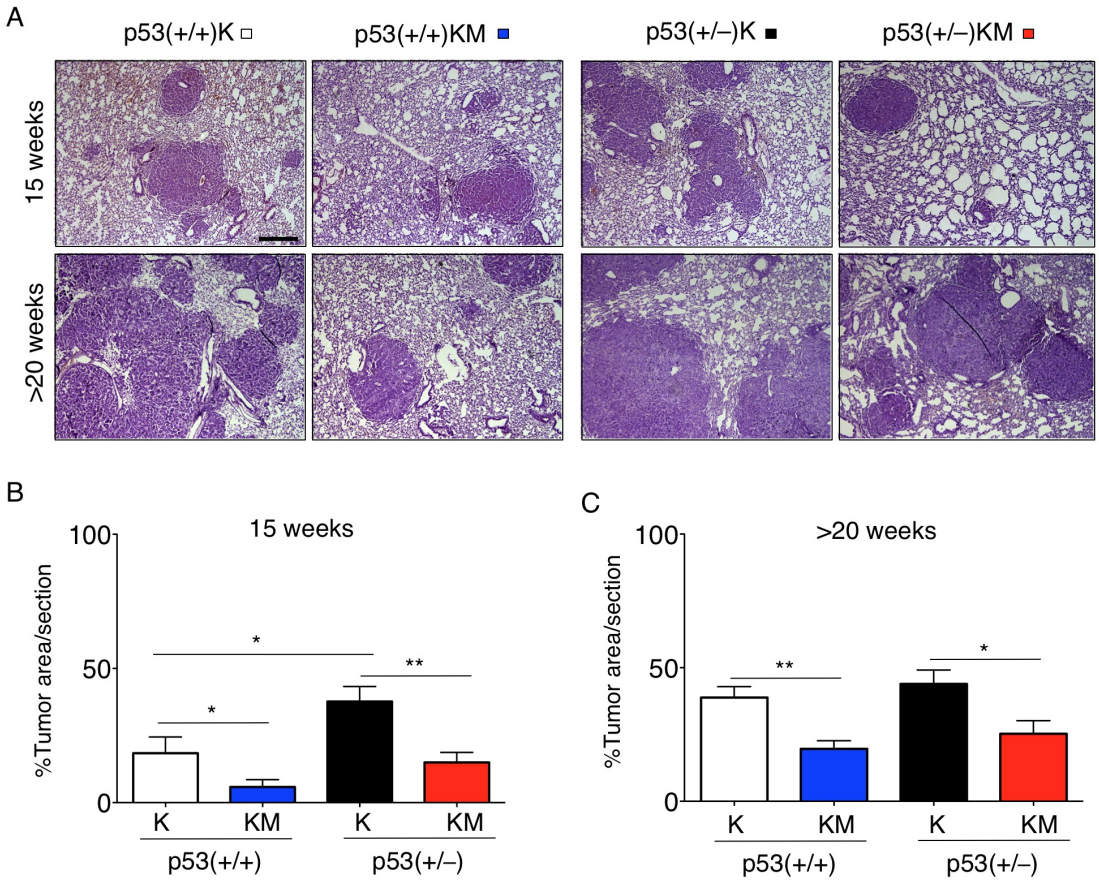

Figure 3.23: Mad2 delays Kras driven lung tumorigenesis at two time points. A) Kinetics of tumorigenesis in p53(+/+)K and p53(+/+)KM, p53(+/–)K and p53(+/–)KM mice. H&E staining at 15 weeks and >20 weeks after transgene induction. Scale bar 500μm. **B**) Percentage of tumor area per lung section after 15 weeks of transgenes induction. Data indicating a delays in tumorigenesis upon Mad2 over-expression, that is more evident in the p53(+/–) than in the p53(+/+) background (p53(+/+)K= 18.42% n=10 mice, p53(+/+)KM= 5.84% n=19 mice, p53(+/–)K = 37.69 % n=10 mice, p53(+/–)KM = 14.95% n=16 mice; unpaired *t*-test $^{*}p<0.05$, $^{**}p<0.01$). **C**) Percentage of tumor area per lung section after >20 weeks of transgenes induction. Data indicating a delays in tumorigenesis upon Mad2 over-expression (p53(+/+)K= 38.81% n=6 mice, p53(+/+)KM= 19.63% n=16 mice, p53(+/–)K = 43.90 % n=11 mice, p53(+/–)KM = 25.29% n=9 mice; unpaired *t*-test $^{**}p<0.01$).

3.6.2 Mad2 over-expression induces p21 and inhibits p53(+/+)Kras tumor proliferation

I reasoned that if one copy of p53 and Mad2 over-expression can induce p21, it is also probably the case in the presence of two copies of p53. In fact, I observed similar induction of the p53 targets in aged tumors with high levels of Mad2 with one or two copies of p53 (Figure 3.17). To confirm the induction of p21 at an early time points and analyze the effect on tumor proliferation, I analyzed tumors coming from p53(+/+)K

and p53(+/+)KM mice. Similarly to the previous analysis tumors were generated by 15 weeks of transgenes induction. Using immunohistochemistry I classified the tumors depending on their genotype and their HA-Mad2 expression (Figure 3.24 A), I analyzed the tumors for p21 induction and BrdU incorporation.

In early stage tumors, I observed a significant increase of p21 positive cells and decrease of BrdU positive cells in High Mad2 nodules compared to the control tumors (Figure 3.24 B and C), suggesting a G1 mediated arrested also in this background. The fact that the control p53(+/+)Kras tumors appears to have more p21 induction than the p53(+/–)K at early time point (23 *Vs*. 48 positive cells per tumor area, Figure 3.12 E and 3.24) together with the fact that p53(+/+)Kras tumors are smaller than p53(+/–)K at 15 weeks (Figure 3.23) suggests that having only one copy of p53 accelerates Kras tumorigenesis in this thesis. I speculate that Kras cells over expressing Mad2 have a reduced chance to accumulate instability compare to the p53(+/–)K cells. With two copies of p53 the Kras cells seem to have a better control of the cell cycle (e.g mitotic block, transformation) than the p53(+/–)K cells. However, even if Kras and Mad2 produces moderate instability compare to the tumors in the p53 heterozygote background, all the tumors over-expressing Mad2 are arrested in G1.

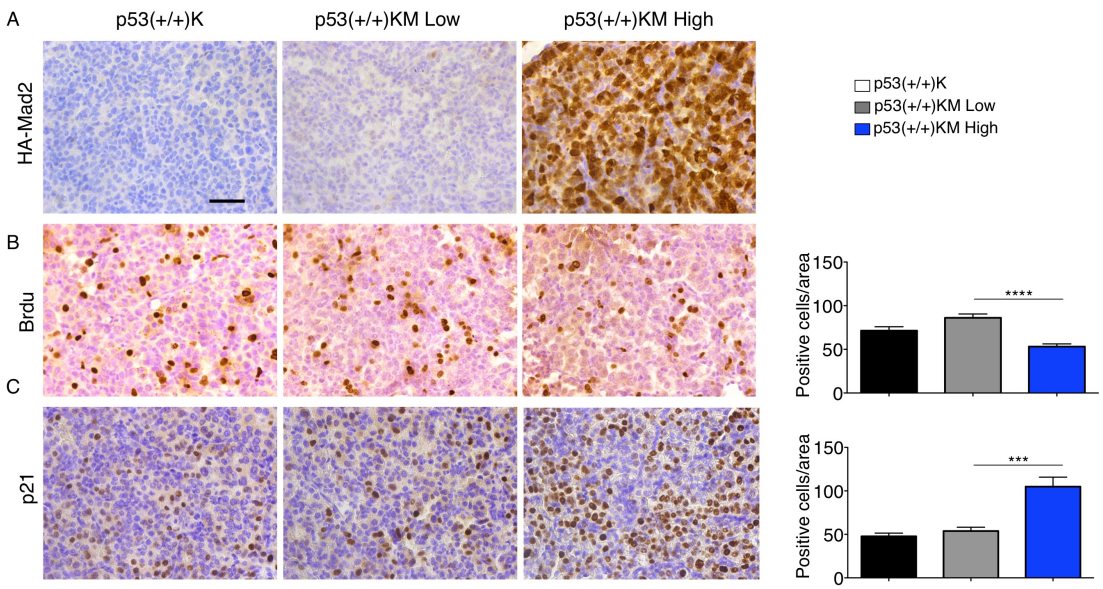

Figure 3.24: Mad2 expression in p53 wild-type Kras lung nodules induces p21 and inhibits proliferation. A) HA immunostaining of early tumors after 15 weeks of transgenes induction. Scale bar 50 µm. **B)** BrdU staining after one day of labelling showing the reduced number of BrdU positive cells in High Mad2 tumors, indicating the decrease of proliferation upon Mad2 over-expression (p53(+/+)K: 71.40 ± 4.528 n=42 tumors from 6 mice, p53(+/+)KM Low: 86.16

± 4.358 n=18 tumors from 4 mice, p53(+/+)KM High : 53.19 ± 3.098 n=24 tumors from 8 mice, unpaired *t*-test ****p<0.0001). **C)** P21 staining showing the high number of p21 positive cells in High Mad2 tumors indicating a G1 arrest upon Mad2 over-expression (p53(+/+)K: 47.73 ± 3. 748 n=37 tumors from 5 mice, p53(+/+)KM Low: 53.84 ± 4.382 n=19 tumors from 4 mice, p53(+/+)KM High : 104.9 ± 10.90 n=20 tumors from 5 mice, unpaired *t*-test ***p<0.001).

I observed that the difference in tumor area in aged p53(+/+)K and p53(+/+)KM remained visible over-time (Figure 3.23 C). I hypothesized that the growth repression induced by p21 could be maintained at later stages during tumor growth. As expected, immunostaining against p21 on aged-tumors (from 25 weeks to 34 weeks of induction) from p53(+/+)KM animals remained positive for p21 upon Mad2 over-expression (Figure 3.25) however, it was also decreased in the p53(+/+)KM high aged-tumors in comparison to the early ones (105 *Vs*. 71 positive cells per tumor area p<0.01 , Figure 3.24 C and 3.25). I observed that p53 (+/–) tumors loose the wild-type copy of p53 that reduce the expression of p21, however it is unlikely that the tumors loose the two alleles of p53. How the p53 wild-type tumors expressing high levels of Mad2 are able to reduce the p21 induction remains unknown and could be addressed in the future.

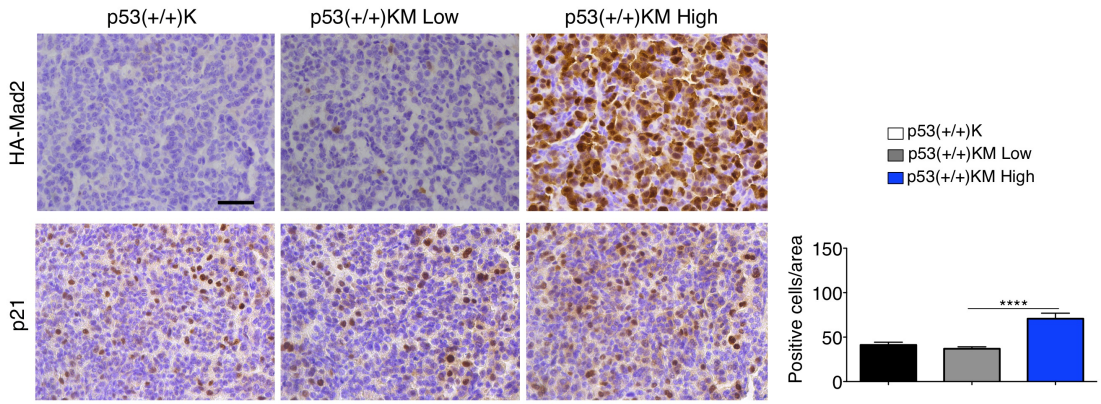

Figure 3.26: Mad2 expression in late stage p53 wild-type Kras lung nodules induces p21. Upper panel) HA immunostaining of early tumors after at least 20 weeks of transgenes induction. Scale bar 50 μm. **Lower panel)** P21 staining in aged tumors showing the activation of p21 upon Mad2 over-expression (p53(+/+)K: 41.21 ± 3.129 n=29 tumors from 5 mice, p53(+/+)KM Low: 36.98 ± 2.188 n=31 tumors from 7 mice, p53(+/+)KM High : 70.74 ± 6.204 n=23 tumors from 8 mice, unpaired t-test ****p<0.0001).

4 Discussion

4.1 Construction of a Model

The results of my work indicate that Mad2 delays Kras and EGFR tumorigenesis in the context of p53 partial inactivation. Work from my colleagues, who are studying similar combinations of oncogenes together with Mad2 in the breast, supports the fact that Mad2 over-expression is detrimental to tumorigenesis. Specifically, in the p53 wild-type mouse model, Mad2 delays Kras-induced breast cancer (in preparation, Konstantina Rowald). Furthermore, Mad2's detrimental effect on Her2 and on Myc-induced breast cancer was previously described in Martina Mantovan's PhD thesis (Autonomous University of Madrid). In addition, my results suggest that the negative effects of Mad2 are exacerbated in the context of p53 partial inactivation in lung tumors driven by the Kras or EGFR oncogene, however it remains unclear if this is the case in other cancer types.

In this thesis, I classified tumorigenesis in three stages (Figure 4.1). Initially, Mad2 over-expression impairs proliferation in both p53 backgrounds due a primary mitotic block. However, the cell fate outcomes differ depending on the p53 background. I hypothesize that, prior to tumorigenesis, the inactivation of one allele of p53 results in a less stringent control of the cell cycle. Firstly, cancer is the result of uncontrolled cell growth and Kras tumorigenesis is enhanced upon p53 partial inactivation. Second, early passage MEFs challenged by Mad2 over-expression do not succumb to mitotic death in the p53 (+/–) background and do not die in interphase during imaging. Reduction of p53 leads to weak cell cycle control, and together with Mad2 over-expression generates highly instable cells, which, in turn, impairs cellular transformation (Figure 4.1 A). The clearance of cells with high levels of aneuploidy in the p53 wild-type tissues may attenuate the detrimental effect of Mad2 on tumorigenesis. The elimination of defective type two pneumocytes could fuel their re-generation and increase the chance for a clone transformation with high levels of Mad2.

In the context of simultaneous Mad2 and Kras over-expression, the p53 background influences the selection of clones, giving rise to tumors. At the tumor stage, one copy of p53 is sufficient to induce G1 arrest. Mad2 over-expression induces the expression of p21 in the p53(+/+) and p53(+/–) tumors, but not in the p53(–/–)tumors. Furthermore, the response to Mad2 over-expression was not restricted to p21, but also included other

p53 targets, confirming the p53-mediated response. As a consequence, the tumors over-expressing Mad2 had decreased proliferative potential with one or two copies of p53 (Figure 4.1 B). At a later stage of tumorigenesis, Mad2 did not influence the loss of the remaining copy of p53. However, complete inactivation of p53 served as a compensatory mechanism to the few nodules expressing high levels of Mad2. In general, the late spontaneous loss of p53 was not sufficient for counteracting the strong selection occurring prior to tumorigenesis in the p53(+/–)KM lung tissues (Figure 4.1 C). A hypothesis for the strong selection in the p53(+/–)KM lung is that the defective type II pneumocytes are not being eliminated due to the impaired p53 function, reducing their chance for transformation. In the p53 wild-type background it remains unclear how the tumors expressing Mad2 compensate for the cell cycle arrest, they could mutate one p53 allele and generate a dominate negative p53 form that would reduce the induction of p21 or act down stream of p21.

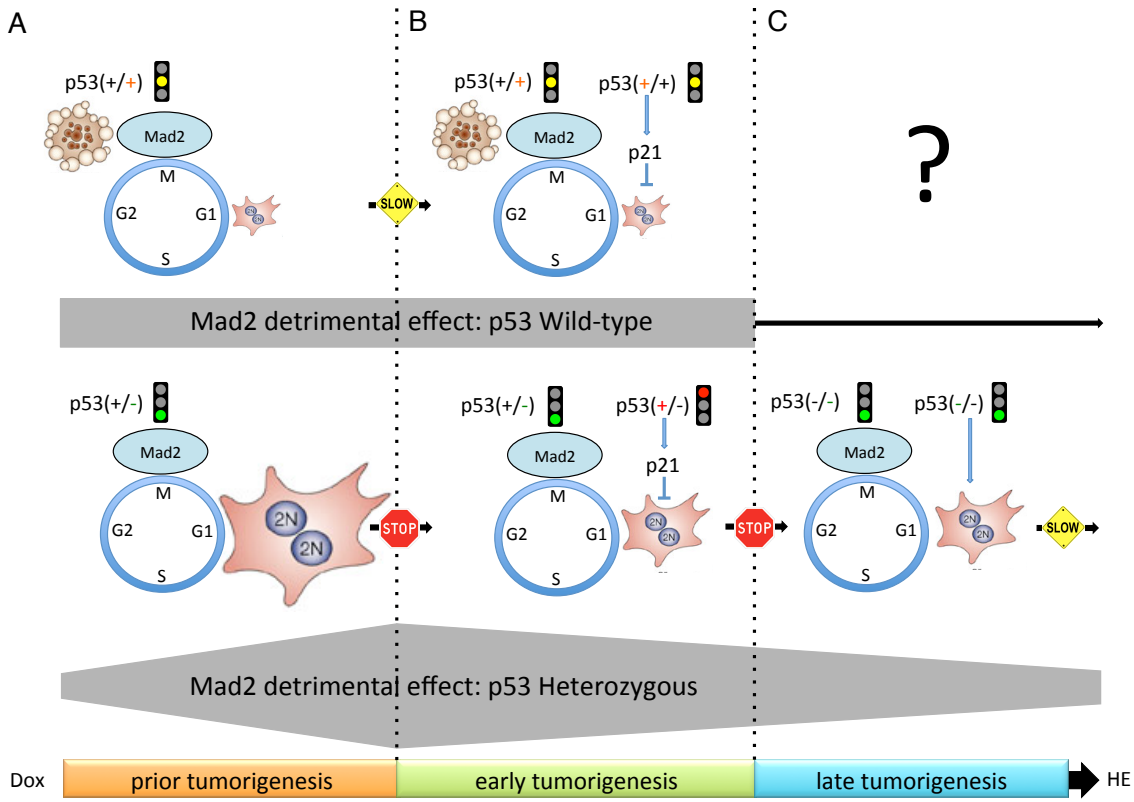

Figure 4.1: Findings model: Tumorigenesis is divided in 3 stages after doxycycline induction (Dox), prior tumorigenesis (orange, **A**): early tumorigenesis (green, **B**), and late tumorigenesis (blue, **C**) until humane end point (HE). The gray shapes represent the intensity of Mad2 detrimental effect on lung tumorigenesis over time. **Upper part** in the p53 wild-type background, **Lower part** in the p53(+/-) background. The blebbing cell represents cell death and the 2 times 2N cell and its size represents the amount of aneuploid cells, always in the

context of Mad2 over expression (bleu round shape). The traffic light signs indicate the effect of p53 dosage in mitosis in **A**, **B** and **C**, and in G1 in **B** and **C**. The left dashed line symbolizes the cell malignant transformation and the right one the tumor progression and it is qualified by the signs STOP or SLOW. **A)** Even if Mad2 induces a mitotic arrest in both conditions Mad2 produces more aneuploid cells in the p53 (+/–) background and impairs cellular transformation, most of the cells arrested in mitosis are eliminated in the p53 wild-type background. **B)** The remaining wild-type copy of p53 activates its target p21 to arrest aneuploidy cells in G1. The Mad2 detrimental effect on tumor progression is more pronounced in the p53 (+/–) since it produces more aneuploidy cells. **C)** Loss of the p53 wild-type copy suppresses the G1 arrest but increase aneuploidy leading to slow tumor progression. It remains unclear how tumor progression occurs in the in the p53 wild-type background and how the G1 arrest is by-passed.

4.2 New mouse models?

In this thesis, the partial inactivation of p53 was achieved by inactivation of one allele from the day of conception modeling of the Li-Fraumeni syndrome, which is characterized by germ-line mutations of p53, for which rare sufferers have predisposition to cancer (Li and Fraumeni, 1969). Because tumorigenesis in mouse models can be time-consuming, the p53(+/–) mouse model (Jacks et al., 1994) has become a tool for the acceleration of tumorigenesis. Additionally, human tumors are more instable than the murine tumors, so model-increasing CIN was used to faithfully mimic the instability of human tumors (Janssen and Medema, 2013). The combination of Mad2 and Kras over-expression in fact led to instable tumors (Sotillo et al., 2010). However, combining the two mouse lines for accelerating tumorigenesis failed and resulted in a further delay. Since partial inactivation of p53 is not directly relevant for lung cancer, the work should be complemented using inducible forms of modified p53 (see section 1.4).

Whether aneuploidy is a cause or a consequence of cellular transformation is frequently debated. The fact that chromosome abnormalities do not occur in isolation together with the fact that mutations of the SAC genes are extremely rare in cancer (Carter et al., 2006), made it challenging to identify aneuploidy as the initiating event. The over-expression of SAC components found in cancer could be the result of tumor-increased proliferation and the inactivation of tumor suppressors (Schvartzman et al., 2011). It is also possible that over-expression of SAC components does not result in SAC over-activation. It would be interesting to determine the stoichiometry of the SAC components in human tumors. Nevertheless, it appears that aneuploidy leads to late latency murine tumors (see section 1.8), though this has been done in extreme settings

such as SAC gene knockdown or over-expression. Importantly, the results could also come from additional SAC-independent protein functions. All together, these findings support the hypothesis that aneuploidy is the result of a deregulated cell cycle by driver oncogenes and tumor-suppressor inactivation. Thus, it might be of interest to decouple tumor generation and the induction of CIN in mouse models. In this thesis, it was not possible since Mad2 and Kras or EGFR were induced simultaneously by doxycycline. To closely simulate human disease, if would be of interest to combine relevant p53 modifications with a mouse model in which transgenes can be induced independently.

4.3 SELECTION

The modulation of the expression of SAC components leads to genomic instability, but has variable effects on tumorigenesis: spontaneous late latency tumors (see section 1.8) or various degrees of delayed tumorigenesis (this thesis). Using the Tet-On transgenic system, I noticed that different tumor populations (expressing low to high levels of Mad2) have co-evolved from an original population of Mad2 expressing type 2 pneumocytes. *In vivo*, low Mad2-expressing nodules were over-represented in almost all mouse models analyzed, suggesting that high Mad2 levels are selected against during tumorigenesis. In addition, MEFs over-expressing Mad2, if not dead, are quickly over-taken in culture by low expressing cells. The use of a moderate over-expression transgenic system would be more appropriate for further *in vitro* experiments.

I propose that co-evolution of the Mad2 tumor types is the result of selection mechanisms occurring prior to tumorigenesis (Figure 4.2). Considering that spontaneous models of tumorigenesis have tissue in quasi-homeostasis (Sotillo et al., 2007) and that transgenic cancer models undergo rapid tumorigenesis, it is possible that different selective pressures take place. In reference to evolution and organisms development, a crucial step during the process of Darwinian evolution is genetic stabilization, making the new species (or tumor) independent of its environment. This requirement is indeed compromised in the models with a rapid onset of cancer. In late latency tumors, the amount of CIN has probably been ‘shaped’ and ‘stabilized’ to a certain degree. Importantly, a slow proliferation rate and putative stabilization have been linked to tumor aggressiveness (Anjomshoaa et al., 2009).

If genetic stabilization is precluded, it is possible for an organism or a tumor cell to adapt to its environment. If Mad2 over-expression is initially normally distributed, the

cells expressing the lowest amount of Mad2 were directionally selected prior to tumor formation (Figure 4.2). Mad2-expressing tumors in the p53(+/–) background were extremely under-represented, suggesting that they persisted until a random event produced the required modification for their development; such as p53 loss of heterozygosity. In other words, implementing strong constraints on organism/cell that preclude stabilization in their environment will frustrate its reproduction/growth and its survival. Random selection is being considered as the mechanism in which cancer clones are generated, with each round of mutation giving growth advantages to a random cell. Genomic instability by means of random selection could benefit the Mad2 opportunistic cells resistant to cancer therapies, giving rise to relapse (Sotillo et al., 2010). Moreover, these scenarios could explain the frequent differences between *in vivo* and *in vitro* observations.

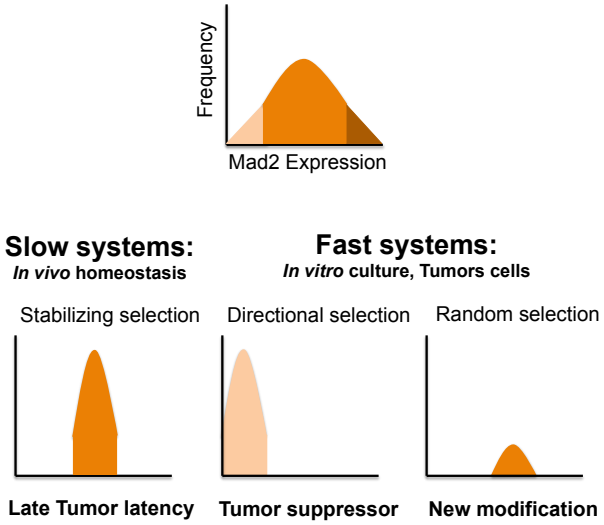

Figure 4.2: Putative selection mechanisms. Assuming that Mad2 is normally distributed among the equipped transgenic cells, some cells should express less Mad2 than average. In systems with slow growth, high Mad2 levels could be integrated and stabilized giving rise to late tumors. In system with high population doubling, Mad2 over-expression is selected against but it can eventually be maintain if a random event allows its tolerance.

4.4 ANEUPLOIDY LEVELS

The generation of low Mad2-expressing tumor can be due to an initial variability of induction, or to mechanisms reducing transgene expression. A hypothesis could be that the transgene promoters have been methylated. In this study, Kras and Mad2 are induced by the same rtTA. Even if I did not verify rtTA and Kras expression, it is very likely that they are expressed in tumors since Kras is required for tumorigenesis (Fisher et al., 2001). A probable explanation in the context of an instable genome is that the Mad2 transgene has been eliminated. However, I verified the presence of the Mad2 transgene by PCR in the low expressing tumors analyzed in section 3.16 (data not shown). It is likely that the mosaic nature of the Tet-On system resulted in low expressing cells from the beginning of the induction. In fact, cells would benefit twice from the low induction of the transgenes given that high levels of Kras would push cells into senescence. The pattern of Kras expression could not be followed due to the lack of reliable antibodies for IHC. In a recent study using the Tet-On system, the over-expression of the two types of Cyclins B produced tumors; whether the tumors maintained transgene expression was not shown (Nam and van Deursen, 2014). *In vivo,* I have analyzed tumors from the opposite spectrum of expression and noticed the detrimental effect of Mad2 in the tumors expressing the most. The impact of low levels of Mad2 over-expression on tumorigenesis remains unclear and, thus, a model inducing uniform lower levels of Mad2 should be used.

The hypothesis that the amount of aneuploidy is responsible for the switch between tumor suppression and promotion has prompted labs to look for a critical aneuploidy threshold. Experiments aimed at determining the extent to which CIN or aneuploidy can be tolerated and affect tumorigenesis are not straightforward since quantitative detection of aneuploidy in tissue samples remains challenging. Often the interpretations on this matter come from extrapolation of results from cells derived from the mouse models (*e.g* MEFs, splenocytes) and the *in vitro* result does not always reflect the *in vivo* phenotypes. In addition, the multitude of ways in which to induce cancer in a mouse adds a layer of complexity when one decides to harmonize the findings. As an example, mice over-expressing Mad2 using the CMV (ubiquitous (Sotillo et al., 2007)) develop lung tumors, but it is not the case when the transgene is over-expressed under the influence of the CCSP promoter (lung epithelium (Sotillo et al., 2010)). Furthermore, the side effects of the transgenic systems could make it difficult to compare studies with

different inducible strategies. If fact, a recent study has shown that doxycycline disturb mitochondrial function in model organisms including mice (Moullan et al., 2015). Harmonization of the "amount of aneuploidy" data could be beneficial to clarify the role of aneuploidy on murine tumorigenesis. One approach could be via centralized pipelines similar to the methodology championed at the International Knockout Mouse Consortium (Bradley et al., 2012). Another way could be to order studies' key experiments from an external platform. Nevertheless, a recent report has suggested that the rate of chromosome mis-segregation was the relevant parameter and not the amount of aneuploidy *per se*. The authors suggested that low rates of chromosome mis-segregation promote tumorigenesis, while increased mis-segregation leads to tumor suppression (Silk et al., 2013). An additional insight coming from the tumor analysis in this thesis is that the faster the tumorigenesis is, the higher the inherent CIN, and the less Mad2 is tolerated. In light of the previous study (Silk et al., 2013), I hypothesize that p53(+/-)K increased the proliferation rate and leads to an increase of mis-segregation rate upon Mad2 over-expression.

4.5 Replicative stress

A simple explanation for the CIN increase in cells with a high proliferation rate with over-activated SAC is that cells are undergoing frequent defective mitosis. Alternatively, but not exclusively, in fast cycling cells, the lack of preparation before replication could result in replicative stress and additional CIN. A study has shown that supplying extra nucleotides to a CIN cell line reduced the segregation errors (Burrell et al., 2013). In line with this, a study has shown that aneuploidy leads to the over-expression of nucleic acid metabolism genes (Torres et al., 2007), suggesting the possibility of replicative stress. Furthermore, lagging chromosomes can be encapsulated in micronuclei and are a major source of DNA damage after mitotic failure (Terradas et al., 2010). Moreover, micronuclei have been shown to be replicating in G2 (Crasta et al., 2012) and their fate is still open to debate. When micronuclei break (Hatch et al., 2013), the DNA can be re-incorporated into the genome, leading to catastrophic DNA rearrangements, a phenomenon called Chromothripsis likened to p53 mutations (Rausch et al., 2012). I noticed the formation of micronuclei during a time-lapse microscopy experiment (data not shown), though this line of research was not investigated. I hypothesize that Mad2-induced failure of mitosis in the context of partially impaired p53 produces micronuclei and might exacerbate the CIN phenotype by inducing

replicative stress. Moreover, the removal of p53 in mouse prone to replicative stress was expected to rescue the DNA damage and the opposite happened (Murga et al., 2009), demonstrating the role of p53 in limiting replicative stress. The expression of the p53 target GADD45a is linked to DNA damage (Walmsley and Tate, 2012); in this thesis, I show the up-regulation of GADD45a in Mad2-expressing tumors. However, I did not observe the induction of DNA damage in pilot experiments (data not shown). Nonetheless, further experiments could investigate the effect of replicative stress on SAC function and mitotic fidelity.

4.6 p53 CELL CYCLE ARREST

Inactivation of one copy of p53 was sufficient to rescue mitotic cell death induced by high levels of Mad2 and leads to the generation of polyploid MEFs after slippage. It is generally accepted that aneuploidy results in gene dosage imbalance and proteotoxicity and impairs cellular fitness and growth (Pavelka et al., 2010; Segal and McCoy, 1974; Tang et al., 2011; Torres et al., 2007; Williams et al., 2008). How aneuploid cells cope with the unbalanced gene dosage remains unclear. Polyploidization has been proposed as a mechanism to reduce the negative effect of aneuploidy (Varetti et al., 2014). Multiple copies of the genome could rescue the loss of single chromosomes. Accordingly, whole-genome doubling was found in 37% of cancers and was associated with p53 mutations (Zack et al., 2013). However, polyploidization induces endoplasmic reticulum stress, which is recognized by an immune-surveillance mechanism for ploidy (Senovilla et al., 2012). It remains unclear in this thesis whether the p53 background altered immune surveillance and impinged on tumor development. The survival of p53 heterozygote MEFs in response to Mad2 over-expression is consistent with previous observations in cell lines. The deletion of the p53 gene enhances mitotic slippage (Marxer et al., 2014), it enhances CIN upon Mad2 deletion, and it is required to generate a CIN phenotype (Burds et al., 2005; Li et al., 2010; Thompson and Compton, 2010). Using high-throughput time-lapse microscopy, a study proposed a model where cell fate after mitotic arrest (death or slippage) depends on what threshold is breached first: apoptotic activity or Cyclin B1 degradation (Gascoigne and Taylor, 2008). Current knowledge indicates that mitotic death is due to the reduction of anti-apoptotic proteins (Harley et al., 2010; Shi et al., 2011), and the fact that cytoplasmic p53 is capable of regulating them (Kim et al., 2014) could explain why p53(+/–)KM MEFs are resistant to mitotic death. Nevertheless, this hypothesis still remains to be addressed, although

information on the role of the cytoplasmic p53 in mitotic death is very limited. Research on the role of p53 in mitotic catastrophe could be further developed using MEFs derived from different p53 mouse models (see section 1.4) together with the use of biosensors that would report its activities in real time.

Increasing evidence from several mouse models have underscored the tumor-suppressor effect of aneuploidy on late-stage tumorigenesis (Varetti et al., 2014). However, the consequences of aneuploidy on tumor progression have not yet been fully addressed. Here, I show that Mad2 over-expression leads to cell cycle arrest by inducing the p53 target gene p21. These results are in line with a previous study, showing that p21 contributes to the maintenance of chromosome stability and prevents lymphomagenesis (Barboza et al., 2006). It is likely that in an impaired p53 context, Mad2 over-expression increases the level of CIN that can be later counteracted by p21 induction in lung tumors. It is unclear whether cell cycle arrest has been induced directly after one or several mitotic blocks given that tetraploid cells can go through mitosis but also arrest in G1 (Kuffer et al., 2013). At an early stage of tumorigenesis, nodules expressing Mad2 in p53(+/–) animals rely on one wild-type copy of p53 to induce G1 arrest. The fate of the arrested cells, since pro-apoptotic genes were up-regulated, remains unclear, and it is possible that they die. However, I did not observe cell death *in vivo*; another alternative is that the cells re-enter the cell cycle.

Analysis of late stage tumors showed that complete loss of p53 increases the tolerance for Mad2 over-expression. This result is not surprising since a study using mitotic drugs on human cell lines has shown that aneuploidy-induced cell cycle arrest mediated by p21 does not occur in p53-deficient cells (Thompson and Compton, 2010). However, lung tumors over-expressing Mad2 in the complete p53 KO model remained smaller. These data show that p53 complete KO would not be sufficient to restore the detrimental effect of Mad2 on lung tumorigenesis. The van Deursen lab has shown that in p53 heterozygous mice, CIN leads to p53 loss of heterozygosity (LOH) and accelerates lymphomagenesis. However, it remains unclear how CIN delayed prostatic cancer in a model heterozygote for the tumor suppressor Pten (Baker et al., 2009). In this thesis, Mad2 over-expression failed to increase p53 LOH because high levels of Mad2 were first selected against. CIN is proposed to actively induce loss of chromosomes containing tumor-suppressor genes (Sotillo et al., 2009). My thesis suggests a rather passive mechanism where clones are selected for LOH to counteract

the negative effect of CIN. This hypothesis should be further confirmed with other tumor suppressors.

4.7 THE SAC AS A THERAPEUTIC TARGET

The result of this study supports the hypothesis that in the long term, mitotic slippage and enhanced instability impairs lung tumor development and growth. Since only 30% of patients with NSCLC show a partial response to taxane-based therapy, a recent study using NSCL cancer cell lines has shown that increasing the duration of mitotic arrest increases the efficacy of the chemotherapeutic agent Paclitaxel (Sinnott et al., 2014). Moreover, the inhibition of the SAC Mps1 kinase increased the sensitivity of cancer cells to chemotherapeutic agents (Tannous et al., 2013). In human breast tumor samples, the clinically relevant concentration of Paclitaxel was low and induces chromosome mis-segregation (Zasadil et al., 2014). Moreover, a low dosage of Paclitaxel induces aneuploidy in cell lines and is sufficient to induce G1 arrest (Giannakakou et al., 2001). Interestingly, using intra-vital imaging in mice has shown that the chemotherapeutical agent Docetaxel had anti-tumor effects by means other than mitotic perturbation (Janssen et al., 2013), suggesting the need for improving the efficacy of chemotherapeutic agents. Kras mutations and p53 dysfunction can initially induce mitotic stress (Luo et al., 2009) and CIN (Burds et al., 2005; Thompson and Compton, 2010). The results of this thesis suggest a therapeutic strategy for lung adenocarcinomas by combining anti-mitotic agents (targeting microtubules or mitotic spindle) with drugs that increase CIN. Determining if and how the SAC is over-activated in tumor would help to find the best strategy.

LITERATURE

Abdel-Rahman, W.M., Katsura, K., Rens, W., Gorman, P.A., Sheer, D., Bicknell, D., Bodmer, W.F., Arends, M.J., Wyllie, A.H., and Edwards, P.A. (2001). Spectral karyotyping suggests additional subsets of colorectal cancers characterized by pattern of chromosome rearrangement. Proc Natl Acad Sci U S A *98*, 2538-2543.

Anjomshoaa, A., Nasri, S., Humar, B., McCall, J.L., Chatterjee, A., Yoon, H.S., McNoe, L., Black, M.A., and Reeve, A.E. (2009). Slow proliferation as a biological feature of colorectal cancer metastasis. British journal of cancer *101*, 822-828.

Baker, D.J., Jin, F., Jeganathan, K.B., and van Deursen, J.M. (2009). Whole chromosome instability caused by Bub1 insufficiency drives tumorigenesis through tumor suppressor gene loss of heterozygosity. Cancer Cell *16*, 475-486.

Bakhoum, S.F., Thompson, S.L., Manning, A.L., and Compton, D.A. (2009). Genome stability is ensured by temporal control of kinetochore-microtubule dynamics. Nature cell biology *11*, 27-35.

Baltimore, D. (1970). RNA-dependent DNA polymerase in virions of RNA tumour viruses. Nature *226*, 1209-1211.

Banfield, W.G., Woke, P.A., Mackay, C.M., and Cooper, H.L. (1965). Mosquito Transmission of a Reticulum Cell Sarcoma of Hamsters. Science *148*, 1239-1240.

Barboza, J.A., Liu, G., Ju, Z., El-Naggar, A.K., and Lozano, G. (2006). p21 delays tumor onset by preservation of chromosomal stability. Proc Natl Acad Sci U S A *103*, 19842-19847.

Bloecher, A., Venturi, G.M., and Tatchell, K. (2000). Anaphase spindle position is monitored by the BUB2 checkpoint. Nature cell biology *2*, 556-558.

Boveri, T. (1914). Frage der Entwicklung maligner Tumoren. (Jena, Germany: G. Fischer).

Bradley, A., Anastassiadis, K., Ayadi, A., Battey, J.F., Bell, C., Birling, M.C., Bottomley, J., Brown, S.D., Burger, A., Bult, C.J., *et al*. (2012). The mammalian gene function resource: the International Knockout Mouse Consortium. Mammalian genome : official journal of the International Mammalian Genome Society *23*, 580-586.

Breasted, J.H., and New York, h.s. (1930). The Edwin Smith surgical papyrus (Chicago, Ill.,: The University of Chicago press).

Brocard, J., Warot, X., Wendling, O., Messaddeq, N., Vonesch, J.L., Chambon, P., and Metzger, D. (1997). Spatio-temporally controlled site-specific somatic mutagenesis in the mouse. Proc Natl Acad Sci U S A *94*, 14559-14563.

Burds, A.A., Lutum, A.S., and Sorger, P.K. (2005). Generating chromosome instability through the simultaneous deletion of Mad2 and p53. Proc Natl Acad Sci U S A *102*, 11296-11301.

Burrell, R.A., McClelland, S.E., Endesfelder, D., Groth, P., Weller, M.C., Shaikh, N., Domingo, E., Kanu, N., Dewhurst, S.M., Gronroos, E., *et al*. (2013). Replication stress links structural and numerical cancer chromosomal instability. Nature *494*, 492-496.

Carter, S.L., Eklund, A.C., Kohane, I.S., Harris, L.N., and Szallasi, Z. (2006). A signature of chromosomal instability inferred from gene expression profiles predicts clinical outcome in multiple human cancers. Nat Genet *38*, 1043-1048.

Chao, C., Hergenhahn, M., Kaeser, M.D., Wu, Z., Saito, S., Iggo, R., Hollstein, M., Appella, E., and Xu, Y. (2003). Cell type- and promoter-specific roles of Ser18 phosphorylation in regulating p53 responses. J Biol Chem *278*, 41028-41033.

Chen, Z., Fillmore, C.M., Hammerman, P.S., Kim, C.F., and Wong, K.K. (2014). Non-small-cell lung cancers: a heterogeneous set of diseases. Nat Rev Cancer *14*, 535-546.

Choi, C.M., Seo, K.W., Jang, S.J., Oh, Y.M., Shim, T.S., Kim, W.S., Lee, D.S., and Lee, S.D. (2009). Chromosomal instability is a risk factor for poor prognosis of adenocarcinoma of the lung: Fluorescence in situ hybridization analysis of paraffin-embedded tissue from Korean patients. Lung cancer *64*, 66-70.

Collado, M., Gil, J., Efeyan, A., Guerra, C., Schuhmacher, A.J., Barradas, M., Benguria, A., Zaballos, A., Flores, J.M., Barbacid, M., *et al*. (2005). Tumour biology: senescence in premalignant tumours. Nature *436*, 642.

Crasta, K., Ganem, N.J., Dagher, R., Lantermann, A.B., Ivanova, E.V., Pan, Y., Nezi, L., Protopopov, A., Chowdhury, D., and Pellman, D. (2012). DNA breaks and chromosome pulverization from errors in mitosis. Nature *482*, 53-58.

Deng, C., Zhang, P., Harper, J.W., Elledge, S.J., and Leder, P. (1995). Mice lacking p21CIP1/WAF1 undergo normal development, but are defective in G1 checkpoint control. Cell *82*, 675-684.

Der, C.J., Krontiris, T.G., and Cooper, G.M. (1982). Transforming genes of human bladder and lung carcinoma cell lines are homologous to the ras genes of Harvey and Kirsten sarcoma viruses. Proc Natl Acad Sci U S A *79*, 3637-3640.

Diaz-Rodriguez, E., Sotillo, R., Schvartzman, J.M., and Benezra, R. (2008). Hec1 overexpression hyperactivates the mitotic checkpoint and induces tumor formation in vivo. Proc Natl Acad Sci U S A *105*, 16719-16724.

Dittmer, D., Pati, S., Zambetti, G., Chu, S., Teresky, A.K., Moore, M., Finlay, C., and Levine, A.J. (1993). Gain of function mutations in p53. Nat Genet *4*, 42-46.

Dryja, T.P., Friend, S., and Weinberg, R.A. (1986). Genetic sequences that predispose to retinoblastoma and osteosarcoma. Symposium on Fundamental Cancer Research *39*, 115-119.

Duijf, P.H., and Benezra, R. (2013). The cancer biology of whole-chromosome instability. Oncogene *32*, 4727-4736.

Duijf, P.H., Schultz, N., and Benezra, R. (2012). Cancer cells preferentially lose small chromosomes. Int J Cancer.

Dulbecco, R. (1967). The induction of cancer by viruses. Scientific American *216*, 28-37.

Duncan, A.W., Taylor, M.H., Hickey, R.D., Hanlon Newell, A.E., Lenzi, M.L., Olson, S.B., Finegold, M.J., and Grompe, M. (2010). The ploidy conveyor of mature hepatocytes as a source of genetic variation. Nature *467*, 707-710.

Ellegren, H. (2004). Microsatellites: simple sequences with complex evolution. Nature reviews Genetics *5*, 435-445.

Evans, T., Rosenthal, E.T., Youngblom, J., Distel, D., and Hunt, T. (1983). Cyclin: a protein specified by maternal mRNA in sea urchin eggs that is destroyed at each cleavage division. Cell *33*, 389-396.

Fearon, E.R., and Vogelstein, B. (1990). A genetic model for colorectal tumorigenesis. Cell *61*, 759-767.

Fisher, G.H., Wellen, S.L., Klimstra, D., Lenczowski, J.M., Tichelaar, J.W., Lizak, M.J., Whitsett, J.A., Koretsky, A., and Varmus, H.E. (2001). Induction and apoptotic regression of lung adenocarcinomas by regulation of a K-Ras transgene in the presence and absence of tumor suppressor genes. Genes Dev *15*, 3249-3262.

Flemming, W. (1878). Zur Kenntniss der Zelle und ihrer Theilungs-Erscheinungen. Schriften des Naturwissenschaftlichen Vereins für Schleswig-Holstein 3: 23–27.

Foster, D.A., Yellen, P., Xu, L., and Saqcena, M. (2010). Regulation of G1 Cell Cycle Progression: Distinguishing the Restriction Point from a Nutrient-Sensing Cell Growth Checkpoint(s). Genes & cancer *1*, 1124-1131.

Galdiero, M.R., Garlanda, C., Jaillon, S., Marone, G., and Mantovani, A. (2013). Tumor associated macrophages and neutrophils in tumor progression. Journal of cellular physiology *228*, 1404-1412.

Gandarillas, A., and Freije, A. (2014). Cycling up the epidermis: reconciling 100 years of debate. Experimental dermatology *23*, 87-91.

Gao, C., Furge, K., Koeman, J., Dykema, K., Su, Y., Cutler, M.L., Werts, A., Haak, P., and Vande Woude, G.F. (2007). Chromosome instability, chromosome transcriptome, and clonal evolution of tumor cell populations. Proc Natl Acad Sci U S A *104*, 8995-9000.

Garcia-Cao, I., Garcia-Cao, M., Martin-Caballero, J., Criado, L.M., Klatt, P., Flores, J.M., Weill, J.C., Blasco, M.A., and Serrano, M. (2002). "Super p53" mice exhibit enhanced DNA damage response, are tumor resistant and age normally. Embo J *21*, 6225-6235.

Gartner, H.V., Seidl, C., Luckenbach, C., Schumm, G., Seifried, E., Ritter, H., and Bultmann, B. (1996). Genetic analysis of a sarcoma accidentally transplanted from a patient to a surgeon. N Engl J Med *335*, 1494-1496.

Gascoigne, K.E., and Taylor, S.S. (2008). Cancer cells display profound intra- and interline variation following prolonged exposure to antimitotic drugs. Cancer Cell *14*, 111-122.

Gey GO, C.W., Kubicek MT. (1952). Tissue culture studies of the proliferative capacity of cervical carcinoma and normal epithelium. Cancer Res

12, 264-265.

Giannakakou, P., Robey, R., Fojo, T., and Blagosklonny, M.V. (2001). Low concentrations of paclitaxel induce cell type-dependent p53, p21 and G1/G2 arrest instead of mitotic arrest: molecular determinants of paclitaxel-induced cytotoxicity. Oncogene *20*, 3806-3813.

Glotzer, M., Murray, A.W., and Kirschner, M.W. (1991). Cyclin is degraded by the ubiquitin pathway. Nature *349*, 132-138.

Gossen, M., and Bujard, H. (1992). Tight control of gene expression in mammalian cells by tetracycline-responsive promoters. Proc Natl Acad Sci U S A *89*, 5547-5551.

Hajdu, S.I. (2011). A note from history: landmarks in history of cancer, part 1. Cancer *117*, 1097-1102.

Hajdu, S.I. (2012). A note from history: landmarks in history of cancer, part 4. Cancer *118*, 4914-4928.

Hajdu, S.I., and Darvishian, F. (2013). A note from history: landmarks in history of cancer, part 5. Cancer *119*, 1450-1466.

Hajdu, S.I., and Vadmal, M.S. (2010). The use of tobacco. Ann Clin Lab Sci *40*, 178-181.

Hanahan, D., and Weinberg, R.A. (2000). The hallmarks of cancer. Cell *100*, 57-70.

Hanahan, D., and Weinberg, R.A. (2011). Hallmarks of cancer: the next generation. Cell *144*, 646-674.

Harley, M.E., Allan, L.A., Sanderson, H.S., and Clarke, P.R. (2010). Phosphorylation of Mcl-1 by CDK1-cyclin B1 initiates its Cdc20-dependent destruction during mitotic arrest. Embo J *29*, 2407-2420.

Harper, J.W., Elledge, S.J., Keyomarsi, K., Dynlacht, B., Tsai, L.H., Zhang, P., Dobrowolski, S., Bai, C., Connell-Crowley, L., Swindell, E.*, et al.* (1995). Inhibition of cyclin-dependent kinases by p21. Molecular biology of the cell *6*, 387-400.

Hartwell, L.H., and Smith, D. (1985). Altered fidelity of mitotic chromosome transmission in cell cycle mutants of S. cerevisiae. Genetics *110*, 381-395.

Hartwell, L.H., and Weinert, T.A. (1989). Checkpoints: controls that ensure the order of cell cycle events. Science *246*, 629-634.

Haruki, N., Saito, H., Harano, T., Nomoto, S., Takahashi, T., Osada, H., Fujii, Y., and Takahashi, T. (2001). Molecular analysis of the mitotic checkpoint genes BUB1, BUBR1 and BUB3 in human lung cancers. Cancer letters *162*, 201-205.

Hassold, T., Hall, H., and Hunt, P. (2007). The origin of human aneuploidy: where we have been, where we are going. Hum Mol Genet *16 Spec No. 2*, R203-208.

Hatch, E.M., Fischer, A.H., Deerinck, T.J., and Hetzer, M.W. (2013). Catastrophic nuclear envelope collapse in cancer cell micronuclei. Cell *154*, 47-60.

Hoyt, M.A., Totis, L., and Roberts, B.T. (1991). S. cerevisiae genes required for cell cycle arrest in response to loss of microtubule function. Cell *66*, 507-517.

Imielinski, M., Berger, A.H., Hammerman, P.S., Hernandez, B., Pugh, T.J., Hodis, E., Cho, J., Suh, J., Capelletti, M., Sivachenko, A.*, et al.* (2012). Mapping the hallmarks of lung adenocarcinoma with massively parallel sequencing. Cell *150*, 1107-1120.

Iwanaga, Y., Chi, Y.H., Miyazato, A., Sheleg, S., Haller, K., Peloponese, J.M., Jr., Li, Y., Ward, J.M., Benezra, R., and Jeang, K.T. (2007). Heterozygous deletion of mitotic arrest-deficient protein 1 (MAD1) increases the incidence of tumors in mice. Cancer Res *67*, 160-166.

Jacks, T. (1996). Lessons from the p53 mutant mouse. J Cancer Res Clin Oncol *122*, 319-327.

Jacks, T., Remington, L., Williams, B.O., Schmitt, E.M., Halachmi, S., Bronson, R.T., and Weinberg, R.A. (1994). Tumor spectrum analysis in p53-mutant mice. Curr Biol *4*, 1-7.

Jackson, E.L., Willis, N., Mercer, K., Bronson, R.T., Crowley, D., Montoya, R., Jacks, T., and Tuveson, D.A. (2001). Analysis of lung tumor initiation and progression using conditional expression of oncogenic K-ras. Genes Dev *15*, 3243-3248.

Janssen, A., Beerling, E., Medema, R., and van Rheenen, J. (2013). Intravital FRET imaging of tumor cell viability and mitosis during chemotherapy. PLoS One *8*, e64029.

Janssen, A., and Medema, R.H. (2013). Genetic instability: tipping the balance. Oncogene *32*, 4459-4470.

Jeganathan, K., Malureanu, L., Baker, D.J., Abraham, S.C., and van Deursen, J.M. (2007). Bub1 mediates cell death in response to chromosome missegregation and acts to suppress spontaneous tumorigenesis. The Journal of cell biology *179*, 255-267.

Jemal, A., Bray, F., Center, M.M., Ferlay, J., Ward, E., and Forman, D. (2011). Global cancer statistics. CA: a cancer journal for clinicians *61*, 69-90.

Johnson, L., Mercer, K., Greenbaum, D., Bronson, R.T., Crowley, D., Tuveson, D.A., and Jacks, T. (2001). Somatic activation of the K-ras oncogene causes early onset lung cancer in mice. Nature *410*, 1111-1116.

Kabeche, L., and Compton, D.A. (2012). Checkpoint-independent stabilization of kinetochore-microtubule attachments by Mad2 in human cells. Curr Biol *22*, 638-644.

Kalitsis, P., Earle, E., Fowler, K.J., and Choo, K.H. (2000). Bub3 gene disruption in mice reveals essential mitotic spindle checkpoint function during early embryogenesis. Genes Dev *14*, 2277-2282.

Kalitsis, P., Fowler, K.J., Griffiths, B., Earle, E., Chow, C.W., Jamsen, K., and Choo, K.H. (2005). Increased chromosome instability but not cancer predisposition in haploinsufficient Bub3 mice. Genes Chromosomes Cancer *44*, 29-36.

Kastan, M.B., Zhan, Q., el-Deiry, W.S., Carrier, F., Jacks, T., Walsh, W.V., Plunkett, B.S., Vogelstein, B., and Fornace, A.J., Jr. (1992). A mammalian cell cycle checkpoint pathway utilizing p53 and GADD45 is defective in ataxia-telangiectasia. Cell *71*, 587-597.

Kazushi Inoue, E.F., Dejan Maglic and Sinan Zhu (2013). (2013). Genetically Engineered Mouse Models for Human Lung Cancer, Oncogenesis, Inflammatory and Parasitic Tropical Diseases of the Lung, Prof. Jean-Marie Kayembe (Ed.), ISBN: 978-953-51-0982-2, InTech, DOI: 10.5772/53721.

Kerbel, R., and Folkman, J. (2002). Clinical translation of angiogenesis inhibitors. Nat Rev Cancer *2*, 727-739.

Kidokoro, T., Tanikawa, C., Furukawa, Y., Katagiri, T., Nakamura, Y., and Matsuda, K. (2008). CDC20, a potential cancer therapeutic target, is negatively regulated by p53. Oncogene *27*, 1562-1571.

Kim, E.M., Park, J.K., Hwang, S.G., Kim, W.J., Liu, Z.G., Kang, S.W., and Um, H.D. (2014). Nuclear and cytoplasmic p53 suppress cell invasion by inhibiting respiratory Complex-I activity via Bcl-2 family proteins. Oncotarget.

Kirby, A.C., Coles, M.C., and Kaye, P.M. (2009). Alveolar macrophages transport pathogens to lung draining lymph nodes. J Immunol *183*, 1983-1989.

Knouse, K.A., Wu, J., Whittaker, C.A., and Amon, A. (2014). Single cell sequencing reveals low levels of aneuploidy across mammalian tissues. Proc Natl Acad Sci U S A *111*, 13409-13414.

Knudson, A.G., Jr. (1971). Mutation and cancer: statistical study of retinoblastoma. Proc Natl Acad Sci U S A *68*, 820-823.

Koshland, D.E., Jr. (1993). Molecule of the year. Science *262*, 1953.

Kuffer, C., Kuznetsova, A.Y., and Storchova, Z. (2013). Abnormal mitosis triggers p53-dependent cell cycle arrest in human tetraploid cells. Chromosoma *122*, 305-318.

Kuukasjarvi, T., Karhu, R., Tanner, M., Kahkonen, M., Schaffer, A., Nupponen, N., Pennanen, S., Kallioniemi, A., Kallioniemi, O.P., and Isola, J. (1997). Genetic heterogeneity and clonal evolution underlying development of asynchronous metastasis in human breast cancer. Cancer Res *57*, 1597-1604.

Landry, J.J., Pyl, P.T., Rausch, T., Zichner, T., Tekkedil, M.M., Stutz, A.M., Jauch, A., Aiyar, R.S., Pau, G., Delhomme, N.*, et al*. (2013). The genomic and transcriptomic landscape of a HeLa cell line. G3 *3*, 1213-1224.

Lane, D.P. (1992). Worrying about p53. Curr Biol *2*, 581-583.

Lebert (1845). Physiologie Pathologique ou Récherches Clinique, Experimentales et Microscopiques. (Paris: Bailliére).

Lengauer, C., Kinzler, K.W., and Vogelstein, B. (1997). Genetic instability in colorectal cancers. Nature *386*, 623-627.

Li, F.P., and Fraumeni, J.F., Jr. (1969). Soft-tissue sarcomas, breast cancer, and other neoplasms. A familial syndrome? Annals of internal medicine *71*, 747-752.

Li, M., Fang, X., Baker, D.J., Guo, L., Gao, X., Wei, Z., Han, S., van Deursen, J.M., and Zhang, P. (2010). The ATM-p53 pathway suppresses aneuploidy-induced tumorigenesis. Proc Natl Acad Sci U S A *107*, 14188-14193.

Li, R., and Murray, A.W. (1991). Feedback control of mitosis in budding yeast. Cell *66*, 519-531.

Li, Y., and Benezra, R. (1996). Identification of a human mitotic checkpoint gene: hsMAD2. Science *274*, 246-248.

Liu, G., McDonnell, T.J., Montes de Oca Luna, R., Kapoor, M., Mims, B., El-Naggar, A.K., and Lozano, G. (2000). High metastatic potential in mice inheriting a targeted p53 missense mutation. Proc Natl Acad Sci U S A *97*, 4174-4179.

Liu, G., Parant, J.M., Lang, G., Chau, P., Chavez-Reyes, A., El-Naggar, A.K., Multani, A., Chang, S., and Lozano, G. (2004). Chromosome stability, in the absence of apoptosis, is critical for suppression of tumorigenesis in Trp53 mutant mice. Nat Genet *36*, 63-68.

Look, A.T. (1997). Oncogenic transcription factors in the human acute leukemias. Science *278*, 1059-1064.

Luo, J., Emanuele, M.J., Li, D., Creighton, C.J., Schlabach, M.R., Westbrook, T.F., Wong, K.K., and Elledge, S.J. (2009). A genome-wide RNAi screen identifies multiple synthetic lethal interactions with the Ras oncogene. Cell *137*, 835-848.

Lynch, H.T., Shaw, M.W., Magnuson, C.W., Larsen, A.L., and Krush, A.J. (1966). Hereditary factors in cancer. Study of two large midwestern kindreds. Archives of internal medicine *117*, 206-212.

Lynch, T.J., Bell, D.W., Sordella, R., Gurubhagavatula, S., Okimoto, R.A., Brannigan, B.W., Harris, P.L., Haserlat, S.M., Supko, J.G., Haluska, F.G., *et al*. (2004). Activating mutations in the epidermal growth factor receptor underlying responsiveness of non-small-cell lung cancer to gefitinib. N Engl J Med *350*, 2129-2139.

Macleod, K.F., Sherry, N., Hannon, G., Beach, D., Tokino, T., Kinzler, K., Vogelstein, B., and Jacks, T. (1995). p53-dependent and independent expression of p21 during cell growth, differentiation, and DNA damage. Genes Dev *9*, 935-944.

MacPherson, D., Kim, J., Kim, T., Rhee, B.K., Van Oostrom, C.T., DiTullio, R.A., Venere, M., Halazonetis, T.D., Bronson, R., De Vries, A., *et al*. (2004). Defective apoptosis and B-cell lymphomas in mice with p53 point mutation at Ser 23. Embo J *23*, 3689-3699.

Mallakin, A., Sugiyama, T., Taneja, P., Matise, L.A., Frazier, D.P., Choudhary, M., Hawkins, G.A., D'Agostino, R.B., Jr., Willingham, M.C., and Inoue, K. (2007). Mutually exclusive inactivation of DMP1 and ARF/p53 in lung cancer. Cancer Cell *12*, 381-394.

Malumbres, M. (2014). Cyclin-dependent kinases. Genome biology *15*, 122.

Mariotto, A.B., Yabroff, K.R., Shao, Y., Feuer, E.J., and Brown, M.L. (2011). Projections of the cost of cancer care in the United States: 2010-2020. J Natl Cancer Inst *103*, 117-128.

Marxer, M., Ma, H.T., Man, W.Y., and Poon, R.Y. (2014). p53 deficiency enhances mitotic arrest and slippage induced by pharmacological inhibition of Aurora kinases. Oncogene *33*, 3550-3560.

Meuwissen, R., and Berns, A. (2005). Mouse models for human lung cancer. Genes Dev *19*, 643-664.

Michel, L., Diaz-Rodriguez, E., Narayan, G., Hernando, E., Murty, V.V., and Benezra, R. (2004). Complete loss of the tumor suppressor MAD2 causes premature cyclin B degradation and mitotic failure in human somatic cells. Proc Natl Acad Sci U S A *101*, 4459-4464.

Michel, L.S., Liberal, V., Chatterjee, A., Kirchwegger, R., Pasche, B., Gerald, W., Dobles, M., Sorger, P.K., Murty, V.V., and Benezra, R. (2001). MAD2 haplo-insufficiency causes premature anaphase and chromosome instability in mammalian cells. Nature *409*, 355-359.

Mills, N.E., Fishman, C.L., Rom, W.N., Dubin, N., and Jacobson, D.R. (1995). Increased prevalence of K-ras oncogene mutations in lung adenocarcinoma. Cancer Res *55*, 1444-1447.

Mitelman, F., Johansson, B., Mandahl, N., and Mertens, F. (1997). Clinical significance of cytogenetic findings in solid tumors. Cancer genetics and cytogenetics *95*, 1-8.

Morgenbesser, S.D., Williams, B.O., Jacks, T., and DePinho, R.A. (1994). p53-dependent apoptosis produced by Rb-deficiency in the developing mouse lens. Nature *371*, 72-74.

Moullan, N., Mouchiroud, L., Wang, X., Ryu, D., Williams, E.G., Mottis, A., Jovaisaite, V., Frochaux, M.V., Quiros, P.M., Deplancke, B., *et al*. (2015). Tetracyclines Disturb Mitochondrial Function across Eukaryotic Models: A Call for Caution in Biomedical Research. Cell Rep.

Muller (1838). Ueber den feinern Bau und die Formen der

krankhaften Geschwulste.

Murchison, E.P., Schulz-Trieglaff, O.B., Ning, Z., Alexandrov, L.B., Bauer, M.J., Fu, B., Hims, M., Ding, Z., Ivakhno, S., Stewart, C., *et al*. (2012). Genome sequencing and analysis of the Tasmanian devil and its transmissible cancer. Cell *148*, 780-791.

Murga, M., Bunting, S., Montana, M.F., Soria, R., Mulero, F., Canamero, M., Lee, Y., McKinnon, P.J., Nussenzweig, A., and Fernandez-Capetillo, O. (2009). A mouse model of ATR-Seckel shows embryonic replicative stress and accelerated aging. Nat Genet *41*, 891-898.

Murgia, C., Pritchard, J.K., Kim, S.Y., Fassati, A., and Weiss, R.A. (2006). Clonal origin and evolution of a transmissible cancer. Cell *126*, 477-487.

Nam, H.J., and van Deursen, J.M. (2014). Cyclin B2 and p53 control proper timing of centrosome separation. Nature cell biology *16*, 538-549.

Nigg, E.A. (2002). Centrosome aberrations: cause or consequence of cancer progression? Nat Rev Cancer *2*, 815-825.

Nowell P, H.D. (1960).

A minute chromosome in chronic granulocytic leukemia. Science *132 (3438): 1497*.

Nowell, P.C. (1976). The clonal evolution of tumor cell populations. Science *194*, 23-28.

Nurse, P.M. (December 9,2001). CYCLIN DEPENDENT KINASES AND CELL CYCLE CONTROL (Nobel Lecture).

O'Farrell, P.H. (2011). Quiescence: early evolutionary origins and universality do not imply uniformity. Philosophical transactions of the Royal Society of London Series B, Biological sciences *366*, 3498-3507.

Pantoja, C., and Serrano, M. (1999). Murine fibroblasts lacking p21 undergo senescence and are resistant to transformation by oncogenic Ras. Oncogene *18*, 4974-4982.

Pao, W., Miller, V., Zakowski, M., Doherty, J., Politi, K., Sarkaria, I., Singh, B., Heelan, R., Rusch, V., Fulton, L., *et al*. (2004). EGF receptor gene mutations are common in lung cancers from "never smokers" and are associated with sensitivity of tumors to gefitinib and erlotinib. Proc Natl Acad Sci U S A *101*, 13306-13311.

Parada, L.F., Land, H., Weinberg, R.A., Wolf, D., and Rotter, V. (1984). Cooperation between gene encoding p53 tumour antigen and ras in cellular transformation. Nature *312*, 649-651.

Pardee, A.B. (1974). A restriction point for control of normal animal cell proliferation. Proc Natl Acad Sci U S A *71*, 1286-1290.

Pavelka, N., Rancati, G., Zhu, J., Bradford, W.D., Saraf, A., Florens, L., Sanderson, B.W., Hattem, G.L., and Li, R. (2010). Aneuploidy confers quantitative proteome changes and phenotypic variation in budding yeast. Nature *468*, 321-325.

Pavletich, N.P. (1999). Mechanisms of cyclin-dependent kinase regulation: structures of Cdks, their cyclin activators, and Cip and INK4 inhibitors. Journal of molecular biology *287*, 821-828.

Perez de Castro, I., Aguirre-Portoles, C., Fernandez-Miranda, G., Canamero, M., Cowley, D.O., Van Dyke, T., and Malumbres, M. (2013). Requirements for Aurora-A in tissue regeneration and tumor development in adult mammals. Cancer Res *73*, 6804-6815.

Politi, K., Zakowski, M.F., Fan, P.D., Schonfeld, E.A., Pao, W., and Varmus, H.E. (2006). Lung adenocarcinomas induced in mice by mutant EGF receptors found in human lung cancers respond to a tyrosine kinase inhibitor or to down-regulation of the receptors. Genes Dev *20*, 1496-1510.

Pulciani, S., Santos, E., Lauver, A.V., Long, L.K., Robbins, K.C., and Barbacid, M. (1982). Oncogenes in human tumor cell lines: molecular cloning of a transforming gene from human bladder carcinoma cells. Proc Natl Acad Sci U S A *79*, 2845-2849.

Rao, C.V., Yang, Y.M., Swamy, M.V., Liu, T., Fang, Y., Mahmood, R., Jhanwar-Uniyal, M., and Dai, W. (2005). Colonic tumorigenesis in BubR1+/-ApcMin/+ compound mutant mice is linked to premature separation of sister chromatids and enhanced genomic instability. Proc Natl Acad Sci U S A *102*, 4365-4370.

Rausch, T., Jones, D.T., Zapatka, M., Stutz, A.M., Zichner, T., Weischenfeldt, J., Jager, N., Remke, M., Shih, D., Northcott, P.A., *et al*. (2012). Genome sequencing of pediatric medulloblastoma links catastrophic DNA rearrangements with TP53 mutations. Cell *148*, 59-71.

Rehen, S.K., Yung, Y.C., McCreight, M.P., Kaushal, D., Yang, A.H., Almeida, B.S., Kingsbury, M.A., Cabral, K.M., McConnell, M.J., Anliker, B., *et al*. (2005). Constitutional aneuploidy in the normal human brain. J Neurosci *25*, 2176-2180.

Ricke, R.M., Jeganathan, K.B., and van Deursen, J.M. (2011). Bub1 overexpression induces aneuploidy and tumor formation through Aurora B kinase hyperactivation. The Journal of cell biology *193*, 1049-1064.

Rothschild, B.M., Witzke, B.J., and Hershkovitz, I. (1999). Metastatic cancer in the Jurassic. Lancet *354*, 398.

Schvartzman, J.M., Duijf, P.H., Sotillo, R., Coker, C., and Benezra, R. (2011). Mad2 is a critical mediator of the chromosome instability observed upon Rb and p53 pathway inhibition. Cancer Cell *19*, 701-714.

Schvartzman, J.M., Sotillo, R., and Benezra, R. (2010). Mitotic chromosomal instability and cancer: mouse modelling of the human disease. Nat Rev Cancer *10*, 102-115.

Sedivy, J.M. (1998). Can ends justify the means?: telomeres and the mechanisms of replicative senescence and immortalization in mammalian cells. Proc Natl Acad Sci U S A *95*, 9078-9081.

Segal, D.J., and McCoy, E.E. (1974). Studies on Down's syndrome in tissue culture. I. Growth rates and protein contents of fibroblast cultures. Journal of cellular physiology *83*, 85-90.

Senovilla, L., Vitale, I., Martins, I., Tailler, M., Pailleret, C., Michaud, M., Galluzzi, L., Adjemian, S., Kepp, O., Niso-Santano, M., *et al*. (2012). An immunosurveillance mechanism controls cancer cell ploidy. Science *337*, 1678-1684.

Serrano, M., Lin, A.W., McCurrach, M.E., Beach, D., and Lowe, S.W. (1997). Oncogenic ras provokes premature cell senescence associated with accumulation of p53 and p16INK4a. Cell *88*, 593-602.

Shames, D.S., and Wistuba, II (2014). The evolving genomic classification of lung cancer. The Journal of pathology *232*, 121-133.

Shi, J., Zhou, Y., Huang, H.C., and Mitchison, T.J. (2011). Navitoclax (ABT-263) accelerates apoptosis during drug-induced mitotic arrest by antagonizing Bcl-xL. Cancer Res *71*, 4518-4526.

Silk, A.D., Zasadil, L.M., Holland, A.J., Vitre, B., Cleveland, D.W., and Weaver, B.A. (2013). Chromosome missegregation rate predicts whether aneuploidy will promote or suppress tumors. Proc Natl Acad Sci U S A *110*, E4134-4141.

Sinnott, R., Winters, L., Larson, B., Mytsa, D., Taus, P., Cappell, K.M., and Whitehurst, A.W. (2014). Mechanisms promoting escape from mitotic stress-induced tumor cell death. Cancer Res *74*, 3857-3869.

Sotillo, R., Dubus, P., Martin, J., de la Cueva, E., Ortega, S., Malumbres, M., and Barbacid, M. (2001). Wide spectrum of tumors in knock-in mice carrying a Cdk4 protein insensitive to INK4 inhibitors. Embo J *20*, 6637-6647.

Sotillo, R., Hernando, E., Diaz-Rodriguez, E., Teruya-Feldstein, J., Cordon-Cardo, C., Lowe, S.W., and Benezra, R. (2007). Mad2 overexpression promotes aneuploidy and tumorigenesis in mice. Cancer Cell *11*, 9-23.

Sotillo, R., Schvartzman, J.M., and Benezra, R. (2009). Very CIN-ful: whole chromosome instability promotes tumor suppressor loss of heterozygosity. Cancer Cell *16*, 451-452.

Sotillo, R., Schvartzman, J.M., Socci, N.D., and Benezra, R. (2010). Mad2-induced chromosome instability leads to lung tumour relapse after oncogene withdrawal. Nature *464*, 436-440.

Soussi, T., and Beroud, C. (2001). Assessing TP53 status in human tumours to evaluate clinical outcome. Nat Rev Cancer *1*, 233-240.

Spencer, F., and Hieter, P. (1992). Centromere DNA mutations induce a mitotic delay in Saccharomyces cerevisiae. Proc Natl Acad Sci U S A *89*, 8908-8912.

Stehelin, D., Varmus, H.E., Bishop, J.M., and Vogt, P.K. (1976). DNA related to the transforming gene(s) of avian sarcoma viruses is present in normal avian DNA. Nature *260*, 170-173.

Stewart, B.W., Wild, C., International Agency for Research on Cancer, and World Health Organization (2014). World cancer report 2014 (Lyon, France

Geneva, Switzerland: International Agency for Research on Cancer

WHO Press).

Storchova, Z., and Kuffer, C. (2008). The consequences of tetraploidy and aneuploidy. J Cell Sci *121*, 3859-3866.

Sullivan, B.A., Blower, M.D., and Karpen, G.H. (2001). Determining centromere identity: cyclical stories and forking paths. Nature reviews Genetics *2*, 584-596.

Tahara, H., Sato, E., Noda, A., and Ide, T. (1995). Increase in expression level of p21sdi1/cip1/waf1 with increasing division age in both normal and SV40-transformed human fibroblasts. Oncogene *10*, 835-840.

Tang, Y.C., Williams, B.R., Siegel, J.J., and Amon, A. (2011). Identification of aneuploidy-selective antiproliferation compounds. Cell *144*, 499-512.

Tannous, B.A., Kerami, M., Van der Stoop, P.M., Kwiatkowski, N., Wang, J., Zhou, W., Kessler, A.F., Lewandrowski, G., Hiddingh, L., Sol, N., *et al*. (2013). Effects of the selective MPS1 inhibitor MPS1-IN-3 on glioblastoma sensitivity to antimitotic drugs. J Natl Cancer Inst *105*, 1322-1331.

Temin, H.M., and Mizutani, S. (1970). RNA-dependent DNA polymerase in virions of Rous sarcoma virus. Nature *226*, 1211-1213.

Terradas, M., Martin, M., Tusell, L., and Genesca, A. (2010). Genetic activities in micronuclei: is the DNA entrapped in micronuclei lost for the cell? Mutation research *705*, 60-67.

Thompson, S.L., and Compton, D.A. (2008). Examining the link between chromosomal instability and aneuploidy in human cells. The Journal of cell biology *180*, 665-672.

Thompson, S.L., and Compton, D.A. (2010). Proliferation of aneuploid human cells is limited by a p53-dependent mechanism. The Journal of cell biology *188*, 369-381.

Thompson, S.L., and Compton, D.A. (2011). Chromosome missegregation in human cells arises through specific types of kinetochore-microtubule attachment errors. Proc Natl Acad Sci U S A *108*, 17974-17978.

Torres, E.M., Sokolsky, T., Tucker, C.M., Chan, L.Y., Boselli, M., Dunham, M.J., and Amon, A. (2007). Effects of aneuploidy on cellular physiology and cell division in haploid yeast. Science *317*, 916-924.

Varetti, G., Pellman, D., and Gordon, D.J. (2014). Aurea Mediocritas: The Importance of a Balanced Genome. Cold Spring Harbor perspectives in biology.

Walmsley, R.M., and Tate, M. (2012). The GADD45a-GFP GreenScreen HC assay. Methods in molecular biology *817*, 231-250.

Warburg, O. (1956). On the origin of cancer cells. Science *123*, 309-314.

Watson, J.D., and Crick, F.H. (1953). Molecular structure of nucleic acids; a structure for deoxyribose nucleic acid. Nature *171*, 737-738.

Weaver, B.A., Silk, A.D., Montagna, C., Verdier-Pinard, P., and Cleveland, D.W. (2007). Aneuploidy acts both oncogenically and as a tumor suppressor. Cancer Cell *11*, 25-36.

Weiss, E., and Winey, M. (1996). The Saccharomyces cerevisiae spindle pole body duplication gene MPS1 is part of a mitotic checkpoint. The Journal of cell biology *132*, 111-123.

Williams, B.R., Prabhu, V.R., Hunter, K.E., Glazier, C.M., Whittaker, C.A., Housman, D.E., and Amon, A. (2008). Aneuploidy affects proliferation and spontaneous immortalization in mammalian cells. Science *322*, 703-709.

Yamamoto, N., Jiang, P., Yang, M., Xu, M., Yamauchi, K., Tsuchiya, H., Tomita, K., Wahl, G.M., Moossa, A.R., and Hoffman, R.M. (2004). Cellular dynamics visualized in live cells in

vitro and in vivo by differential dual-color nuclear-cytoplasmic fluorescent-protein expression. Cancer Res *64*, 4251-4256.

Zack, T.I., Schumacher, S.E., Carter, S.L., Cherniack, A.D., Saksena, G., Tabak, B., Lawrence, M.S., Zhang, C.Z., Wala, J., Mermel, C.H., *et al*. (2013). Pan-cancer patterns of somatic copy number alteration. Nat Genet *45*, 1134-1140.

Zasadil, L.M., Andersen, K.A., Yeum, D., Rocque, G.B., Wilke, L.G., Tevaarwerk, A.J., Raines, R.T., Burkard, M.E., and Weaver, B.A. (2014). Cytotoxicity of paclitaxel in breast cancer is due to chromosome missegregation on multipolar spindles. Science translational medicine *6*, 229ra243.

Zhivotovsky, B., and Kroemer, G. (2004). Apoptosis and genomic instability. Nature reviews Molecular cell biology *5*, 752-762.

Zienolddiny, S., Ryberg, D., Arab, M.O., Skaug, V., and Haugen, A. (2001). Loss of heterozygosity is related to p53 mutations and smoking in lung cancer. British journal of cancer *84*, 226-231.